ERDC/CRREL TR-16-7

US Army Corps
of Engineers®
Engineer Research and
Development Center

New Hampshire DOT SPR2 Program

Assessment of Asphalt Concrete Reinforcement Grid in Flexible Pavements

Lynette A. Barna, Charles E. Smith Jr., Andrew Bernier, Aaron Smart, and Ann M. Scholz

May 2016

Cold Regions Research
and Engineering Laboratory

The U.S. Army Engineer Research and Development Center (ERDC) solves the nation's toughest engineering and environmental challenges. ERDC develops innovative solutions in civil and military engineering, geospatial sciences, water resources, and environmental sciences for the Army, the Department of Defense, civilian agencies, and our nation's public good. Find out more at www.erdc.usace.army.mil.

To search for other technical reports published by ERDC, visit the ERDC online library at http://acwc.sdp.sirsi.net/client/default.

ERDC/CRREL TR-16-7
May 2016

Assessment of Asphalt Concrete Reinforcement Grid in Flexible Pavements

Lynette A. Barna, Charles E. Smith Jr., and Andrew Bernier

U.S. Army Engineer Research and Development Center (ERDC)
Cold Regions Research and Engineering Laboratory (CRREL)
72 Lyme Road
Hanover, NH 03755-1290

Aaron Smart and Ann Scholz

New Hampshire Department of Transportation (NHDOT)
PO Box 483, 5 Hazen Drive
Concord, NH 03302-0483

Final Report

Prepared for New Hampshire Department of Transportation (NHDOT) in cooperation with the U.S. Department of Transportation, Federal Highway Administration

Under Cooperative Research and Development Agreement (CRADA) 13-CRL-01 and project 26962A, "Assessment of Asphalt Concrete Reinforcement Grid in Flexible Pavements"

Abstract

This report investigated the application of accepted methods of pavement structural evaluation to independently assess the potential structural benefit of asphalt geogrid reinforcement of an operational flexible highway pavement. The asphalt interlayer consisted of an elastomeric polymer coated fiberglass grid with an open configuration. The reinforcing grid was installed in the asphalt layer during construction of a maintenance overlay and has been subjected to trafficking for several years.

Our structural evaluation included a geotechnical investigation and nondestructive testing using a falling weight deflectometer. Field testing was conducted when both air temperatures were above 50°F and no recent precipitation events had occurred. Standard testing methods were applied during the field data collection and back-calculation procedure.

The back-calculation results showed no clear quantifiable benefit from including the reinforcing grid in the asphalt layer, but this study developed a methodology to test and evaluate in situ flexible pavements with asphalt grid reinforcement. We recommend that a future structural evaluation be completed to monitor any changes in the pavement's performance.

Contents

Illustrations

Figures

Tables

Preface

This project was funded by the New Hampshire Department of Transportation (NHDOT) in cooperation with the U.S. Department of Transportation, Federal Highway Administration under Cooperative Research and Development Agreement (CRADA) 13-CRL-01 and project 26962A, "Assessment of Asphalt Concrete Reinforcement Grid in Flexible Pavements." The technical monitor was Glenn Roberts, NHDOT.

This report was prepared by Lynette Barna (Force Projection and Sustainment Branch, Dr. Toyoaki Nogami, Chief) and Charles Smith and Andrew Bernier (Engineering Resources Branch, Jared Oren, Chief), U.S. Army Engineer Research and Development Center (ERDC) Cold Regions Research and Engineering Laboratory (CRREL), and Aaron Smart and Ann Scholz, NHDOT Bureau of Materials and Research. At the time of publication, Dr. Loren Wehmeyer was Chief of the Research and Engineering Division, ERDC-CRREL. The Deputy Director of ERDC-CRREL was Dr. Lance Hansen, and the Director was Dr. Robert Davis.

The authors acknowledge the generous project support from NHDOT District 6 and the NHDOT coring crew during the field testing and the post-field laboratory testing done by the NHDOT Bureau of Materials and Testing.

COL Bryan S. Green was Commander of ERDC, and Dr. Jeffery P. Holland was the Director.

Acronyms and Abbreviations

AASHTO	Association of State Highway and Transportation Officials
CBR	California Bearing Ratio
CRREL	Cold Regions Research and Engineering Laboratory
CRADA	Cooperative Research and Development Agreement
DCP	Dynamic Cone Penetrometer
DOD	Department of Defense
EB	Eastbound
ERDC	U.S. Army Engineer Research and Development Center
FWD	Falling Weight Deflectometer
GPS	Global Position System
ISM	Impulse Stiffness Modulus
LEEP	Layered Elastic Evaluation Program
MM	Mile Marker
NCDC	National Climatic Data Center
NHDOT	New Hampshire Department of Transportation
PCASE	Pavement-Transportation Computer Assisted Structural Engineering
WB	Westbound
WESDEF	Waterways Experiment Station Deflection

Unit Conversion Factors

Multiply	By	To Obtain
degrees (angle)	0.01745329	radians
degrees Fahrenheit	(F-32)/1.8	degrees Celsius
feet	0.3048	meters
inches	0.0254	meters
miles (U.S. statute)	1,609.347	meters
mils	0.0254	millimeters
pounds (force)	4.448222	newtons
pounds (force) per square inch	6.894757	kilopascals
square inches	6.4516 E-04	square meters

1 Introduction

1.1 Background

Geogrid manufacturers have promoted including reinforcing grid in the asphalt concrete layer of a flexible pavement as an effective rehabilitation method to reduce or arrest cracking. The New Hampshire Department of Transportation (NHDOT) installed GlasGrid 8501, a commercially available fiberglass grid, in sections of New Hampshire Route 101 (NH 101) during maintenance overlays to address the pavement deterioration and advancing distress from numerous cracks that formed primarily from traffic loading. During the rehabilitation project, the pavement surface was milled and overlain with a thin leveling course, the reinforcing grid was placed, and an asphalt overlay was constructed. Over the past several years since the completion of the rehabilitation project, visual observations by NHDOT personnel suggest that the inclusion of the grid reinforcement in the asphalt layer has effectively impeded the formation of reflective cracks or continued cracking in the roadway sections where it was placed. U.S. Army Cold Regions Research and Engineering Laboratory (CRREL) conducted structural evaluation testing in test sections with and without reinforcing grid in an effort to evaluate and quantify the benefit of using the reinforcing grid.

NHDOT and CRREL collaborated on this project under a cooperative research and development agreement (CRADA).

1.2 Objective

The objective of this project was to independently assess the potential structural benefit from the installation of reinforcing grid in the asphalt concrete layer in a New Hampshire flexible pavement. To the extent possible, any benefit would also consider variables such as the grid geometry and the depth of the reinforcing grid installation within the asphalt layer.

1.3 Scope

Pavement testing focused on a section of NH 101, both the east- and westbound directions, between mile markers 123.2 and 131.5 near the southern town of Exeter in Rockingham County. Within these designated roadway mileposts were roadway sections where commercial reinforcing grid had

been installed, which were compared with sections without reinforcing grid (control sections). The thickness of the asphalt layer varied from 5.75 to 10 in. During a joint initial site visit, NHDOT and CRREL identified six test sections for structural evaluation testing, which included a geotechnical investigation and non-destructive testing.

The non-destructive structural evaluation used CRREL's Falling Weight Deflectometer (FWD) testing equipment, calibrated in accordance with the American Association of State Highway and Transportation Officials (AASHTO) Designation R 32-11, *Standard Practice for Calibrating the Load Cell and Deflection Sensors for a Falling Weight Deflectometer* (AASHTO 2011). Pavement evaluation testing in the field was completed in keeping with AASHTO T256, *Standard Method of Test for Pavement Deflection Measurements* (AASHTO 2005) or ASTM standards as applicable.

1.4 Technical approach

We completed the initial site visit in July 2014 with the information collected forming the basis of the field-test plan. NHDOT provided site-specific background information on the test sites, conducted core sampling and geotechnical analysis at each of the six designated test locations, and provided traffic control. CRREL performed the structural pavement evaluation using the FWD mobile testing apparatus, the back-calculation of the deflection data, and the data analysis.

Field testing was conducted under ideal conditions so as to minimize the variability from the effects of temperature and moisture in an uncontrolled environment. To ensure the reliability of the FWD measurements, CRREL recommended defining the requirements for ideal weather conditions. CRREL specified for FWD testing that the minimum air temperature threshold was 50°F and no significant precipitation events should have occurred during the previous seven days.

The back-calculation procedure, with some modification, conformed to the U.S. Army Corps of Engineers approach actively used in pavement evaluation.

2 Cracking in Flexible Pavements

Roadway pavements surfaced with hot mix asphalt are commonly used for high-speed, high-volume highway applications. The purpose of the surface is to provide a stable, durable, and reliable interface between the vehicle and the underlying supporting materials across all types of climates. Pavement design uses a number of input parameters. The AASHTO *Guide for the Design of Pavement Structures* (1993) remains in use and describes in detail the accepted procedures for both the design and maintenance of pavement structures. Design considerations include pavement performance, traffic, subgrade soil, construction materials, environment, drainage, reliability, life-cycle costs, and shoulder design.

The pavement's safety, functional performance, and structural performance are important characteristics in determining the overall performance (AASHTO 1993). Safety-related performance is tied to the frictional resistance at the interface between the tire and road surface; the functional performance is described as how well the pavement serves the user through riding comfort and smoothness (AASHTO 1993). Maintaining and continuing the load-carrying capacity are related to the pavement's structural performance, which is impacted by the pavement's physical condition and any deterioration that might reduce the load-carrying capacity.

The asphalt concrete layer serves to distribute the traffic loads to the underlying support layers to reduce the stress effect. It is well documented that the thickness of asphalt roads is designed to reduce the tensile strain at the bottom of the asphalt layer and the vertical stress at the top of the subgrade. Over time, visual evidence of the development of distresses, such as fatigue cracking and rutting, occurs in the pavement, impacting the structural capacity (Hassan et al. 2003). Cracking in the asphalt layer is a common distress that results from load repetition and from continuous exposure to the environment (Doré and Zubeck 2009). The presence of cracks in the asphalt layer is problematic, leading to continued deterioration of the pavement as cracks are a direct pathway for water infiltration or increased oxidation (Caltabiano and Brunton 1991).

Eventual fatigue of the asphalt layer due to the combination of repetitive strains, often caused by traffic or thermally induced, and the reduced tensile strength lead to fatigue cracking (Roberts et al. 1996). Figure 1 shows an example of fatigue cracking.

Figure 1. An example of fatigue cracking in flexible pavement (DOD 2001).

When the extent of cracking reaches a certain threshold, maintenance is required. When cracking occurs in the pavement layer, it is important to correctly assess the distress type to select the best method of rehabilitation (Francken 2005; Roberts et al. 1996; Romeo et al. 2014; Hassan et al. 2003). Asphalt overlays are customarily used as a rehabilitation method to preserve the structural capacity of the roadway. However, overlays are frequently subject to reflective cracking leading to premature failure (Roberts et al. 1996; Romeo et al. 2014).

Reflection cracks are visually observed on the surface of the overlay as a result of discontinuities that begin in the lower pavement layers and propagate (Roberts et al. 1996). The crack propagates from the relative movement (Roberts et al. 1996) of an existing crack (Caltabiano and Brunton 1991) or joint (Lee 2008; Francken 2005) in the lower layers. Reflective cracks are non-structural (Caltabiano and Brunton 1991) and may occur soon after placement of the overlay (Darling and Woolstencroft 2004) as a result of excessive traffic volume or environmental factors (Lee 2008) or construction procedures (Francken 2005). Roberts et al. (1996) reported that reflective cracks can appear within the surface of the overlay in as little as 1–2 years on pavements that use a standard tack coat as the bond between the old and new layers. This leads to increased roadway maintenance and costs.

To address the issue of reflective cracking in overlays and to improve resistance to cracking (Romeo et al. 2014), the literature describes two approaches: increasing the thickness of the asphalt layer and using interlayers within the asphalt layer. The purpose of the interlayer is to prevent or

delay the development of reflective cracks by absorbing the movement of the underlying layers and attenuating the stresses and strains within the layer before cracking and crack growth progress to the upper layers (Roberts et al. 1996). Roberts et al. (1996) reported that materials successfully used as interlayers include asphalt rubber and geotextiles, and the application of recycling techniques to rework the upper 2–4 in. of the old asphalt surface has also shown to be effective.

The type of reinforcing grid installed in NH 101 was GlasGrid 8501, consisting of an open grid configuration from strands of fiberglass coated with an elastomeric polymer (Tensar 2011). The grid size was 0.5 × 0.5 in. (Saint-Gobain ADFORS 2011), as shown in Figure 2.

Figure 2. A photograph of GlasGrid fiberglass mesh installed in NH 101.

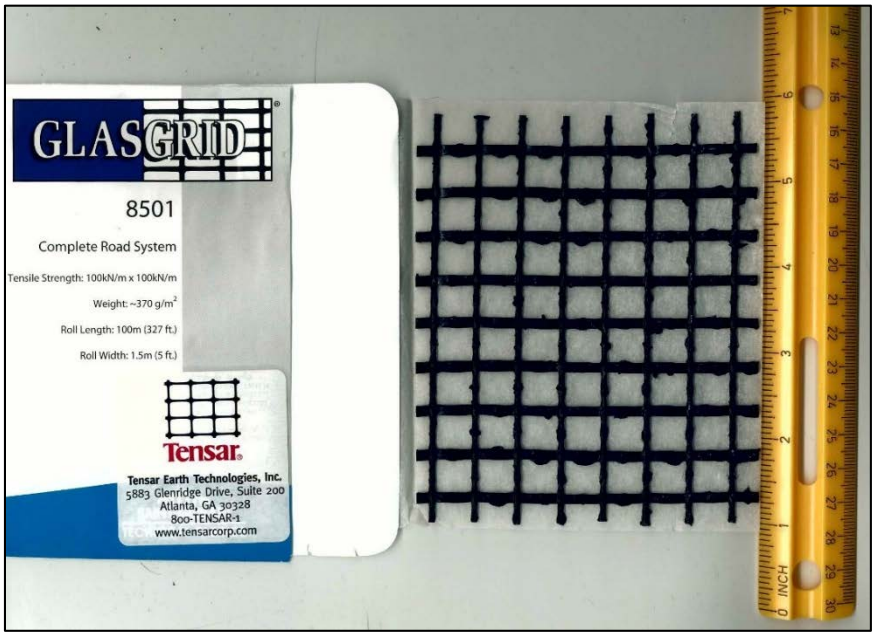

A literature search showed that including reinforcing grid within the asphalt layer has been used for some time but has had mixed results. A continued unmet need is an unbiased, non-destructive evaluation to quantify any structural benefit derived from using grid reinforcement within the asphalt layer, particularly in the in situ condition (Francken 2005). This information would help to evaluate the cost and benefits of adding grid reinforcement to asphalt concrete, to improve design models, to provide needed material characteristics, and to further develop testing methods and field validations (Francken 2005).

We found in our literature review one study by Pasquini et al. (2013) that conducted laboratory testing and used FWD testing during a full-scale field trial. The focus of this research study was the performance of test sections with grid reinforcement and emphasized the proper installation of the grid layer. Pasquini et al. (2013) constructed and trafficked several test sections, one of which was a control section. They conducted FWD testing on the existing pavement prior to the reconstruction and shortly after reconstruction. As reported in the article, the applied load level during the FWD testing was approximately 14 kip. The results of the FWD testing did not clearly indicate a structural benefit provided by the presence of grid reinforcement within the test sections. The authors reasoned that the early age of the pavement sections obscured the positive influence of the grid. The authors, based on laboratory testing results, postulated that under field conditions the pavement may need to sustain some level of damage due to traffic loading before non-destructive testing would show perceptible results.

Our investigation looked at a section of NH 101 that was rehabilitated using grid reinforcement. Prior to the rehabilitation, a pilot project conducted FWD testing (Smart 2011). This data may be limited in its use as the total thickness of the asphalt layer increased significantly during reconstruction. Additionally, no FWD baseline measurements were collected after rehabilitation. For several years, the pavement has been subjected to steady traffic conditions and environmental oscillations (seasonal temperature cycling and precipitation). Therefore, a structural evaluation with FWD testing may well present evidence of a benefit from grid reinforcement.

3 Pavement Test Sections

The section of NH 101 tested in this investigation was oriented east–west in the vicinity of Exits 9 to 13 between Epping and Hampton, NH (Figure 3). The roadway is an asphalt-surfaced divided highway operating mixed traffic at highway speed.

Figure 3. A map view indicating the test area on NH 101. The six test sections are identified with the *yellow circles*—note that two *yellow circles* are obscured due to the close proximity of stations. (Adapted from NHDOT).

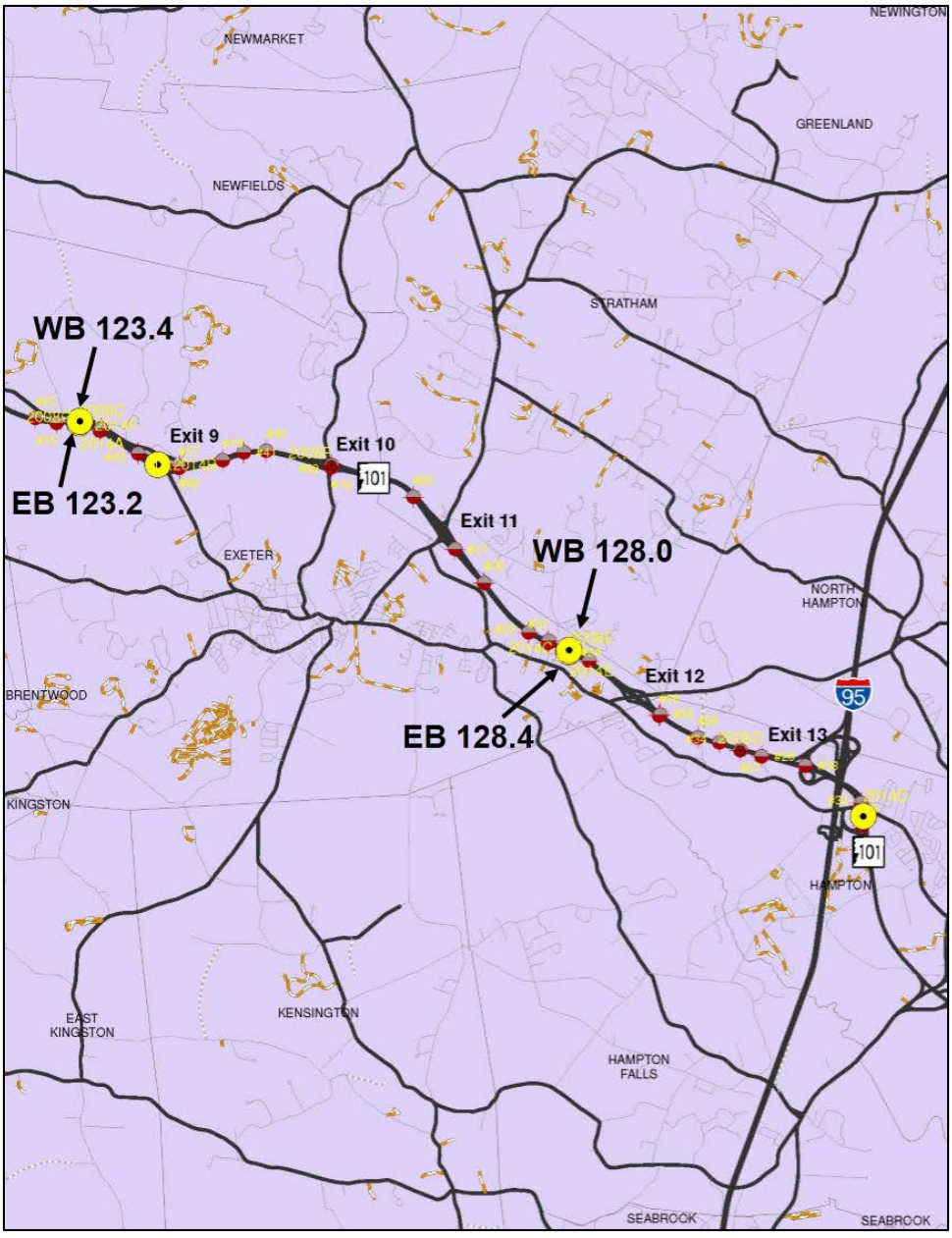

The site visit in July 2014 allowed NHDOT and CRREL to identify suitable test-section locations, to observe the condition of the pavement and the traffic, and to consider both safety and logistical requirements. To the greatest extent practical, the grid-reinforced test sections were located adjacent to a control test section without reinforcement. We also selected locations near the FWD test points used in a 2008 pilot study evaluating nondestructive pavement testing methods prior to the reinforcing grid installation during the roadway reconstruction project (Smart 2011). During the initial site visit, NHDOT demarcated each test section with paint, identified a location for core sampling, and flagged the test section by tying white survey tape to the mile marker sign (or as near as possible). Figure 4 shows the test section markings at mile marker 123.2 eastbound. Generally, the condition of the pavement surface was good at all test section locations with no significant deterioration observed.

Figure 4. Photographs of the test section in the eastbound travel lane at mile marker 123.3.

Factors considered in test section selection were grid reinforcement location, pavement treatment, asphalt thickness, direction of traffic, and safety. Specifically, factors such as traffic count, slope, and aspect were assumed to have negligible effects for the structural evaluation. Our intention was to select a suitable number of test sections to minimize traffic disruptions yet maintain the safety of personnel and equipment during the field testing and yield a sufficient quantity of data for analysis. Another criteria was to collect the data during a sequential time period when the environmental conditions would stay relatively constant; consequently, we needed to conduct the testing during warm and dry conditions.

During the rehabilitation project, NHDOT installed reinforcing grid in sections of NH 101. Figures 5 and 6 illustrate where the grid reinforcement, depicted as blue hatched areas, was placed along NH 101 between mile marker (MM) 115.1 and 132.5 in the eastbound direction and MM 117.6 and 132.5 in the westbound direction. These figures also show the similar pavement treatment types during construction. Note in
Figure 5 in the eastbound direction that the reinforcing grid was installed in the travel lane, whereas in the westbound direction (

Figure 6), reinforcing grid was installed in a significant portion of the travel lane with smaller installations in the passing lane.

Another selection factor was asphalt thickness. In the eastbound lanes, the asphalt thickness at MM 123.2 (control without grid) and 124.2 (with grid) were similar at 10 in. These two locations offered a side-by-side comparison of the pavement at relatively close proximity to each other while allowing a good offset distance between test sections. At MM 128.4 (with grid) in the eastbound lane, the asphalt thickness decreased to 6 in.

In the westbound lanes, MM 131.5 (control without grid) and MM 128.0 (with grid) were comparable with asphalt layer thicknesses of 5.75 and 7 in., respectively. At MM 123.4 in the westbound lane, the asphalt thickness increased to a 9 in. depth.

For the 10 in. nominal asphalt thickness, the three test sections were eastbound (EB) MM 123.2 (control), EB MM 124.2, and a replicate at westbound (WB) MM 123.4.

Figure 5. NH 101 eastbound lanes, showing the three test sections in the eastbound lane. In the upper graphic, the blue hatched areas indicate locations where grid reinforcement was installed in the asphalt layer. Each individual test section was approximately 500 ft long. (Adapted from NHDOT.)

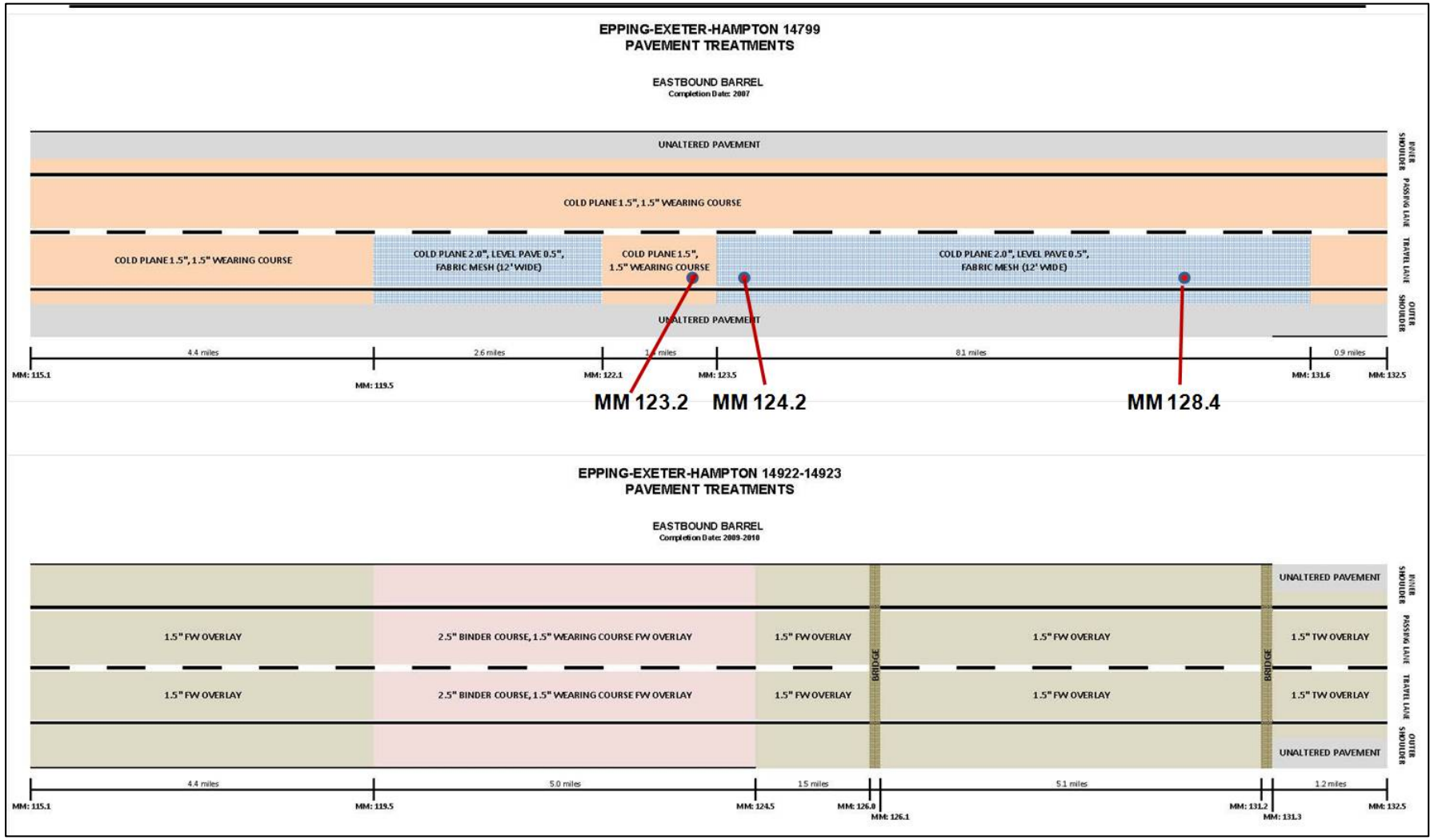

Figure 6. NH 101 westbound lanes, showing the three test sections in the westbound lane. The blue hatched areas in the upper graphic indicate locations where grid reinforcement was installed in the asphalt layer. Each individual test section was approximately 500 ft long. (Adapted from NHDOT.)

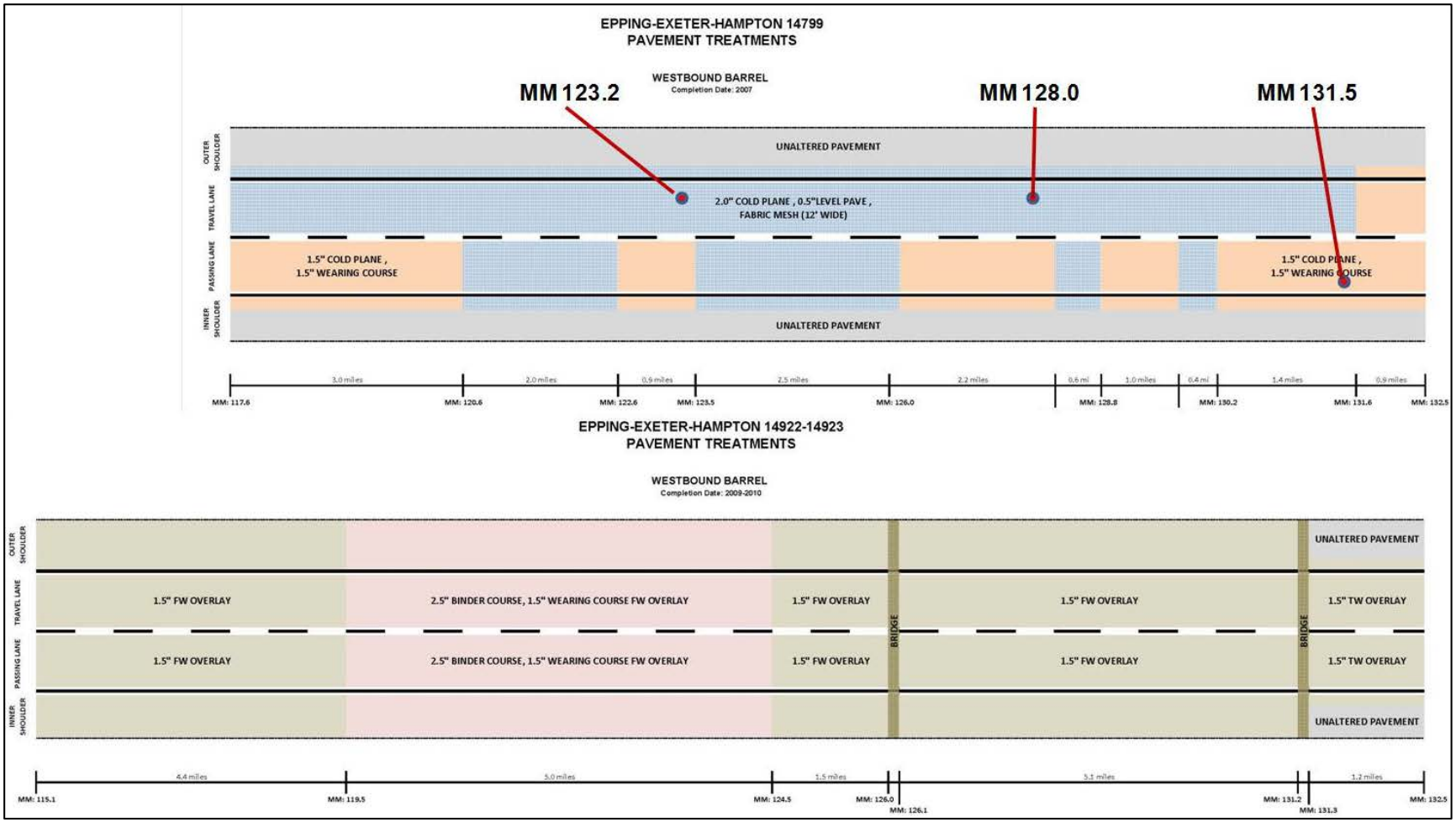

Table 1 lists the six test sections. For the 6 in. nominal asphalt thickness, the three test sections were WB MM 131.5 (control), WB MM 128.0, and a replicate at EB MM 128.4. The control location at WB MM 131.5 was a slightly different condition compared to the other two test sections. It had decreased traffic exposure given that it was located east of the I-95 on ramp. However, this was not considered a significant factor.

Table 1. Proposed test sections from site survey.

Direction	Mile Marker	Pavement Overlay Thickness (in.)	Total Asphalt Thickness (in.)	Grid	Grid Depth* (in.)
EB	123.2	5.5	10	NO	N/A
EB	124.2	5.5	10	YES	5.5
EB	128.4	1.5	6.5	YES	3.0
WB	123.4	5.5	9	YES	5.5
WB	128.0	1.5	7	YES	2.5
WB	131.5	1.5	5.75	NO	N/A

* Measured from the top of the core

Each of the six test sections was approximately 500 ft long and contained a minimum of ten FWD test points all within the same lane and spaced roughly 100 ft apart. Five test points were located in the wheel path, and five were located at a 3 ft offset from the wheel path toward the midlane (should the distance of the offset be greater, these test points would occur in the other wheel path). The layout of the test points is further described in Figure 14 in Section 4.

4 Field Data Collection

4.1 Field-testing overview

NHDOT and CRREL conducted initial field testing on 4 September 2014. At four of the six test sections, pavement and soil cores were collected, and subsurface soil strength was measured. No FWD data was collected at any of the test sites due to a communications error between the FWD testing equipment and the data collection computer. Because of this equipment malfunction, CRREL suspended testing. Shortly thereafter, CRREL's FWD equipment was shipped to the manufacturer for a planned system upgrade that included calibration of the load cell and deflection sensors. The field-testing dates were rescheduled soon after the FWD was returned to CRREL and placed back into service. Field testing on NH 101 resumed on 28 October 2014 during a period of favorable weather conditions. The remaining two cores were collected from the test sections WB MM 123.2 and WB MM 124.2, and FWD testing was completed at all six test sections.

4.2 Field-testing schedule

For safety reasons, given the schedule and volume of traffic along NH 101, we anticipated completing the field testing over two consecutive days with testing beginning mid- to late morning and ending about mid-afternoon on both days. Next, we watched the weather forecast to identify a timeframe for field testing that would meet the testing criteria.

We continuously monitored the 10-day weather forecast for the Exeter area by using online commercial weather forecasts to identify possible dates and to coordinate availability for NHDOT and CRREL. Given the variability in the forecasts, we generally monitored three different sites simultaneously to watch for a potential test window. The web page for the Skyhaven Airport in Rochester, NH (www.skyhavennh.com), roughly 25 miles north of the test area, offered ready access and reported a 3-day weather history used to track rain events that occurred in the area. Continuous temperature and precipitation data for Epping, NH* (approximately 8 miles west), and precipitation data for Exeter, NH†, were available from

* GHCND: USC00272800; Latitude: 43.030° North, Longitude: 71.084° West.
† GHCND: US1NHRC0007; Latitude: 42.973° North, Longitude: 70.920° West.

the National Climatic Data Center (NCDC) in Asheville, NC, accessed via the website (http://www.ncdc.noaa.gov/) and are included in Figure 7.

The weather conditions were ideal on 4 September 2014 with clear, sunny skies and no precipitation in the forecast. As shown in Figure 7, the air temperature reading reached a high that day of 81°F following a low the previous night of 65°F based on NCDC's recorded climate observations for Exeter, NH. Prior to the test date, both the Epping and Exeter dataset reported rain events that occurred on 1 and 3 September. Precipitation on 1 September was similar at the two sites with Epping recording 0.11 in. and Exeter 0.14 in. Precipitation amounts on 3 September, the day before testing, varied with Epping reporting 0.27 in. and Exeter 0.43 in. On the day of testing, we observed no standing water on the pavement (Figure 8). When the asphalt core was removed at test section EB MM 123.2, no excess water was present in the core hole. The top of the base course was moist; however, this may have resulted from the water used to cool the core barrel while cutting through the pavement layer.

When testing resumed on 28 and 29 October 2014, there was a period of several days when the air temperature consistently reached highs in the upper 50s to mid-60s (Figure 7) with overnight lows reaching the mid-30s. On 27 October, the air temperature readings were mid-40s by 0700 hr with no rain in the forecast. The NCDC precipitation measurements for Exeter, NH, recorded a significant rain event of 1.5 in. on 24 October 2014 followed by only trace amounts of precipitation on 25 October and on the mornings of both testing days. We considered any impacts from the precipitation minimal. On the first day of testing, the weather conditions were good with clear skies. As an example, the photographs in Figures 9–12 show the testing conditions and test-section layout at WB MM 128.0. Fog delayed the start of testing on 29 October; but by late morning, it lifted for acceptable visibility to continue testing (Figure 13). Skies remained overcast throughout the remainder of testing that day. Testing was completed by late afternoon on 29 October.

Figure 7. Observed daily maximum and minimum air temperatures and precipitation readings from Epping, NH, station GHCND:USC00272800. (Data from the National Climatic Data Center, www.ncdc.noaa.gov.)

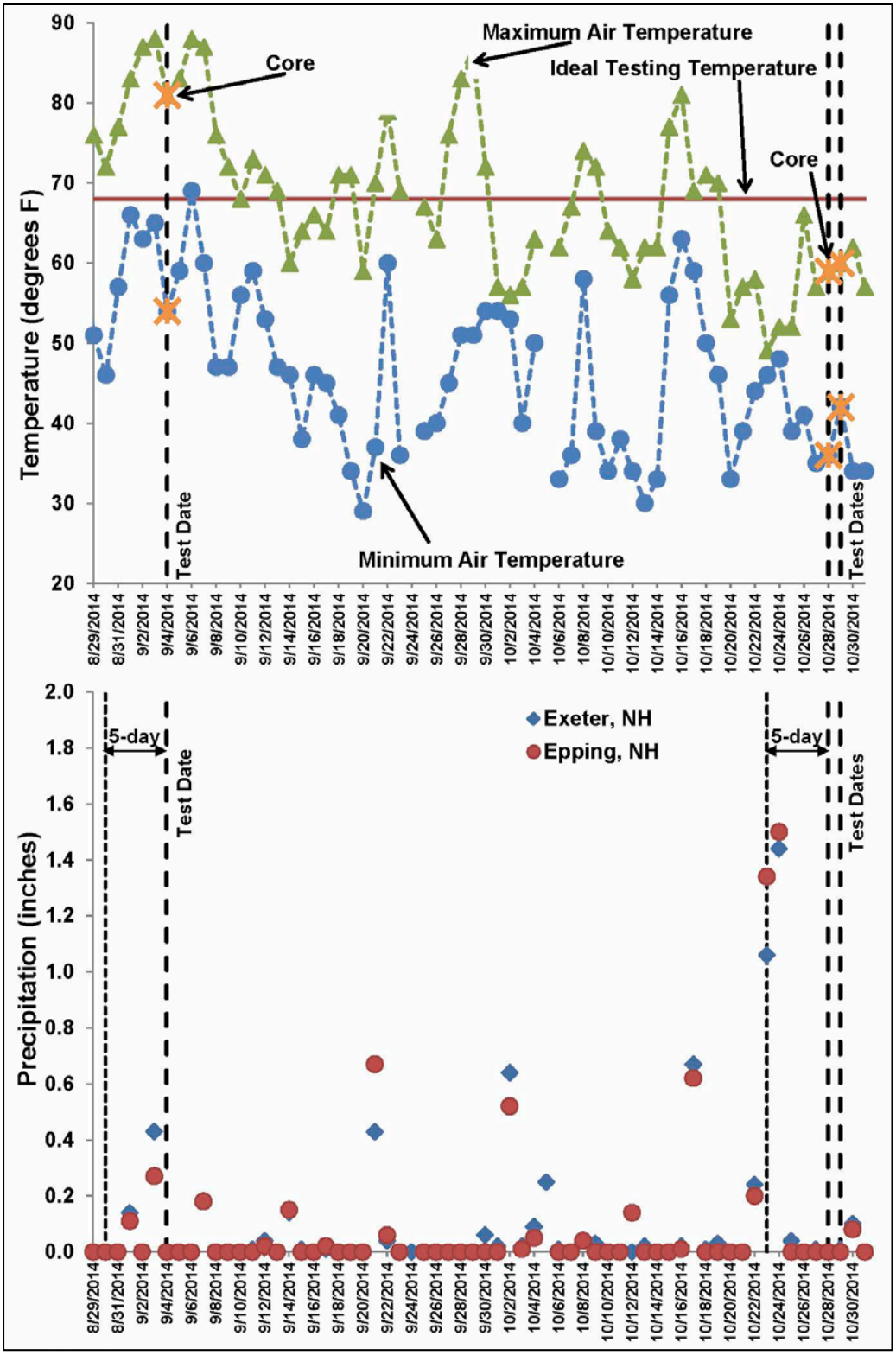

Figure 8. Conditions of the pavement and weather at WB MM 131.5, at 0930 hr on 4 September 2014.

Figure 9. Test section at WB MM 128.0.

Figure 10. Test section drill rig setup at WB MM 128.0 for core hole sampling and geotechnical soil sampling.

Figure 11. At test section WB MM 128.0, removing standing water from the bottom of the core hole prior to dynamic cone penetrometer (DCP) testing.

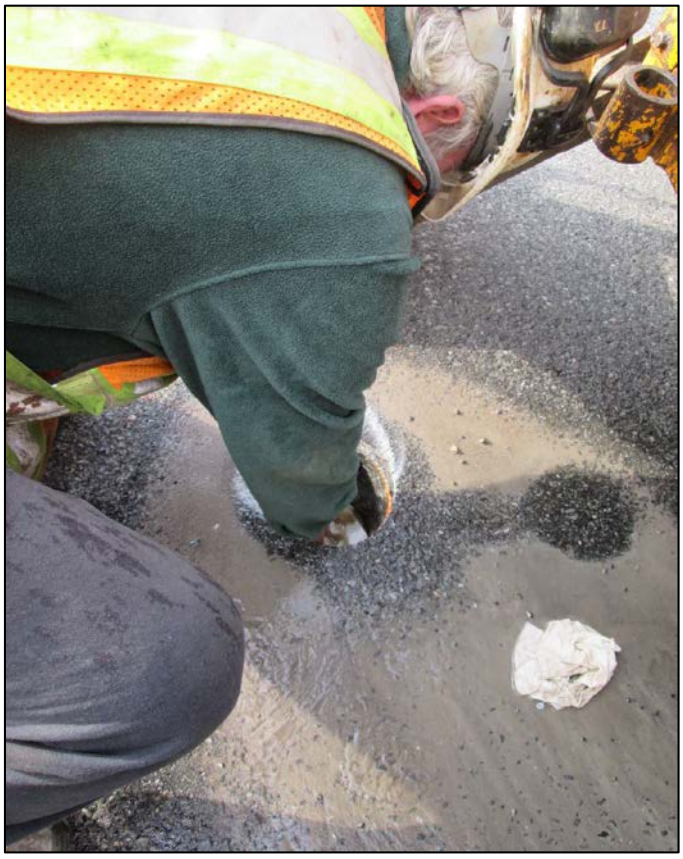

Figure 12. Test section WB MM 128.0 FWD test point locations. The photograph shows the two test points located nearest the core hole: one in the wheel path and six midlane. In this view, the remaining test points continued in the direction of traffic and were spaced approximately 100 ft apart.

Figure 13. Pavement and weather conditions at the start of testing on 29 October 2014. Fog initially delayed testing but lifted by midmorning.

4.3 Test-section layout

Each test section was approximately 500 ft long. Figure 14 shows a sketch of the layout within each test section of the core location and FWD test points. FWD testing was conducted in the direction of traffic, and all test points were located beyond the core location. Five FWD test points were located in the wheel path with the remaining five offset by approximately 3 ft toward the midlane. There was about 100 ft between each FWD test point. The reason for this was to select a representative portion of the pavement as some variability is to be expected. Test points spaced too closely together may not completely represent the section of roadway. Of the six test sections, five were located in the travel lane. WB MM 131.5 was the exception where the test section followed the same layout and number of test points but, for safety reasons, it was located in the passing lane.

Figure 14. Test section layout at all mile markers, except at WB MM 131.5 where testing was conducted in the passing lane.

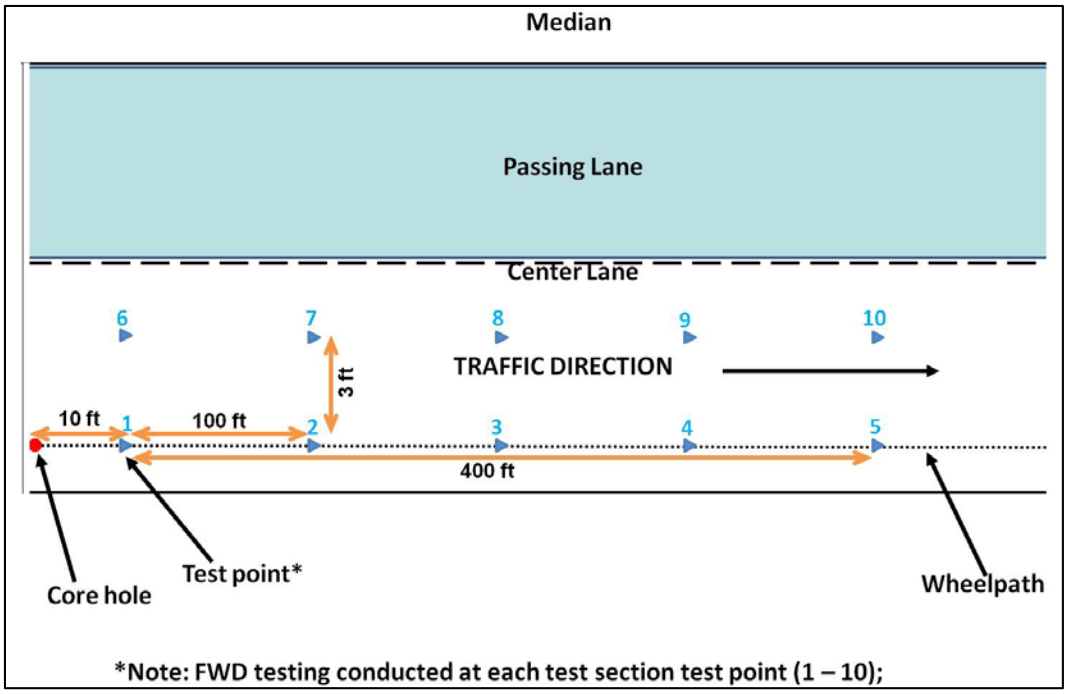

4.4 Testing sequence

Once NHDOT removed the asphalt core from the pavement, CRREL used a sliding drop hammer device to measure the supporting soil strength (described in Section 4.4.1). NHDOT collected soil samples using a split spoon sampler. FWD test points were measured out and marked on the pave-

ment surface. To begin the testing sequence, the FWD was moved into position at the first test point. All five of the test points in the wheel path were completed first (these were test points 1 to 5), then the FWD backed up to test point 6 (midlane nearest to the core hole), and testing continued for test points 6 to 10.

4.4.1 Subsurface soil strength

The strength of the underlying supporting soil layers is needed in flexible pavement evaluation, and it is also used as an input parameter in the back-calculation procedure (Air Force 2002). The dual mass DCP is a sliding drop hammer on a steel rod with a diameter of 5/8 in. (Webster et al. 1992), shown in Figure 15. The tip is a disposable cone with a 60° angle. The equipment is portable and useful for expedient field-testing applications.

To establish the strength, the number of blows needed to penetrate the soil is recorded. Should the rod penetrate less than 1 in. after 25 blows, this is termed refusal; and the test at that location is discontinued. Under normal circumstances when there is sufficient space, another DCP test would be conducted, except the available area within the core hole diameter was too small for the first test not to be a detrimental influence. Relationships based on the blow count and the cumulative depth of the rod penetration are used to estimate the soil strength correlated to the California Bearing Ratio (CBR), as shown in Figure 16. The CBR data is plotted with depth to determine soil strength and the thicknesses of different material layers.

An initial modulus value may be estimated using the soil strength value from the DCP. The relationship to estimate the soil elastic modulus (MPa) for granular soils uses the DCP Index (Doré and Zubeck 2009) and is given in Equation 1:

$$\log(E_{FWD}) = -0.62x\log(DCPIndex) + 2.56 \quad (1)$$

Figure 15. Sketch of the DCP testing equipment (modified from Air Force 2002).

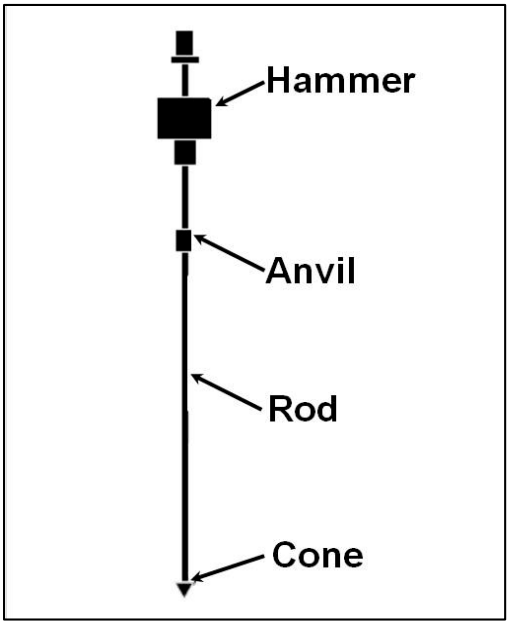

Figure 16. Relationships to determine the soil CBR from the DCP index value (from Air Force 2002).

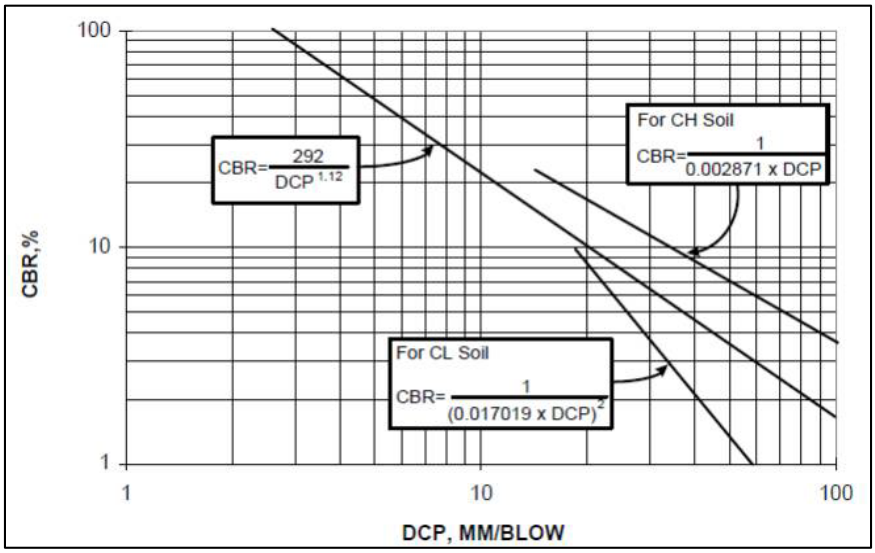

4.4.2 Deflection testing

The Dynatest Model 8000 FWD test apparatus simulates the loading from the wheel of a moving vehicle by imparting an impulse load to the pavement surface and measuring the resulting response of the vertical deflections. The vertical deflections are measured using geophones placed in contact with the pavement surface, oriented radially outward from the point of impact along the load axis. CRREL's FWD equipment setup uses a

total of seven geophones: one at the center of the loading plate and six more spaced 12 in. apart out to a total distance of 72 in. (Figure 17). The impulse load is generated from a set of weights dropped from increasingly greater predetermined heights onto a rubber buffer system connected to a 12 in. diameter segmented load plate set in contact with the pavement surface. In theory, the load should approximate the shape of a haversine or half-sine wave (ASTM 2009; AASHTO 1993). The load level is read by a load cell. CRREL's FWD test equipment is trailer mounted and is towed with a dedicated test vehicle that houses the data-acquisition equipment and ancillary test gear.

Figure 17. Test section WB MM 128.0 FWD testing showing loading plate and proximity of geophone spacing on the pavement surface.

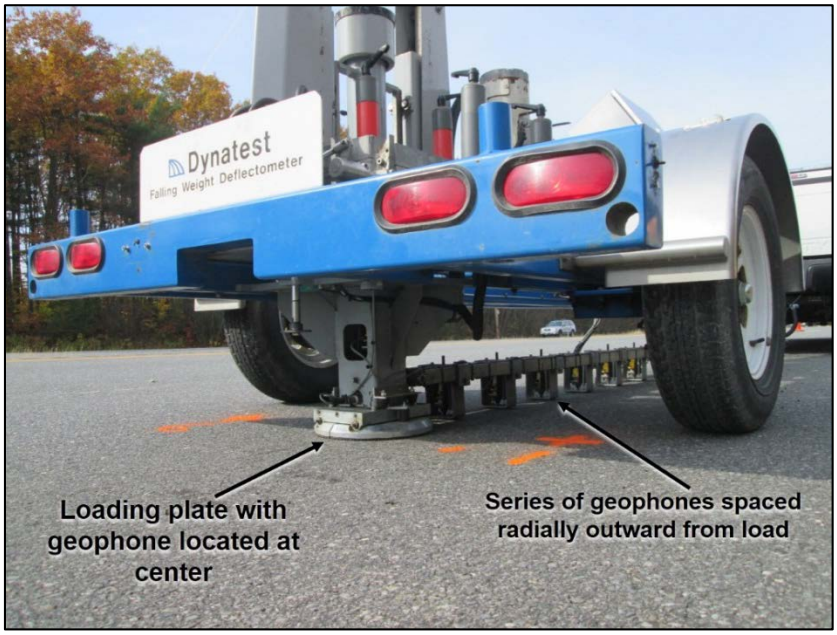

While the FWD is capable of producing controlled load levels, multiple drops are conducted at increasing loads during testing. For testing on NH 101, the target was four drops at four load levels, or a total of 16 drops at each test point. There were ten designated test points within each test section, or a minimum of 160 drops per test section. The four load levels used were 6, 9, 12, and 16 kip. Typically, the first set of four drops at the 6 kip load level is used as a seating load.

At each test point, a cursory check was done of the deflection data. In the event that the deflection readings did not appear reasonable, the test was rerun by moving the vehicle forward approximately 10 ft and repeating the test. Testing was repeated at several locations; this is normal.

5 Data Analysis

5.1 GPS coordinates

NHDOT collected the global positioning system (GPS) coordinates at each core location during the initial site visit in July 2014 (Table 2). We should note that the locations for the field investigation were modified slightly after NHDOT conducted a safety review. EB MM 124.0 was adjusted to 124.2, WB MM 123.2 was adjusted to 123.4, and WB MM 128.4 was adjusted to 128.0.

Table 2. GPS coordinates of proposed core locations collected during initial site visit in July 2014.

Mile Marker	Direction	Easting(X)	Northing(Y)
123.2	E	1164949.77	185558.24
124.0	E	1168649.60	183596.42
128.4	E	1188147.20	174716.24
131.5	W	1202143.11	166920.93
128.4	W	1188181.01	174796.16
123.2	W	1164959.13	185645.40

5.2 Asphalt thickness

The asphalt cores were measured to determine the thickness and depth of the reinforcement grid in the test sections where it was installed. A 6 in. diameter core barrel was used to cut through the asphalt layer. Figures 18 to 23 show photographs of the asphalt core from each test section containing grid reinforcement (labeled). In Figure 18 for EB MM 123.2, the dark line in the photo is where the core broke during transport, this test section did not have grid reinforcement. In the cores that included grid reinforcement, it was difficult to visually see the grid layer embedded in the core. We generally identified by touch where the grid layer was located. Typically, the reinforcing grid was located approximately in the middle of the total asphalt thickness.

Figure 18. Asphalt core for EB MM 123.2 (no grid reinforcement).

Figure 19. Asphalt core for EB MM 124.2. The *solid arrow* indicates the location of grid.

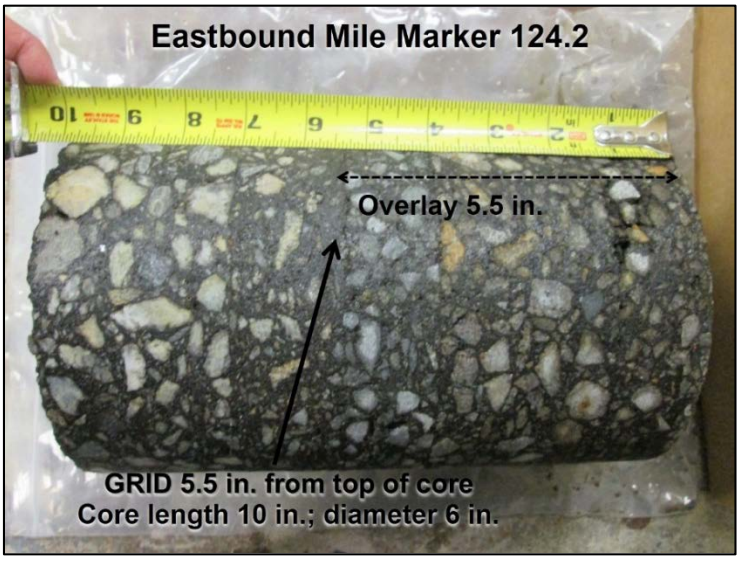

Figure 20. Asphalt core for WB MM 123.4.

Figure 21. Asphalt core for EB MM 128.4.

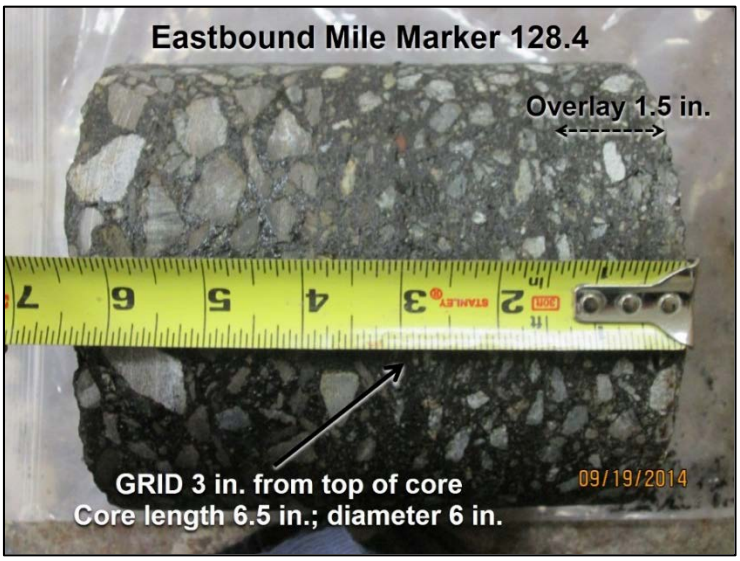

Figure 22. Asphalt core for WB MM 128.0.

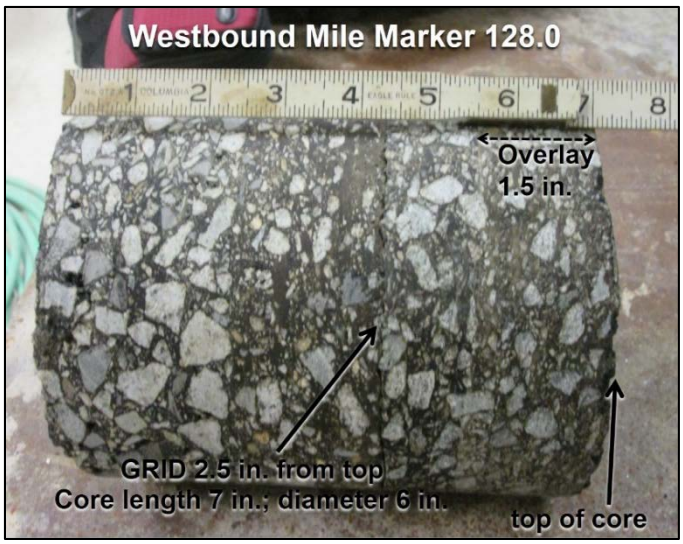

Figure 23. Asphalt core for WB MM 131.5.

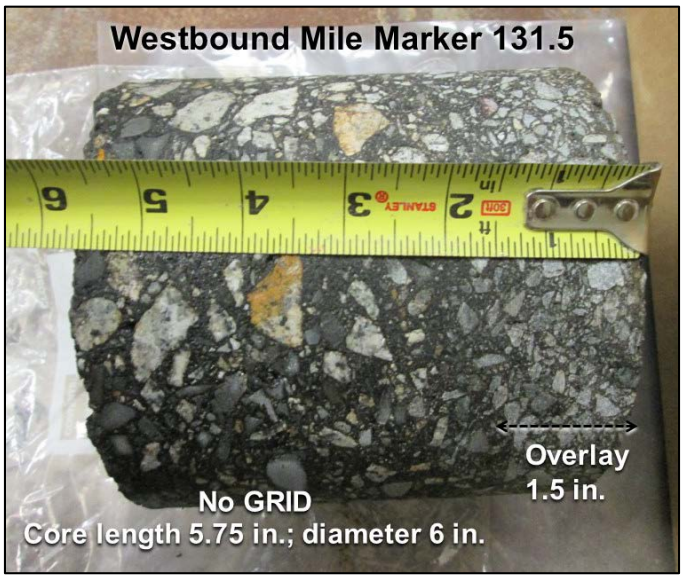

5.3 Subsurface soil strength

In general, the strength of the soil below the asphalt layer was satisfactory. Figures 24 and 25 show the calculated CBR profile values for the thick (approximately 10 in.) and thin (approximately 6 in.) asphalt layers, respectively. In all six test sections, the uppermost 2–4 in. of the base layer below the asphalt layer showed a decrease in strength. This is not uncommon with this test as the readings from the uppermost part of the soil layer tend to be slightly different due to the reduced confinement of the material. Once past this upper layer, the strength consistently reached the maximum 100 CBR, or the equivalent of a crushed limestone material.

The depth of DCP penetration ranged as shallow as 4 in., due to refusal, at the two west test sections of 123.4 and 128.0 and as deep as nearly 28 in. at the west test section 131.5. In general, there was good consistency in the readings at all six test sections.

Figure 24. Subsurface soil strength, shown as the CBR, for the thick (approximately 10 in.) asphalt test sections.

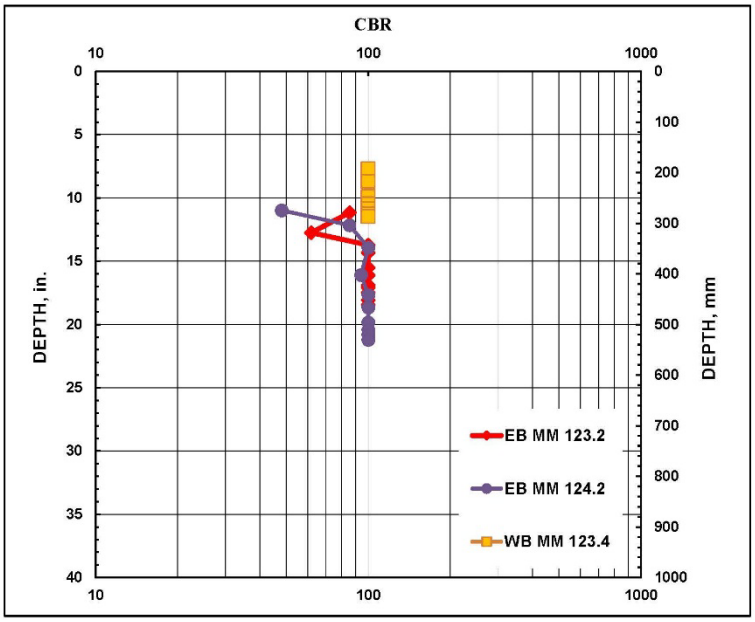

Figure 25. Subsurface soil strength, shown as the CBR, for the thin (approximately 6 in.) asphalt test sections.

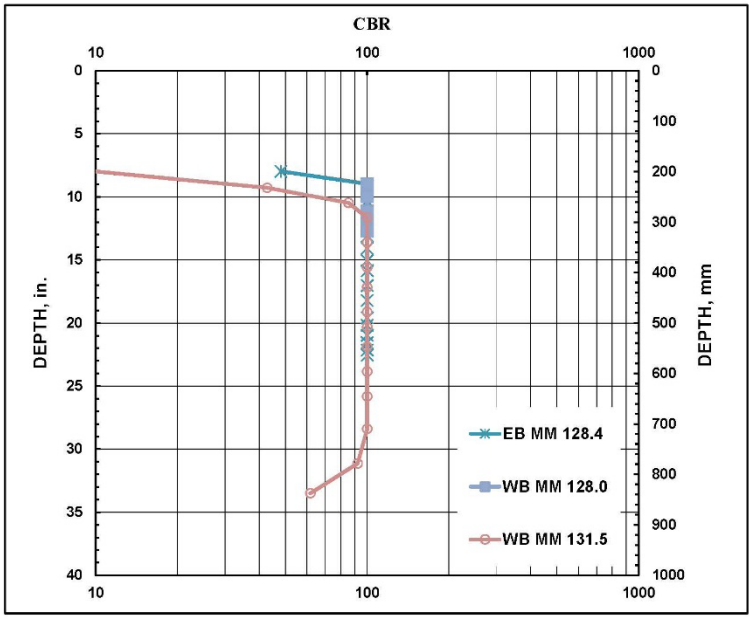

5.4 Soil analysis

NHDOT conducted the laboratory testing to determine the soil type and the moisture content. This information was used to determine the layer thicknesses used in the back-calculation. Testing followed the methods described in AASHTO T 27-14 (2014) and T 11-09 (2009). Figures 26 to 29 give the results of the grain size analysis with soil classification from the cores collected on 4 September 2014. Appendix A provides the test boring logs and laboratory grain size distribution sheets.

Figure 26. Grain size analysis for base and subbase materials at EB MM 123.2 and EB MM 124.2.

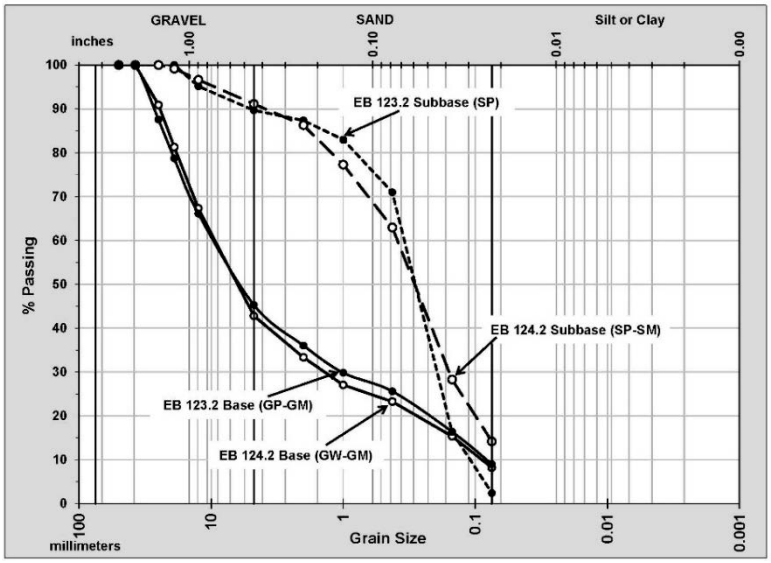

Figure 27. Grain size analysis for subgrade materials at EB MM 123.2 and EB MM 124.2.

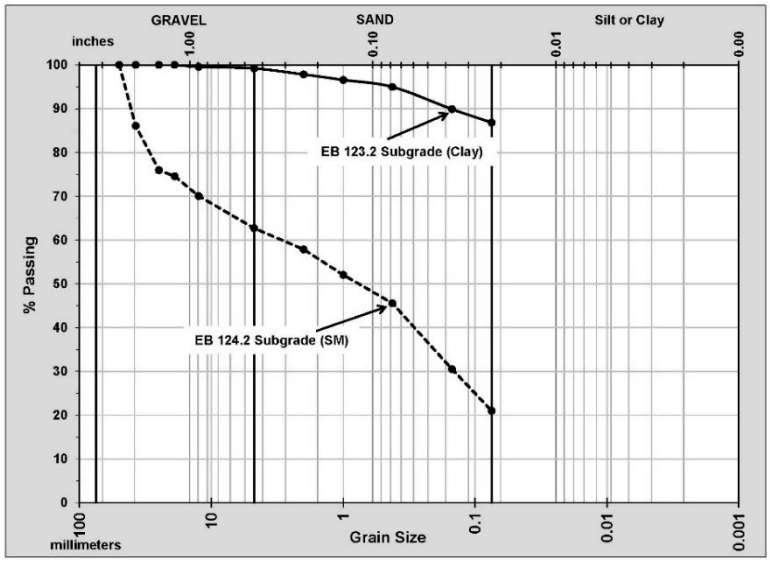

Figure 28. Grain size analysis for base and subbase materials at EB MM 128.4 and WB MM 131.5.

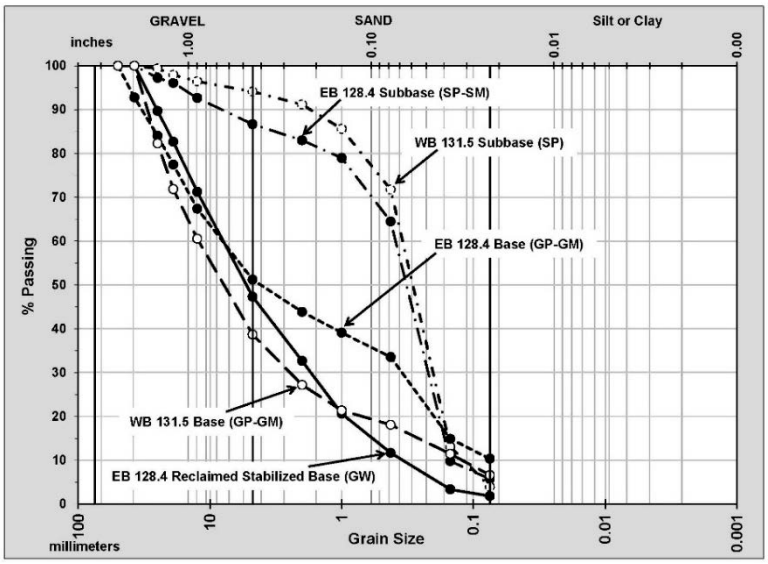

Figure 29. Grain size analysis for subgrade materials at EB MM 128.4 and WB MM 131.5.

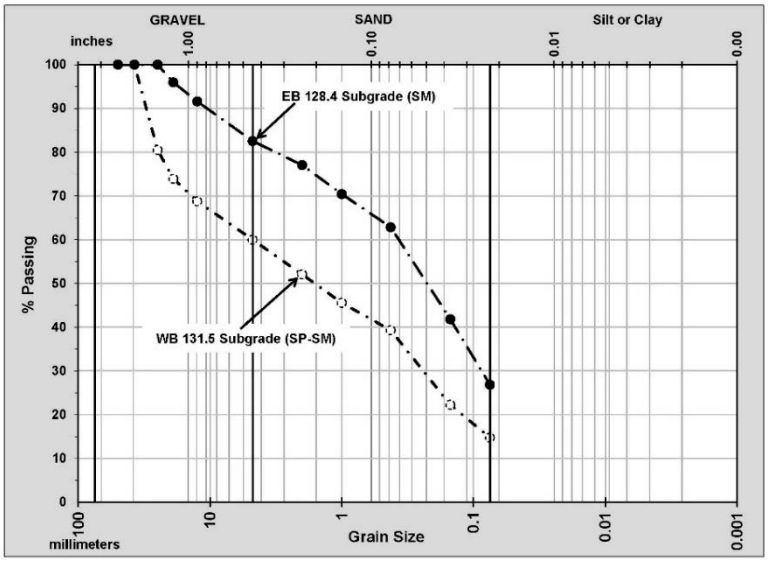

5.5 Deflection data

The measured deflection readings for each test ranged throughout the testing, and the data given in Tables 3 to 8 are for drops 13 to 16 (the highest load level). The raw deflection data were reviewed prior to further analysis confirming that the geophone at d_0 reading responds with the largest deflection measurement and that d_7 (at 72 in.), the geophone furthest away from the load, has the smallest readings with successively decreasing deflection readings between d_0 and d_7. The profile forms a basin, as shown

for test section WB MM 128.0 (Figure 30) at the third drop height (16 kip load level). The numbers 41 through 50 correspond to the test points within this test section. Deflection basins at test points that do not exhibit this pattern were not used in the analysis. Consequently, several test points were not included in Tables 3 through 8. Similarly, the measured deflection readings at the center of the plate are examined for excessive values. Unreasonable values may occur at the center of the plate as a result of the plate not sitting evenly on the pavement surface, or a small stone or piece of debris may be lodged under the plate.

An initial comparison of the measured deflections was made between test sections with grid reinforcement and the corresponding control sections. Figures 31 and 32 are examples of the deflection measurements for the thin and thick asphalt sections, respectively. Each of the deflection readings shown are for the third drop at the 16 kip load level for test points in the wheel path. In the figures, there is no clear difference between the measured deflection from the reinforced and non-reinforced test sections.

In Tables 3 to 8 there are several data points marked with an asterisk. The table note describes this as "data point dropped." At EB MM 123.2 test point 6, the four deflection readings at d_0 (at the center of the plate) at the fourth drop height (16 kip) were unreasonably high. This is seen in the table under the "0" column heading with the deflection readings of 101.37, 64.23, and 74.95 mil. The third set of readings at the fourth drop height were still high but were processed through the back-calculation. At test point 6, only the third drop was used in the calculations; the other readings were not used as the d_0 readings were high. To address any unreasonable deflection readings, we retested by repositioning the FWD forward approximately 10–20 ft, resulting in the fractional test points, such as 6.1, 6.2, etc.

This was similar at EB MM 124.2. The readings at the designated test points (14 and 17) were unreasonable, and the FWD was pulled forward 20 ft and retested at points 14.1 and 17.1.

Figure 30. An example deflection basin from FWD data from WB MM 128.0 comparing the deflections from the third drop resulting from a 16 kip load.

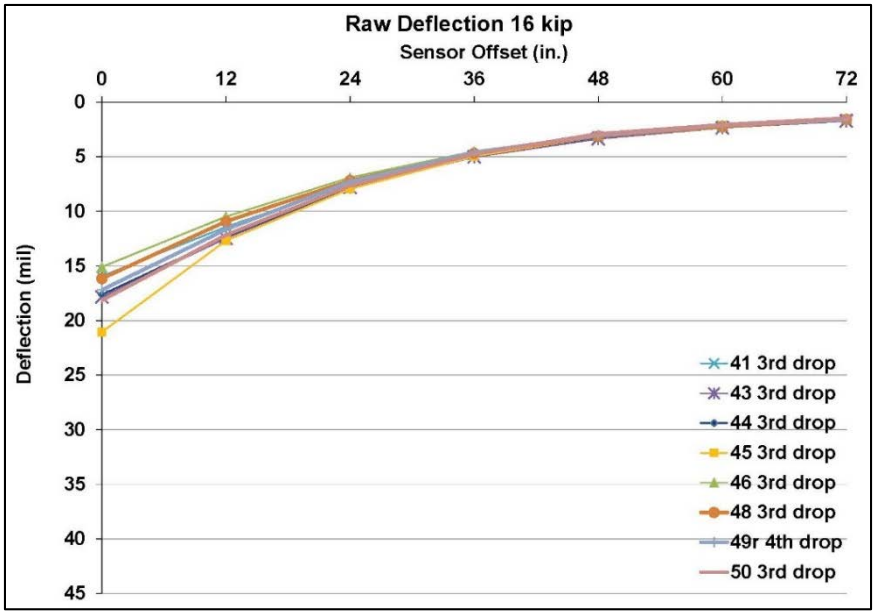

Figure 31. Deflection measurements comparing readings located in the wheel path from grid-reinforced and non-reinforced thin asphalt test sections.

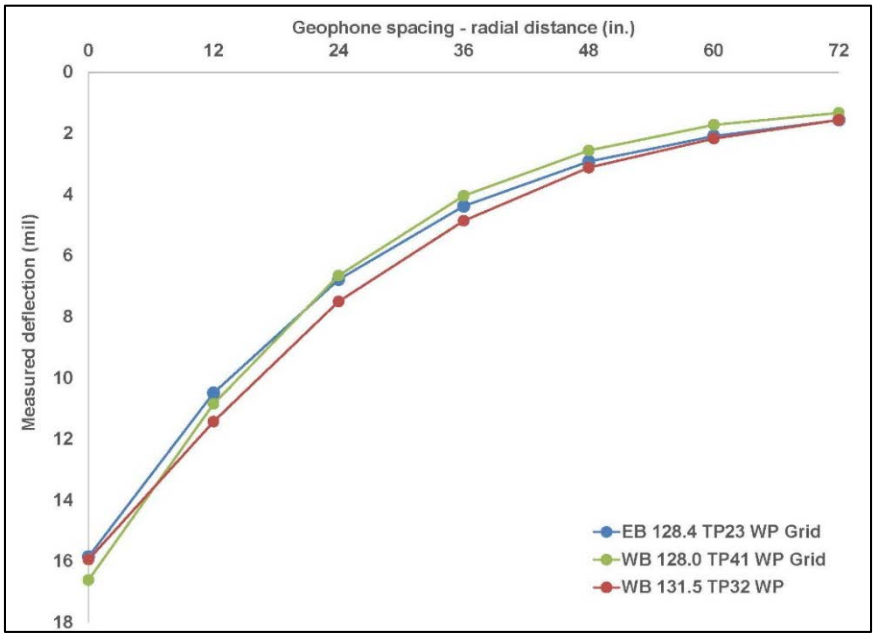

Figure 32. Deflection measurements comparing readings located in the wheel path from grid-reinforced and non-reinforced thick asphalt test sections.

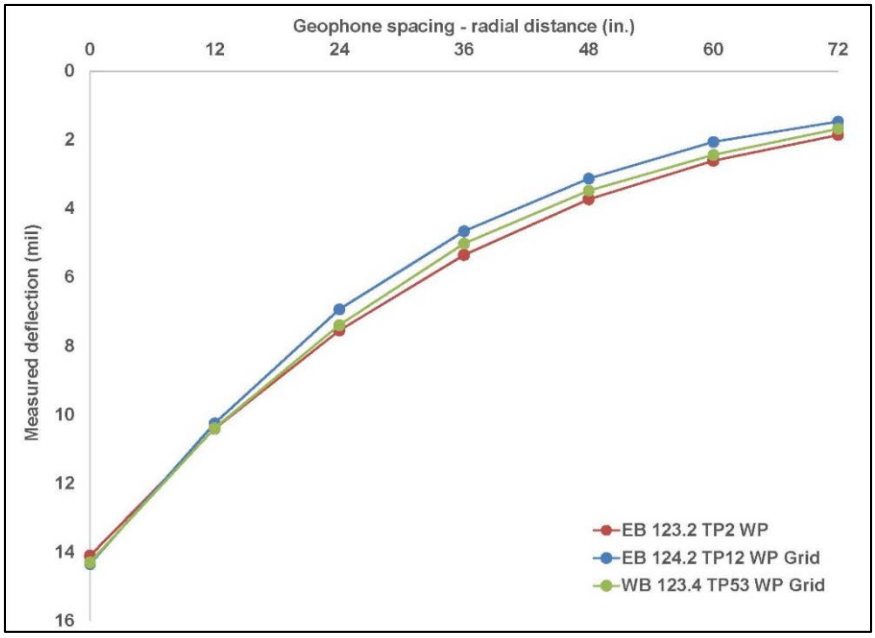

Table 3. Measured deflections for thick asphalt section EB MM 123.2 without reinforcement.

Lane Location	Point	Distance* (ft)	Time	Temperature		Load (lb)	Deflection (mil)							Drop Number
				Pavement (°F)	Air (°F)		0	12	24	36	48	60	72	
WP	1	10	10:40:00	56.7	54	16,501	12.15	8.53	6.13	4.14	2.75	1.91	1.44	13
						16,422	11.97	8.45	6.12	4.12	2.74	1.91	1.43	14
						16,399	11.98	8.44	6.11	4.13	2.74	1.94	1.43	15
						16,388	12.00	8.43	6.09	4.13	2.74	1.94	1.43	16
WP	2	110	10:43:00	56.9	54	16,309	14.48	10.48	7.59	5.37	3.74	2.61	1.83	13
						16,252	14.31	10.41	7.56	5.35	3.72	2.61	1.83	14
						16,229	14.11	10.41	7.55	5.35	3.73	2.61	1.86	15
						16,218	13.98	10.39	7.54	5.34	3.72	2.61	1.85	16
WP	3	210	10:45:00	57	54	16,196	13.89	10.28	7.34	5.20	3.68	2.65	1.99	13
						16,139	13.85	10.20	7.24	5.15	3.65	2.63	1.96	14
						16,128	13.80	10.20	7.26	5.17	3.67	2.67	1.98	15
						16,116	13.73	10.17	7.29	5.18	3.67	2.67	1.98	16
WP	4	310	10:48:00	57.1	54	16,184	12.80	9.04	6.72	4.78	3.16	2.48	1.70	13
						16,150	12.72	9.01	6.67	4.77	3.24	2.45	1.71	14
						16,128	12.85	8.98	6.69	4.76	3.24	2.46	1.74	15
						16,139	12.95	8.99	6.65	4.76	3.24	2.46	1.72	16
WP	5	410	10:50:00	57.2	54	16,173	11.76	7.76	5.56	3.67	2.40	1.54	1.02	13
						16,139	12.06	7.74	5.54	3.67	2.41	1.56	1.03	14
						16,105	11.98	7.72	5.52	3.67	2.41	1.55	1.03	15
						16,071	11.69	7.71	5.50	3.66	2.40	1.55	1.03	16
CL	6	10	10:59:00	57.2	54	16,150	101.37	8.51	6.15	4.28	2.87	2.07	1.56	13†
						16,082	64.23	8.46	6.11	4.25	2.84	2.08	1.55	14†
						16,082	21.53	8.45	6.11	4.26	2.87	2.07	1.57	15
						16,105	74.95	8.46	6.11	4.25	2.85	2.07	1.55	16†
CL	6.1	20	11:02:00	57.5	54	16,105	14.79	8.91	6.37	4.44	2.98	2.03	1.44	13
						16,037	13.56	8.86	6.33	4.43	2.99	2.03	1.45	14
						16,082	12.65	8.85	6.35	4.44	2.98	2.05	1.46	15
						16,071	11.99	8.85	6.33	4.44	2.98	2.03	1.46	16
CL	6.2	30	11:05:00	56.9	56	16,082	11.65	8.83	6.44	4.64	3.22	2.31	1.72	13
						16,105	11.62	8.84	6.40	4.66	3.21	2.33	1.72	14
						16,026	11.63	8.83	6.43	4.65	3.23	2.33	1.74	15
						16,026	11.62	8.80	6.44	4.65	3.24	2.33	1.74	16
CL	6.3	40	11:08:00	56.8	56	16,071	11.34	8.36	6.02	4.25	2.87	2.02	1.49	13
						16,037	11.34	8.31	6.01	4.25	2.88	2.04	1.51	14
						16,015	11.28	8.32	6.00	4.25	2.87	2.04	1.49	15
						15,992	11.31	8.32	6.00	4.24	2.87	2.03	1.48	16
CL	7	110	11:11:00	57.1	56	16,003	12.56	9.81	7.37	5.31	3.69	2.67	1.93	13
						15,958	12.49	9.74	7.33	5.28	3.68	2.64	1.92	14
						15,981	12.49	9.74	7.32	5.29	3.69	2.64	1.94	15
						15,958	12.46	9.76	7.34	5.30	3.69	2.65	1.94	16
CL	8.1	220	0.46944	56.8	56	15,879	14.59	10.76	7.81	5.50	3.87	2.82	2.10	13
						15,856	14.55	10.67	7.80	5.48	3.79	2.80	2.09	14
						15,856	14.46	10.62	7.74	5.45	3.80	2.80	2.08	15
						15,856	14.61	10.62	7.76	5.46	3.76	2.79	2.08	16
CL	9	310	0.47083	57.1	56	15,879	13.22	9.64	6.76	4.82	3.24	2.34	1.77	13
						15,834	13.19	9.59	6.79	4.80	3.28	2.35	1.80	14
						15,811	13.16	9.58	6.78	4.82	3.26	2.39	1.78	15
						15,822	13.14	9.58	6.77	4.83	3.28	2.37	1.80	16
CL	10	410	11:20:00	57	56	15,856	12.40	7.80	5.65	3.77	2.44	1.53	0.98	13
						15,845	11.64	7.77	5.65	3.74	2.43	1.56	1.01	14
						15,834	11.34	7.80	5.65	3.74	2.44	1.55	1.01	15
						15,811	11.11	7.85	5.63	3.76	2.46	1.54	0.98	16

WP = wheel path

CL = center of lane

* Linear distance from the core hole to the test point (following Figure 15)

† Data point dropped—d_0 deflection excessive

Table 4. Measured deflections for thick asphalt section EB MM 124.2 with reinforcement.

Lane Location	Point	Distance* (ft)	Time	Temperature		Load (lb)	Deflection (mil)							Drop Number
				Pavement (°F)	Air (°F)		0	12	24	36	48	60	72	
WP	11	10	11:45:00	57.5	56	16,241	11.58	7.84	5.33	3.58	2.33	1.70	1.02	13
						16,128	11.48	7.81	5.33	3.58	2.43	1.63	1.18	14
						16,082	11.42	7.79	5.32	3.58	2.44	1.63	1.19	15
						16,071	11.43	7.78	5.32	3.58	2.47	1.58	1.23	16
WP	12	110	11:47:00	57.8	56	16,071	14.37	10.30	6.99	4.67	3.07	2.12	1.42	13
						16,026	14.39	10.26	6.95	4.67	3.11	2.10	1.46	14
						15,992	14.35	10.25	6.93	4.66	3.13	2.06	1.47	15
						15,992	14.33	10.25	6.92	4.67	3.11	2.08	1.45	16
WP	13	210	11:50:00	58.2	56	16,026	15.46	11.13	7.41	4.67	2.93	1.85	1.25	13
						15,992	15.40	11.07	7.39	4.66	2.93	1.85	1.29	14
						16,003	15.39	11.07	7.37	4.66	2.92	1.89	1.20	15
						15,947	15.34	11.04	7.35	4.65	2.92	1.87	1.21	16
WP	14	310	11:52:00	58.1	56	16,015	54.22	9.56	6.55	4.28	2.69	1.67	1.20	13†
						15,969	44.53	9.52	6.59	4.30	2.70	1.65	1.24	14†
						15,981	70.11	9.51	6.56	4.29	2.70	1.65	1.24	15†
						15,924	17.93	9.50	6.56	4.28	2.69	1.69	1.19	16
WP	14.1	320	11:57:00	58.3	56	16,015	13.33	9.49	6.48	4.22	2.66	1.70	1.15	13
						15,992	13.34	9.49	6.56	4.24	2.67	1.70	1.15	14
						15,947	13.26	9.48	6.44	4.21	2.67	1.69	1.18	15
						15,947	13.31	9.51	6.46	4.24	2.65	1.69	1.15	16
WP	15	410	11:59:00	58.7	58	15,958	16.07	11.76	8.14	5.38	3.51	2.34	1.65	13
						15,913	15.98	11.74	8.22	5.46	3.46	2.36	1.64	14
						15,901	15.94	11.71	8.20	5.44	3.45	2.34	1.61	15
						15,901	16.01	11.69	8.15	5.40	3.49	2.35	1.66	16
CL	16	10	12:09:00	58.7	58	16,105	9.52	6.34	4.43	2.99	2.07	1.41	1.05	13
						16,071	9.44	6.38	4.43	3.00	2.10	1.42	1.07	14
						16,037	9.39	6.31	4.44	3.00	2.09	1.43	1.07	15
						16,015	9.36	6.32	4.43	3.00	2.10	1.42	1.07	16
CL	17	110	12:12:00	58.7	58	15,969	47.97	8.80	6.33	4.33	2.95	1.98	1.41	13†
						15,890	43.38	8.76	6.32	4.33	2.96	2.01	1.43	14†
						15,879	37.22	8.74	6.29	4.34	2.96	2.02	1.46	15†
						15,856	13.18	8.74	6.28	4.33	2.96	2.00	1.42	16
CL	17.1	120	12:14:00	58.7	58	15,913	11.81	8.71	6.26	4.33	2.95	2.00	1.41	13
						15,856	11.77	8.70	6.27	4.35	2.96	1.99	1.40	14
						15,868	11.78	8.70	6.27	4.34	2.96	2.00	1.44	15
						15,856	11.79	8.68	6.26	4.31	2.94	1.98	1.38	16
CL	18	210	0.51181	58.8	58	15,901	12.55	9.37	6.59	4.47	2.88	1.85	1.28	13
						15,856	12.43	9.30	6.53	4.42	2.82	1.80	1.18	14
						15,822	12.36	9.28	6.54	4.44	2.84	1.83	1.24	15
						15,800	12.35	9.27	6.52	4.40	2.81	1.79	1.17	16
CL	19	310	12:19:00	58.7	58	15,901	12.57	8.62	5.94	3.90	2.54	1.62	1.11	13
						15,845	12.40	8.59	5.91	3.89	2.52	1.62	1.11	14
						15,845	12.39	8.59	5.92	3.90	2.54	1.62	1.08	15
						15,845	12.26	8.58	5.91	3.88	2.52	1.62	1.11	16
CL	20	410	12:29:00	58.8	58	16,015	13.39	10.17	7.35	5.09	3.42	2.31	1.59	13
						15,981	13.34	10.14	7.34	5.09	3.42	2.31	1.59	14
						15,935	13.36	10.09	7.32	5.07	3.41	2.30	1.61	15
						15,969	13.34	10.10	7.32	5.08	3.41	2.30	1.60	16

WP = wheel path

CL = center of lane

* Linear distance from the core hole to the test point (following Figure 15)

† Data point dropped—d_0 deflection excessive

Table 5. Measured deflections for thick asphalt section WB MM 123.4 with reinforcement.

Lane Location	Point	Distance* (ft)	Time	Temperature		Load (lb)	Deflection (mil)							Drop Number
				Pavement (°F)	Air (°F)		0	12	24	36	48	60	72	
WP	51	10	13:26:00	65	61	16,376	15.21	10.86	7.37	4.82	3.15	2.16	1.51	13
						16,309	15.11	10.81	7.34	4.82	3.16	2.17	1.52	14
						16,252	15.02	10.80	7.34	4.77	3.15	2.23	1.50	15
						16,229	15.00	10.79	7.32	4.76	3.13	2.24	1.49	16
WP	52	110	13:33:00	66.1	61	16,275	15.79	11.49	7.76	5.20	3.60	2.48	1.73	13
						16,162	15.67	11.40	7.75	5.19	3.60	2.50	1.80	14
						16,150	15.66	11.40	7.72	5.20	3.62	2.50	1.76	15
						16,082	15.61	11.33	7.72	5.17	3.61	2.48	1.83	16
WP	53	210	13:36:00	66.4	61	16,196	14.44	10.44	7.36	5.05	3.46	2.45	1.70	13
						16,128	14.34	10.41	7.43	5.06	3.50	2.48	1.74	14
						16,082	14.30	10.39	7.39	5.02	3.48	2.44	1.68	15
						16,060	14.27	10.35	7.36	5.01	3.46	2.44	1.68	16
WP	54	310	13:39:00	66.2	61	16,218	27.23	9.15	6.16	3.97	2.57	1.69	1.20	13†
						16,139	15.03	9.11	6.19	3.97	2.62	1.70	1.24	14
						16,094	13.93	9.09	6.15	3.96	2.59	1.71	1.22	15
						16,094	12.90	9.09	6.15	3.94	2.59	1.69	1.24	16
WP	55	410	13:43:00	65.5	61	16,105	14.70	10.77	7.45	4.97	3.32	2.37	1.72	13
						16,060	14.71	10.71	7.46	4.99	3.39	2.38	1.82	14
						16,060	14.68	10.67	7.41	4.95	3.35	2.37	1.72	15
						16,003	14.47	10.66	7.38	4.95	3.39	2.33	1.77	16
CL	56	10	13:47:00	64.6	61	16,048	13.24	9.44	6.63	4.39	2.96	2.11	1.45	13
						15,992	13.08	9.37	6.56	4.37	2.94	2.11	1.44	14
						15,992	13.06	9.31	6.57	4.37	2.91	2.11	1.42	15
						15,958	13.01	9.33	6.54	4.37	2.91	2.10	1.44	16
CL	58	210	0.580556	64.1	61	15,935	13.56	9.65	6.83	4.77	3.32	2.33	1.65	13
						15,879	13.47	9.57	6.79	4.76	3.33	2.34	1.65	14
						15,856	13.45	9.56	6.80	4.76	3.34	2.35	1.66	15
						15,845	13.41	9.56	6.79	4.75	3.32	2.33	1.63	16
CL	60	410	0.588194	64.3	63	15,992	14.68	9.37	6.75	4.75	3.30	2.35	1.69	13
						15,924	14.00	9.50	6.70	4.72	3.30	2.35	1.69	14
						15,924	14.05	9.48	6.71	4.72	3.30	2.36	1.68	15
						15,890	14.14	9.42	6.72	4.72	3.30	2.35	1.67	16

WP = wheel path

CL = center of lane

* Linear distance from the core hole to the test point (following Figure 15)

† Data point dropped—d_0 deflection excessive

Table 6. Measured deflections for thin asphalt section WB MM 131.5 without reinforcement.

Lane Location	Point	Distance* (ft)	Time	Temperature		Load (lb)	Deflection (mil)							Drop Number
				Pavement (°F)	Air (°F)		0	12	24	36	48	60	72	
WP	31	10	14:58:00	61.4	56	16,591	18.30	11.78	6.89	3.96	2.40	1.56	1.19	13
						16,512	18.12	11.68	6.81	3.92	2.38	1.60	1.20	14
						16,490	18.02	11.65	6.80	3.95	2.40	1.59	1.21	15
						16,456	17.93	11.61	6.79	3.93	2.39	1.60	1.21	16
WP	32	110	15:02:00	62	58	16,399	17.12	10.97	6.69	4.05	2.52	1.72	1.27	13
						16,354	16.73	10.87	6.63	4.03	2.52	1.73	1.30	14
						16,331	16.61	10.85	6.65	4.04	2.56	1.72	1.33	15
						16,320	16.51	10.82	6.61	4.03	2.55	1.73	1.33	16
WP	33	210	15:06:00	61.6	58	16,388	15.30	10.69	6.94	4.33	2.79	1.90	1.39	13
						16,297	15.08	10.60	6.85	4.31	2.80	1.91	1.40	14
						16,275	14.96	10.58	6.85	4.30	2.80	1.91	1.40	15
						16,252	14.89	10.56	6.85	4.31	2.80	1.91	1.40	16
WP	34	310	15:09:00	60.9	58	16,196	20.80	13.52	8.06	4.57	2.59	1.71	1.07	13
						16,139	20.33	13.34	7.94	4.54	2.67	1.72	1.16	14
						16,139	20.17	13.29	7.91	4.52	2.61	1.74	1.09	15
						16,139	20.10	13.28	7.93	4.56	2.66	1.75	1.17	16
WP	35	410	15:14:00	61.3	58	16,015	53.75	12.09	6.84	3.88	2.48	1.83	1.28	13†
						16,003	20.52	11.98	6.78	3.89	2.53	1.77	1.38	14
						15,981	20.18	11.94	6.78	3.86	2.49	1.83	1.34	15
						15,958	19.74	11.92	6.78	3.88	2.50	1.84	1.33	16
WP	35.2	430	15:19:00	61.3	58	15,969	18.55	11.52	6.59	3.89	2.52	1.82	1.35	13
						15,981	18.36	11.43	6.55	3.93	2.59	1.84	1.44	14
						15,924	18.19	11.34	6.52	3.83	2.48	1.85	1.38	15
						15,890	18.09	11.36	6.49	3.86	2.50	1.83	1.41	16
CL	36	10	15:23:00	61.3	58	16,343	16.06	10.64	6.31	3.63	2.17	1.41	1.01	13
						16,297	15.92	10.55	6.26	3.61	2.16	1.42	1.02	14
						16,309	15.87	10.52	6.25	3.61	2.17	1.42	1.04	15
						16,275	15.78	10.50	6.24	3.60	2.16	1.41	1.02	16
CL	37	110	15:26:00	61.2	58	16,275	17.57	10.76	6.49	3.83	2.37	1.67	1.16	13
						16,286	16.80	10.70	6.46	3.82	2.39	1.65	1.20	14
						16,241	16.39	10.67	6.44	3.83	2.40	1.65	1.24	15
						16,263	16.22	10.67	6.45	3.83	2.38	1.66	1.21	16
CL	38	210	15:28:00	60.1	58	16,331	14.33	10.04	6.41	3.99	2.54	1.72	1.18	13
						16,297	14.22	10.02	6.38	3.99	2.56	1.73	1.21	14
						16,263	14.17	9.98	6.37	3.98	2.56	1.72	1.22	15
						16,252	14.17	9.98	6.37	3.98	2.54	1.72	1.20	16
CL	39	310	15:31:00	60.4	58	16,105	18.40	12.31	7.29	4.16	2.41	1.51	0.93	13
						16,060	18.20	12.17	7.20	4.13	2.41	1.53	0.91	14
						16,060	18.13	12.13	7.22	4.14	2.44	1.54	0.97	15
						16,071	18.12	12.12	7.20	4.15	2.45	1.54	0.98	16
CL	40	410	15:41:00	61.2	58	16,128	17.94	11.29	6.40	3.75	2.39	1.64	1.23	13
						16,071	17.80	11.15	6.32	3.72	2.40	1.65	1.26	14
						16,037	17.77	11.11	6.31	3.72	2.39	1.65	1.24	15
						16,037	17.75	11.11	6.29	3.71	2.35	1.65	1.24	16

WP = wheel path

CL = center of lane

* Linear distance from the core hole to the test point (following Figure 15)

† Data point dropped—d_0 deflection excessive

Table 7. Measured deflections for thin asphalt section EB MM 128.4 with reinforcement.

Lane Location	Point	Distance* (ft)	Time	Temperature		Load (lb)	Deflection (mil)							Drop Number
				Pavement (°F)	Air (°F)		0	12	24	36	48	60	72	
WP	21	10	13:08:00	61	59	16,343	17.64	11.82	7.50	4.80	3.19	2.28	1.74	13
						16,275	17.48	11.75	7.45	4.77	3.19	2.26	1.76	14
						16,196	17.70	11.72	7.42	4.76	3.20	2.23	1.75	15
						16,196	18.01	11.71	7.46	4.80	3.17	2.39	1.65	16
WP	22	110	13:11:00	61.6	59	16,343	16.38	10.82	7.09	4.65	3.07	2.27	1.72	13
						16,275	16.24	10.86	7.07	4.66	3.00	2.30	1.74	14
						16,275	16.30	10.78	7.04	4.57	3.18	2.26	1.73	15
						16,252	16.16	10.79	7.05	4.60	3.13	2.28	1.74	16
WP	23	210	13:14:00	61.2	59	16,343	15.97	10.57	6.80	4.38	2.92	2.06	1.57	13
						16,309	15.92	10.52	6.78	4.37	2.93	2.06	1.57	14
						16,275	15.85	10.49	6.78	4.38	2.92	2.09	1.56	15
						16,286	15.83	10.49	6.79	4.38	2.91	2.10	1.56	16
WP	24	310	13:16:00	61.2	59	16,173	15.57	10.45	6.75	4.41	2.98	2.17	1.65	13
						16,196	15.52	10.45	6.78	4.44	3.07	2.14	1.71	14
						16,173	15.50	10.45	6.78	4.44	3.02	2.19	1.66	15
						16,128	15.43	10.43	6.76	4.43	3.01	2.19	1.65	16
WP	25.2	430	13:24:00	61.3	59	16,060	15.44	10.30	6.78	4.56	3.15	2.26	1.74	13
						15,992	15.25	10.27	6.78	4.56	3.17	2.29	1.76	14
						15,981	15.17	10.24	6.76	4.57	3.17	2.29	1.76	15
						16,003	15.15	10.24	6.77	4.57	3.17	2.29	1.76	16
WP	25.4	450	13:29:00	61.3	59	15,868	14.29	10.20	7.04	4.84	3.44	2.52	1.95	13
						15,834	14.26	10.19	7.00	4.83	3.44	2.51	1.95	14
						15,811	14.25	10.14	7.01	4.83	3.43	2.54	1.93	15
						15,822	14.24	10.16	7.03	4.85	3.44	2.54	1.94	16
CL	26.1	20	13:37:00	62	59	15,935	15.25	10.13	6.58	4.24	2.86	1.97	1.48	13
						15,913	15.21	10.11	6.57	4.24	2.87	1.97	1.49	14
						15,890	15.17	10.08	6.57	4.26	2.83	2.01	1.48	15
						15,890	15.17	10.07	6.57	4.26	2.84	2.00	1.49	16
CL	27	110	13:40:00	62.6	59	15,788	15.11	10.10	6.61	4.36	2.97	2.11	1.57	13
						15,754	14.99	10.05	6.58	4.36	2.98	2.12	1.59	14
						15,766	14.98	10.02	6.60	4.38	2.98	2.13	1.57	15
						15,721	14.94	10.01	6.58	4.36	2.98	2.12	1.57	16
CL	28	210	13:43:00	62.8	59	15,935	14.81	10.03	6.57	4.28	2.86	2.00	1.53	13
						15,935	14.78	10.01	6.57	4.29	2.85	2.02	1.51	14
						15,890	14.68	10.00	6.56	4.29	2.86	2.02	1.50	15
						15,890	14.67	9.99	6.56	4.28	2.86	2.01	1.51	16
CL	29.1	320	13:49:00	62.2	61	15,958	14.71	9.74	6.38	4.16	2.81	2.00	1.55	13
						15,924	14.63	9.72	6.39	4.16	2.81	2.01	1.56	14
						15,901	14.59	9.70	6.36	4.15	2.81	2.01	1.56	15
						15,890	14.48	9.72	6.40	4.17	2.81	2.01	1.56	16
CL	30	410	13:53:00	62.2	61	15,913	13.75	9.59	6.52	4.52	3.24	2.34	1.82	13
						15,901	13.69	9.57	6.52	4.53	3.24	2.37	1.84	14
						15,868	13.53	9.50	6.50	4.51	3.22	2.35	1.82	15
						15,879	13.68	9.55	6.52	4.53	3.24	2.39	1.82	16

WP = wheel path

CL = center of lane

* Linear distance from the core hole to the test point (following Figure 15)

† Data point dropped—d_0 deflection excessive

Table 8. Measured deflections for thin asphalt section WB MM 128.0 with reinforcement.

Lane Location	Point	Distance* (ft)	Time	Temperature		Load (lb)	Deflection (mil)							Drop Number
				Pavement (°F)	Air (°F)		0	12	24	36	48	60	72	
WP	41	10	11:22:00	57.8	54	15,766	16.17	11.52	7.54	4.91	3.08	2.25	1.49	13
						15,709	16.02	11.47	7.51	4.85	3.17	2.15	1.57	14
						15,732	15.94	11.43	7.50	4.86	3.12	2.17	1.56	15
						15,732	15.96	11.46	7.50	4.87	3.14	2.20	1.55	16
WP	43	210	11:36:00	59.4	54	16,162	18.03	12.56	7.86	5.03	3.33	2.33	1.72	13
						16,105	17.89	12.50	7.82	5.02	3.33	2.34	1.74	14
						16,094	17.85	12.46	7.80	5.02	3.35	2.34	1.73	15
						16,094	17.81	12.43	7.78	5.00	3.32	2.33	1.74	16
WP	44	310	11:39:00	59.6	54	16,105	17.67	12.45	7.88	4.95	3.19	2.20	1.59	13
						16,037	17.54	12.36	7.83	4.94	3.21	2.19	1.61	14
						16,026	17.63	12.33	7.82	4.94	3.21	2.20	1.62	15
						16,026	17.69	12.30	7.80	4.93	3.22	2.21	1.63	16
CL	46	10	11:54:00	60.6	54	16,275	15.27	10.61	7.02	4.56	3.01	2.00	1.53	13
						16,241	15.13	10.52	6.98	4.53	3.00	2.04	1.49	14
						16,241	15.10	10.49	6.91	4.51	3.00	2.07	1.48	15
						16,218	15.11	10.48	6.98	4.53	3.01	2.00	1.54	16
CL	48	210	12:01:00	61.1	56	16,218	16.32	11.05	7.24	4.71	3.11	2.22	1.61	13
						16,082	16.14	10.92	7.16	4.68	3.12	2.22	1.62	14
						16,162	16.16	10.93	7.19	4.69	3.11	2.26	1.59	15
						16,150	16.10	10.89	7.14	4.68	3.12	2.24	1.63	16
CL	49.1	315	12:06:00	62.3	56	16,082	17.33	11.93	7.40	4.63	3.02	2.11	1.52	13
						16,048	17.20	11.85	7.33	4.60	3.00	2.11	1.50	14
						16,026	17.20	11.67	7.30	4.61	3.03	2.12	1.58	15
						16,015	17.08	11.63	7.28	4.59	3.02	2.12	1.58	16
CL	50	410	12:08:00	62.3	56	16,116	18.91	12.41	7.76	4.86	2.95	2.11	1.48	13
						16,026	18.29	12.20	7.69	4.76	2.93	2.04	1.45	14
						16,048	18.15	12.17	7.65	4.76	2.91	2.07	1.46	15
						16,037	18.09	12.18	7.64	4.78	2.93	2.06	1.46	16

WP = wheel path

CL = center of lane

* Linear distance from the core hole to the test point (following Figure 15)

5.5.1 Basin area

As described above, the response of the deflection measurements forms a pattern, or a basin. The basin area is a fundamental parameter calculated from the deflection data (Horak 1987), and Equation 2 gives the approach used by DOD (2001).

$$Area = \frac{1}{2} x\left(Deflection_n + Deflection_{n+1}\right) x\left(SensorOffset_{n+1} - SensorOffset_n\right) \quad (2)$$

In Equation 2, the x-axis is used to determine the sensor offset distance while the y-axis determines the deflection measurement. The shape between each sensor spacing is assumed to be trapezoidal. Figure 33 illus-

trates this (DOD 2001). This calculation was performed using the measured deflection readings to see if there was subtle, but clear, distinction between the basin areas with grid reinforcement and the control test sections. Figures 34 and 35 show the calculated basin area for the thin and thick asphalt test sections as a function of the distance from the core hole. Similar to the measured deflection readings, no clear trend was present between grid and control sections.

Figure 33. The calculation for the basin area (DOD 2001).

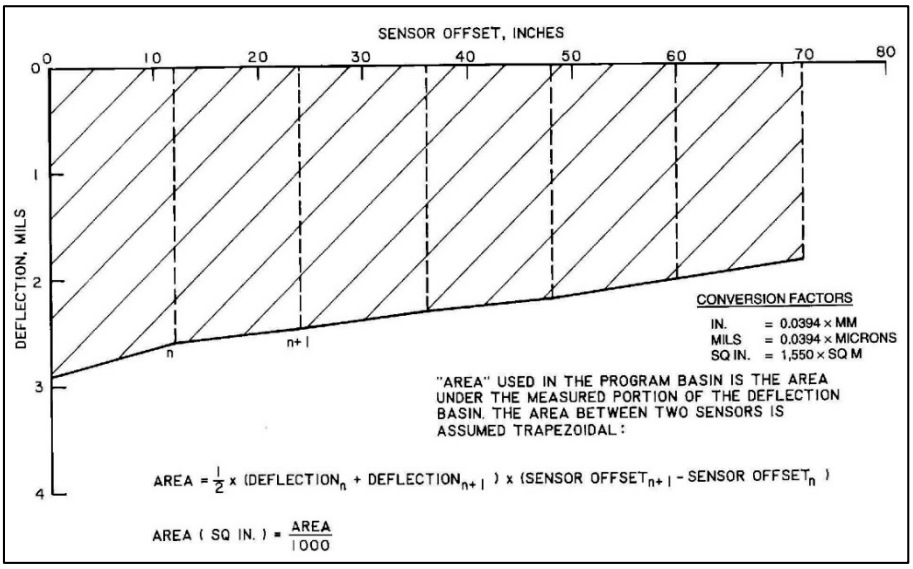

Figure 34. The calculated basin area using measured deflections for thin asphalt test sections.

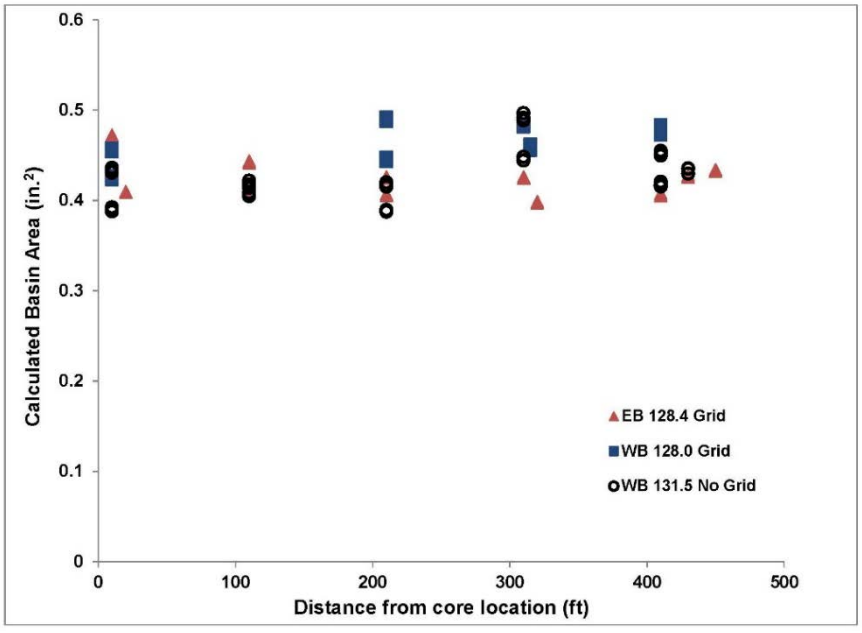

Figure 35. The calculated basin area using measured deflections for thick asphalt test sections.

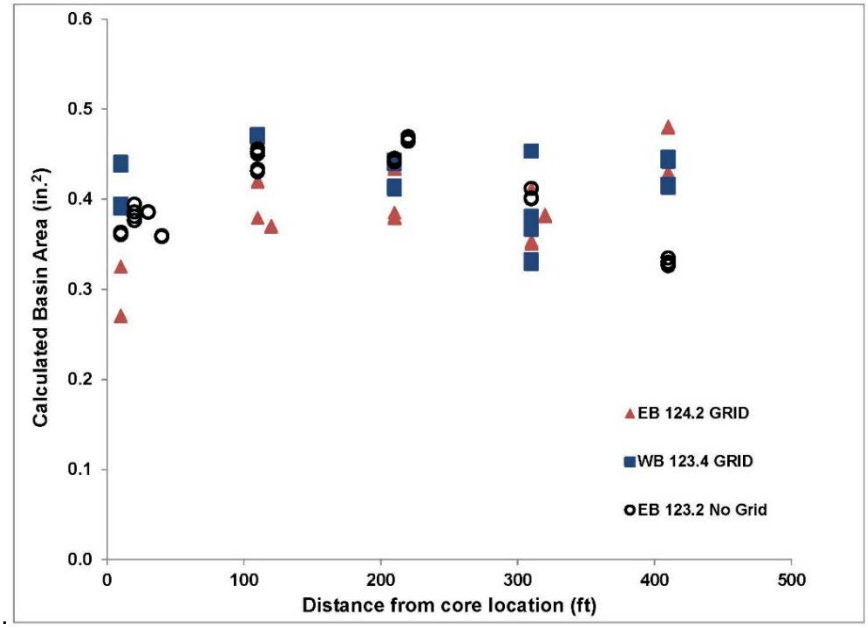

5.5.2 Impulse Stiffness Modulus

The Impulse Stiffness Modulus (ISM) provides a qualitative stiffness and compares similar structural characteristics between the test points within each test section and between all of the test sections (DOD 2001). The ISM is the load (kip) divided by the center deflection (inches) (Equation 3). The ISM was calculated for each test section. When plotted, the ISM identifies inconsistencies between test points and pavement sections.

$$ISM = \frac{load\,(kips)}{d_0\,(inches)} \tag{3}$$

The plots in Figures 36 and 37 show the calculated ISM for the thick and thin test sections as a function of linear distance from the core hole and compare the test points to the average, minimum, and maximum values. The calculations used the values from only the four drops at the highest load level (16 kip load).

Figure 35 suggests that the calculated ISM values were essentially the same for locations containing grid reinforcement as for locations without grid reinforcement. There is some scatter in the ISM values, but this is expected and is considered within reasonable limits. As shown in Figures 36 and 37, the average ISM value for the thinner pavement was 912 kip/in.

whereas for the thicker pavement it was 1170 kip/in. In general, the ISM values for the thicker pavements were slightly higher than those for the thinner pavement sections. A higher stiffness modulus would be consistent with a thicker asphalt layer. No clear relationship is present in the ISM values between test section with reinforcing grid and the control sections.

Figure 36. Comparison of ISM values for all test points within the approximately 10 in. thick pavement sections.

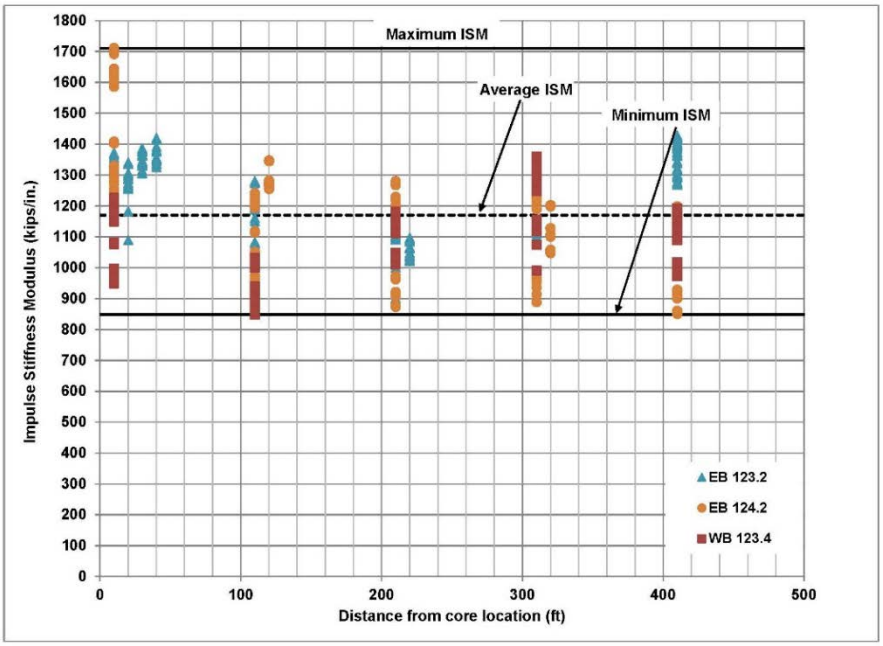

Figure 37. Comparison of ISM values for all test points within the approximately 6 in. thick pavement sections.

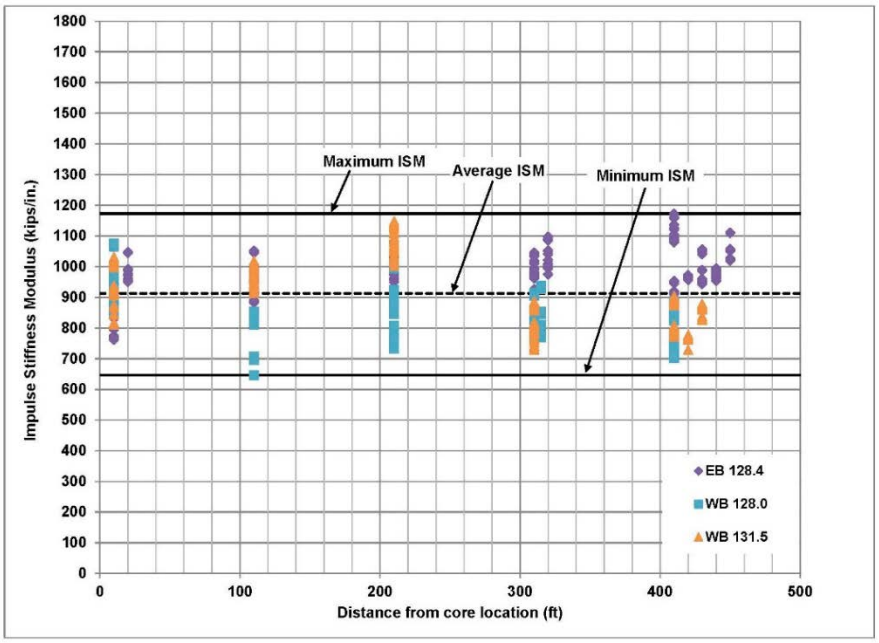

5.5.1 Radius of curvature

Another parameter that may be determined using the deflection measurements is the radius of curvature (R). This value describes the structural state of the base layer (Horak 1987; Doré and Zubeck 2009). Equation 4 shows this calculation (Doré and Zubeck 2009).

$$R = \frac{(d_0 - d_x)^2 + a^2}{2(d_0 - d_x)} \cong \frac{a^2}{2(d_0 - d_x)} \quad (4)$$

where d_x is the deflection measurement (in millimeters) obtained from the sensor outside of the loading plate and a is the loading plate radius in millimeters. The radius of curvature was calculated for each test point for both the thick and thin asphalt test sections. The deflection at the center of the plate was designated as d_0, and the value from d_1 was the sensor spaced 12 in. away. The results were plotted as a function of the linear distance in the test section (Figures 38 and 39).

The radius of curvature values for the thicker asphalt test sections were higher than that of the thin asphalt sections. Some difference in the radius of curvature value would be expected given the different asphalt thicknesses. There is a good amount of scatter in the calculated value, and no clear trend emerges to differentiate between the test sections with grid reinforcement and those without for either asphalt thickness.

Figure 38. The calculated radius of curvature for test points in the thick (10 in.) asphalt test sections.

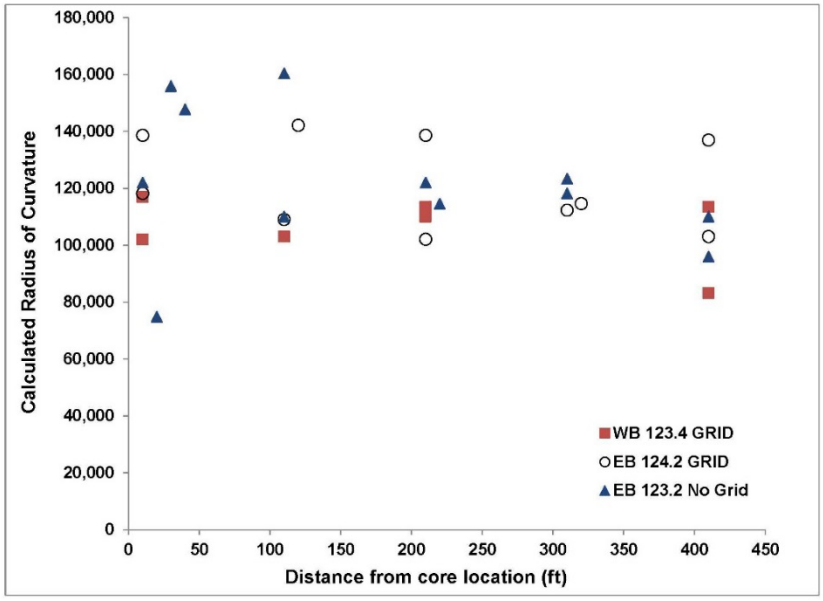

Figure 39. The calculated radius of curvature for test points in the thin (6 in.) asphalt test sections.

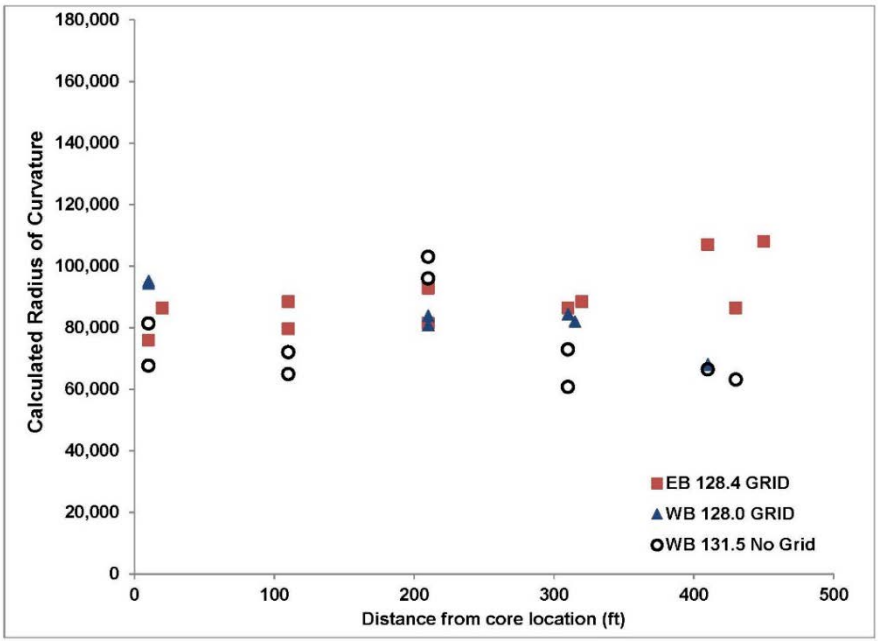

5.5.2 Normalized deflection readings

Consistent with DOD (2001) pavement evaluation procedures, the deflection data was then normalized to a common load. As the target load level was 16,000 lb, this was the load to which the deflections were normalized. It is common during FWD testing for the load to vary slightly for each drop. Normalizing the deflection data to a common load removes this variability. A load ratio is determined by dividing the common load by the load value for each deflection reading. Each measured deflection reading is then multiplied by the load ratio. Tables 9–11 gives the normalized deflections for the thin asphalt sections, and Tables 12–14 gives those for the thick asphalt sections.

The ISM was recalculated using the normalized deflection data. The test points selected were distances common to the test sections of similar thicknesses (or all similar distances for the thin asphalt test sections and the thick asphalt test sections). The ISM was then plotted against the test point number. Figures 40 and 41 show the results. Note in the thin asphalt test section a distinct upward trend for the test sections EB MM 128.4 and WB MM 128.0; both test sections had grid reinforcement. In test section WB MM 128.0, the trend is downward for the latter test points. An explanation of the reason for the trend is unclear; but compared to test section WB MM 131.5 without grid reinforcement, this is the first indication of a

difference in the values. However, the trend did not continue for the thick asphalt test sections. There remained a great deal of scatter in the ISM value for the grid reinforced sections and the control.

Table 9. Normalized deflections for thin asphalt section EB MM 128.4 (grid).

Test Section	Test Point	Drop Number	Deflection (mil)							Calculated ISM
			Sensor Number							
			D0	D1	D2	D3	D4	D5	D6	
			Sensor Offset (in.)							
			0	12	24	36	48	60	72	
EB MM 128.4	21	13	18.02	12.07	7.66	4.90	3.26	2.33	1.78	888
	21	14	17.78	11.95	7.58	4.85	3.24	2.30	1.79	900
	21	15	17.92	11.86	7.51	4.82	3.24	2.26	1.77	893
	21	16	18.23	11.85	7.55	4.86	3.21	2.42	1.67	878
	23	13	16.31	10.80	6.95	4.47	2.98	2.10	1.60	981
	23	14	16.23	10.72	6.91	4.45	2.99	2.10	1.60	986
	23	15	16.12	10.67	6.90	4.46	2.97	2.13	1.59	992
	23	16	16.11	10.68	6.91	4.46	2.96	2.14	1.59	993
	24	13	15.74	10.56	6.82	4.46	3.01	2.19	1.67	1017
	24	14	15.71	10.58	6.86	4.49	3.11	2.17	1.73	1018
	24	15	15.67	10.56	6.85	4.49	3.05	2.21	1.68	1021
	24	16	15.55	10.51	6.81	4.47	3.03	2.21	1.66	1029
	26.1	13	15.19	10.09	6.55	4.22	2.85	1.96	1.47	1053
	26.1	14	15.13	10.06	6.53	4.22	2.85	1.96	1.48	1058
	26.1	15	15.07	10.01	6.52	4.23	2.81	2.00	1.47	1062
	26.1	16	15.07	10.00	6.52	4.23	2.82	1.99	1.48	1062
	28	13	14.75	9.99	6.54	4.26	2.85	1.99	1.52	1085
	28	14	14.72	9.97	6.54	4.27	2.84	2.01	1.50	1087
	28	15	14.58	9.93	6.51	4.26	2.84	2.01	1.49	1097
	28	16	14.57	9.92	6.51	4.25	2.84	2.00	1.50	1098
	29.1	13	14.67	9.71	6.36	4.15	2.80	1.99	1.55	1091
	29.1	14	14.56	9.67	6.36	4.14	2.80	2.00	1.55	1099
	29.1	15	14.50	9.64	6.32	4.12	2.79	2.00	1.55	1103
	29.1	16	14.38	9.65	6.36	4.14	2.79	2.00	1.55	1113
	30	13	13.68	9.54	6.48	4.50	3.22	2.33	1.81	1170
	30	14	13.61	9.51	6.48	4.50	3.22	2.36	1.83	1176
	30	15	13.42	9.42	6.45	4.47	3.19	2.33	1.80	1192
	30	16	13.58	9.48	6.47	4.50	3.22	2.37	1.81	1179

Table 10. Normalized deflections for thin asphalt section WB MM 128.0 (grid).

Test Section	Test Point	Drop Number	Deflection (mil)							Calculated ISM
			Sensor Number							
			D0	D1	D2	D3	D4	D5	D6	
			Sensor Offset (in.)							
			0	12	24	36	48	60	72	
WB MM 128.0	41	13	15.93	11.35	7.43	4.84	3.03	2.22	1.47	1004
	41	14	15.73	11.26	7.37	4.76	3.11	2.11	1.54	1017
	41	15	15.67	11.24	7.37	4.78	3.07	2.13	1.53	1021
	41	16	15.69	11.27	7.37	4.79	3.09	2.16	1.52	1020
	43	13	18.21	12.69	7.94	5.08	3.36	2.35	1.74	879
	43	14	18.01	12.58	7.87	5.05	3.35	2.36	1.75	889
	43	15	17.95	12.53	7.85	5.05	3.37	2.35	1.74	891
	43	16	17.91	12.50	7.83	5.03	3.34	2.34	1.75	893
	44	13	17.79	12.53	7.93	4.98	3.21	2.21	1.60	900
	44	14	17.58	12.39	7.85	4.95	3.22	2.20	1.61	910
	44	15	17.66	12.35	7.83	4.95	3.22	2.20	1.62	906
	44	16	17.72	12.32	7.81	4.94	3.23	2.21	1.63	903
	46	13	15.53	10.79	7.14	4.64	3.06	2.03	1.56	1030
	46	14	15.36	10.68	7.09	4.60	3.05	2.07	1.51	1042
	46	15	15.33	10.65	7.01	4.58	3.05	2.10	1.50	1044
	46	16	15.32	10.62	7.08	4.59	3.05	2.03	1.56	1045
	48	13	16.54	11.20	7.34	4.77	3.15	2.25	1.63	967
	48	14	16.22	10.98	7.20	4.70	3.14	2.23	1.63	986
	48	15	16.32	11.04	7.26	4.74	3.14	2.28	1.61	980
	48	16	16.25	10.99	7.21	4.72	3.15	2.26	1.65	985
	49.1	13	17.42	11.99	7.44	4.65	3.04	2.12	1.53	919
	49.1	14	17.25	11.89	7.35	4.61	3.01	2.12	1.50	927
	49.1	15	17.23	11.69	7.31	4.62	3.03	2.12	1.58	929
	49.1	16	17.10	11.64	7.29	4.59	3.02	2.12	1.58	936
	50	13	19.05	12.50	7.82	4.90	2.97	2.13	1.49	840
	50	14	18.32	12.22	7.70	4.77	2.93	2.04	1.45	873
	50	15	18.20	12.21	7.67	4.77	2.92	2.08	1.46	879
	50	16	18.13	12.21	7.66	4.79	2.94	2.06	1.46	882

Table 11. Normalized deflections for thin asphalt section WB MM 131.5 (no grid).

Test Section	Test Point	Drop Number	Deflection (mil)							Calculated ISM
			Sensor Number							
			D0	D1	D2	D3	D4	D5	D6	
			Sensor Offset (in.)							
			0	12	24	36	48	60	72	
WB MM 131.5	31	13	18.98	12.22	7.14	4.11	2.49	1.62	1.23	843
	31	14	18.70	12.05	7.03	4.05	2.46	1.65	1.24	856
	31	15	18.57	12.01	7.01	4.07	2.47	1.64	1.25	862
	31	16	18.44	11.94	6.98	4.04	2.46	1.65	1.24	868
	33	13	15.67	10.95	7.11	4.44	2.86	1.95	1.42	1021
	33	14	15.36	10.80	6.98	4.39	2.85	1.95	1.43	1042
	33	15	15.22	10.76	6.97	4.37	2.85	1.94	1.42	1051
	33	16	15.12	10.73	6.96	4.38	2.84	1.94	1.42	1058
	34	13	21.05	13.69	8.16	4.63	2.62	1.73	1.08	760
	34	14	20.51	13.46	8.01	4.58	2.69	1.73	1.17	780
	34	15	20.35	13.41	7.98	4.56	2.63	1.76	1.10	786
	34	16	20.27	13.40	8.00	4.60	2.68	1.77	1.18	789
	36	13	16.40	10.87	6.45	3.71	2.22	1.44	1.03	975
	36	14	16.22	10.75	6.38	3.68	2.20	1.45	1.04	987
	36	15	16.18	10.72	6.37	3.68	2.21	1.45	1.06	989
	36	16	16.05	10.68	6.35	3.66	2.20	1.43	1.04	997
	38	13	14.63	10.25	6.54	4.07	2.59	1.76	1.20	1094
	38	14	14.48	10.21	6.50	4.06	2.61	1.76	1.23	1105
	38	15	14.40	10.14	6.47	4.05	2.60	1.75	1.24	1111
	38	16	14.39	10.14	6.47	4.04	2.58	1.75	1.22	1112
	39	13	18.52	12.39	7.34	4.19	2.43	1.52	0.94	864
	39	14	18.27	12.22	7.23	4.15	2.42	1.54	0.91	876
	39	15	18.20	12.18	7.25	4.16	2.45	1.55	0.97	879
	39	16	18.20	12.17	7.23	4.17	2.46	1.55	0.98	879
	40	13	18.08	11.38	6.45	3.78	2.41	1.65	1.24	885
	40	14	17.88	11.20	6.35	3.74	2.41	1.66	1.27	895
	40	15	17.81	11.14	6.32	3.73	2.40	1.65	1.24	898
	40	16	17.79	11.14	6.30	3.72	2.36	1.65	1.24	899

Table 12. Normalized deflections for thick asphalt sections EB MM 124.2 (grid).

Test Section	Test Point	Drop Number	Deflection (mil)							Calculated ISM
			Sensor Number							
			D0	D1	D2	D3	D4	D5	D6	
			Sensor Offset (in.)							
			0	12	24	36	48	60	72	
EB MM 124.2	11	13	11.33	7.67	5.21	3.50	2.28	1.66	1.00	1,412
	11	14	11.15	7.59	5.18	3.48	2.36	1.58	1.15	1,435
	11	15	11.06	7.55	5.15	3.47	2.36	1.58	1.15	1,446
	11	16	11.07	7.53	5.15	3.47	2.39	1.53	1.19	1,446
	12	13	13.91	9.97	6.77	4.52	2.97	2.05	1.37	1,150
	12	14	13.89	9.91	6.71	4.51	3.00	2.03	1.41	1,152
	12	15	13.82	9.87	6.68	4.49	3.02	1.98	1.42	1,157
	12	16	13.81	9.87	6.67	4.50	3.00	2.00	1.40	1,159
	13	13	14.93	10.75	7.15	4.51	2.83	1.79	1.21	1,072
	13	14	14.84	10.66	7.12	4.49	2.82	1.78	1.24	1,078
	13	15	14.84	10.67	7.10	4.49	2.81	1.82	1.16	1,078
	13	16	14.74	10.61	7.06	4.47	2.81	1.80	1.16	1,086
	14.1	13	12.86	9.16	6.25	4.07	2.57	1.64	1.11	1,244
	14.1	14	12.85	9.14	6.32	4.08	2.57	1.64	1.11	1,245
	14.1	15	12.74	9.11	6.19	4.04	2.56	1.62	1.13	1,256
	14.1	16	12.79	9.14	6.21	4.07	2.55	1.62	1.10	1,251
	15	13	15.45	11.31	7.83	5.17	3.37	2.25	1.59	1,036
	15	14	15.32	11.25	7.88	5.23	3.32	2.26	1.57	1,044
	15	15	15.27	11.22	7.85	5.21	3.30	2.24	1.54	1,048
	15	16	15.34	11.20	7.81	5.17	3.34	2.25	1.59	1,043
	16	13	9.24	6.15	4.30	2.90	2.01	1.37	1.02	1,732
	16	14	9.14	6.18	4.29	2.90	2.03	1.37	1.04	1,751
	16	15	9.07	6.10	4.29	2.90	2.02	1.38	1.03	1,764
	16	16	9.03	6.10	4.27	2.89	2.03	1.37	1.03	1,772
	18	13	12.02	8.98	6.31	4.28	2.76	1.77	1.23	1,331
	18	14	11.87	8.88	6.24	4.22	2.69	1.72	1.13	1,348
	18	15	11.78	8.85	6.23	4.23	2.71	1.74	1.18	1,358
	18	16	11.75	8.82	6.21	4.19	2.67	1.70	1.11	1,361
	20	13	12.92	9.81	7.09	4.91	3.30	2.23	1.53	1,239
	20	14	12.84	9.76	7.07	4.90	3.29	2.22	1.53	1,246
	20	15	12.82	9.69	7.03	4.87	3.27	2.21	1.55	1,248
	20	16	12.83	9.72	7.04	4.89	3.28	2.21	1.54	1,247

Table 13. Normalized deflections for thick asphalt section WB MM 123.4 (grid).

Test Section	Test Point	Drop Number	Deflection (mil)							Calculated ISM
			Sensor Number							
			D0	D1	D2	D3	D4	D5	D6	
			Sensor Offset (in.)							
			0	12	24	36	48	60	72	
WB MM 123.4	51	13	15.00	10.71	7.27	4.75	3.11	2.13	1.49	1,066
	51	14	14.85	10.62	7.21	4.74	3.10	2.13	1.49	1,078
	51	15	14.71	10.57	7.19	4.67	3.08	2.18	1.47	1,088
	51	16	14.66	10.55	7.16	4.65	3.06	2.19	1.46	1,091
	52	13	15.48	11.27	7.61	5.10	3.53	2.43	1.70	1,034
	52	14	15.26	11.10	7.55	5.05	3.51	2.43	1.75	1,049
	52	15	15.24	11.09	7.51	5.06	3.52	2.43	1.71	1,050
	52	16	15.12	10.98	7.48	5.01	3.50	2.40	1.77	1,058
	53	13	14.09	10.19	7.18	4.93	3.38	2.39	1.66	1,136
	53	14	13.93	10.11	7.22	4.92	3.40	2.41	1.69	1,148
	53	15	13.85	10.07	7.16	4.86	3.37	2.36	1.63	1,155
	53	16	13.81	10.01	7.12	4.85	3.35	2.36	1.63	1,159
	54	14	14.61	8.86	6.02	3.86	2.55	1.65	1.21	1,095
	54	15	13.51	8.81	5.96	3.84	2.51	1.66	1.18	1,185
	54	16	12.51	8.81	5.96	3.82	2.51	1.64	1.20	1,279
	55	13	14.26	10.45	7.23	4.82	3.22	2.30	1.67	1,122
	55	14	14.23	10.36	7.22	4.83	3.28	2.30	1.76	1,124
	55	15	14.20	10.32	7.17	4.79	3.24	2.29	1.66	1,127
	55	16	13.95	10.28	7.11	4.77	3.27	2.25	1.71	1,147
	56	13	12.80	9.13	6.41	4.24	2.86	2.04	1.40	1,250
	56	14	12.60	9.03	6.32	4.21	2.83	2.03	1.39	1,270
	56	15	12.58	8.97	6.33	4.21	2.80	2.03	1.37	1,272
	56	16	12.51	8.97	6.29	4.20	2.80	2.02	1.38	1,279
	58	13	13.02	9.26	6.56	4.58	3.19	2.24	1.58	1,229
	58	14	12.88	9.15	6.50	4.55	3.19	2.24	1.58	1,242
	58	15	12.85	9.13	6.50	4.55	3.19	2.24	1.59	1,245
	58	16	12.80	9.13	6.48	4.53	3.17	2.22	1.56	1,250
	60	13	14.14	9.03	6.50	4.58	3.18	2.26	1.63	1,131
	60	14	13.43	9.11	6.43	4.53	3.17	2.25	1.62	1,191
	60	15	13.48	9.09	6.44	4.53	3.17	2.26	1.61	1,187
	60	16	13.54	9.02	6.43	4.52	3.16	2.25	1.60	1,182

Table 14. Normalized deflections for thick asphalt section EB MM 123.2 (no grid).

Test Section	Test Point	Drop Number	Deflection (mil)							Calculated ISM
			Sensor Number							
			D0	D1	D2	D3	D4	D5	D6	
			Sensor Offset (in.)							
			0	12	24	36	48	60	72	
EB MM 123.2	1	13	12.53	8.80	6.32	4.27	2.84	1.97	1.49	1,277
	1	14	12.29	8.67	6.28	4.23	2.81	1.96	1.47	1,302
	1	15	12.28	8.65	6.26	4.23	2.81	1.99	1.47	1,303
	1	16	12.29	8.63	6.24	4.23	2.81	1.99	1.46	1,302
	2	13	14.76	10.68	7.74	5.47	3.81	2.66	1.87	1,084
	2	14	14.54	10.57	7.68	5.43	3.78	2.65	1.86	1,101
	2	15	14.31	10.56	7.66	5.43	3.78	2.65	1.89	1,118
	2	16	14.17	10.53	7.64	5.41	3.77	2.65	1.88	1,129
	3	13	14.06	10.41	7.43	5.26	3.73	2.68	2.01	1,138
	3	14	13.97	10.29	7.30	5.19	3.68	2.65	1.98	1,145
	3	15	13.91	10.28	7.32	5.21	3.70	2.69	2.00	1,150
	3	16	13.83	10.24	7.34	5.22	3.70	2.69	1.99	1,157
	4	13	12.95	9.14	6.80	4.83	3.20	2.51	1.72	1,236
	4	14	12.84	9.09	6.73	4.81	3.27	2.47	1.73	1,246
	4	15	12.95	9.05	6.74	4.80	3.27	2.48	1.75	1,235
	4	16	13.06	9.07	6.71	4.80	3.27	2.48	1.73	1,225
	5	13	11.89	7.84	5.62	3.71	2.43	1.56	1.03	1,346
	5	14	12.16	7.81	5.59	3.70	2.43	1.57	1.04	1,315
	5	15	12.06	7.77	5.56	3.69	2.43	1.56	1.04	1,327
	5	16	11.74	7.74	5.52	3.68	2.41	1.56	1.03	1,363
	6.1	13	14.89	8.97	6.41	4.47	3.00	2.04	1.45	1,075
	6.1	14	13.59	8.88	6.34	4.44	3.00	2.03	1.45	1,177
	6.1	15	12.71	8.90	6.38	4.46	3.00	2.06	1.47	1,258
	6.1	16	12.04	8.89	6.36	4.46	2.99	2.04	1.47	1,329
	8.1	13	14.48	10.68	7.75	5.46	3.84	2.80	2.08	1,105
	8.1	14	14.42	10.57	7.73	5.43	3.76	2.77	2.07	1,110
	8.1	15	14.33	10.52	7.67	5.40	3.77	2.77	2.06	1,117
	8.1	16	14.48	10.52	7.69	5.41	3.73	2.76	2.06	1,105
	10	13	12.29	7.73	5.60	3.74	2.42	1.52	0.97	1,302
	10	14	11.53	7.69	5.60	3.70	2.41	1.54	1.00	1,388
	10	15	11.22	7.72	5.59	3.70	2.41	1.53	1.00	1,426
	10	16	10.98	7.76	5.56	3.72	2.43	1.52	0.97	1,457

Figure 40. Calculated ISM using normalized deflection data for the thin asphalt test sections.

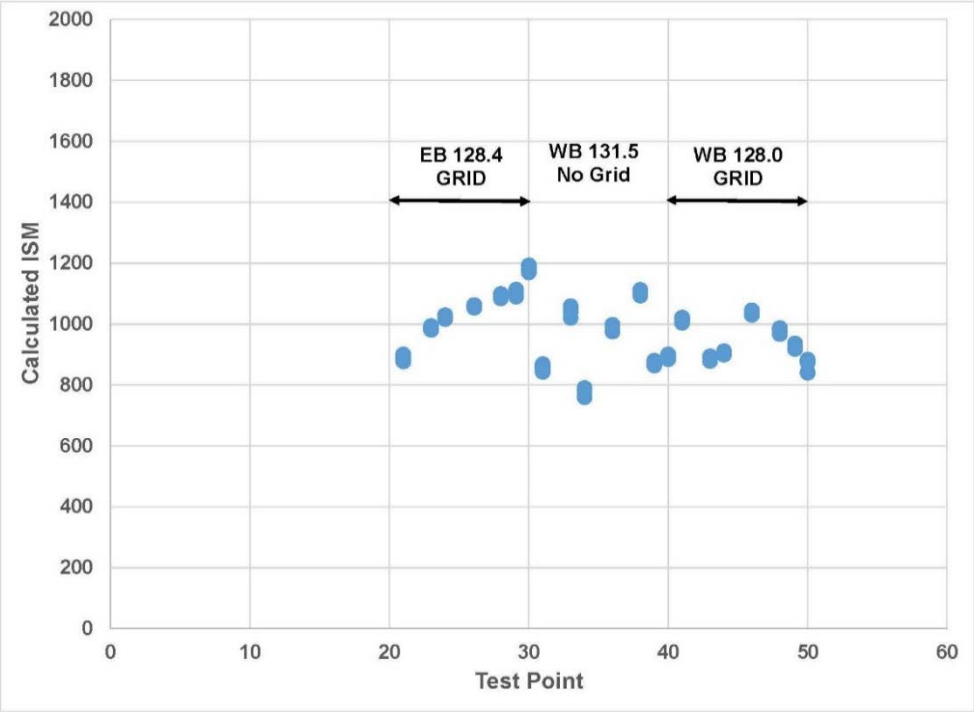

Figure 41. Calculated ISM using normalized deflection data for the thick asphalt test sections.

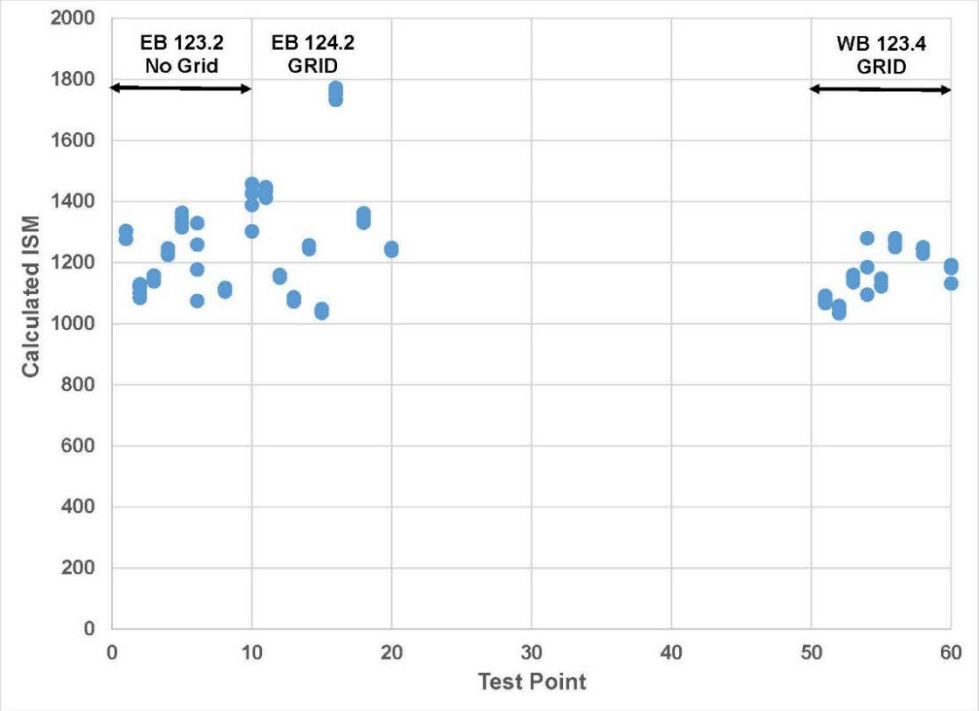

5.5.3 Asphalt temperature correction factor

Asphalt strength is temperature dependent. At lower ambient temperatures, the material is stiffer. The relationship between the asphalt condition and the temperature impacts the deflection measurements. Consequently, an adjustment factor was needed to correct for the effects of the ambient temperature during the time the data was collected (Lukanen et al. 2000). The temperature at mid-depth of the asphalt layer (3 in. and 5 in.) was estimated using the measured pavement surface temperature taken during FWD testing as input in the model from Lukanen et al. (2000) (Equation 5). The standard reference temperature of 68°F was used.

$$\begin{aligned} T_d &= 0.95 + 0.892 \cdot IR \\ &+ (\log(d) - 1.25) \cdot \left(-0.448 \cdot IR + 0.621 \cdot (1 - day) + 1.83 \cdot \sin\left(\frac{2\pi(h_1 - 15.5)}{18} \right) \right) \\ &+ 0.042 \cdot IR \cdot \sin\left(\frac{2\pi(h_2 - 13.5)}{18} \right) \end{aligned} \quad (5)$$

where

T_d = the pavement temperature at depth,
IR = the infrared pavement surface temperature (°C),
D = the asphalt depth to estimate the temperature (mm),
1-day = the average air temperature from the day prior to testing, and
h_1 and h_2 = values according to Lukanen et al. (2002) (Doré and Zubeck 2009).

Once temperatures are determined, the asphalt modification factor is calculated from Lukanen et al. (2002) (Equation 6):

$$ATAF = 10^{slope*(T_r - T_m)} \quad (6)$$

where

ATAF = the computed asphalt temperature adjustment factor,
slope = log modulus as a function of temperature relationship,
T_r = the reference temperature at mid-depth of the asphalt, and
T_m = the estimated temperature at mid-depth during testing.

The calculated asphalt moduli correction factor was determined to be 0.855. This multiplier was applied to all of the asphalt modulus values from the back-calculation procedure.

5.5.4 Summary of data analysis

As a way to assess possible structural benefit from grid reinforcement, the measured deflection data for each test section was used to calculate the basin area, ISM, and radius of curvature and to compare between grid-reinforced asphalt test sections and the corresponding control test sections. No convincing trend emerged. The deflection data was then normalized to a common (16,000 lb) load to reduce the variability. The ISM was recalculated using the normalized deflection values. In the thin asphalt test sections, there appeared to be a weak correlation between the ISM value and the presence of grid reinforcement in the test sections. This relationship did not translate to the thick asphalt test sections.

The next section describes the process used to back-calculate the asphalt layer modulus by using both the measured and normalized deflection data.

6 Back Calculation

In this project, we used the software program WESDEF (Waterways Experiment Station Deflection), developed by the U.S. Army Engineer Research and Development Center Geotechnical and Structures Laboratory), to back-calculate the material layer modulus values. WESDEF provides a numerical solution capability for a multi-layer structure and easily operates on a desktop digital platform (Van Cauwelaert et al. 1989; DOD 2001). Forming the basis of this computer program is the elastic layer design procedures limiting the stresses and strains within a pavement structure at critical locations (Van Cauwelaert et al. 1989; DOD 2001). The back-calculation procedure produces theoretical deflection measurements that are compared to the measured deflection readings (Hassan et al. 2003). The Layered Elastic Evaluation Program (LEEP) incorporates the WESDEF program as one of several modules within the Pavement-Transportation Computer Assisted Structural Engineering (PCASE) software suite used in infrastructure design and evaluation of airfields, roads, and railroads. The PCASE program is available from www.pcase.com. The program is actively used for structural evaluations completed on roadways and airfields on military installations.

The linear elastic program pavement response model is based on the following assumptions (DOD 2001):

- The pavement system consists of multiple and distinct material layers where each layer is described by a thickness, modulus of elasticity, and Poisson's ratio.
- Individual layers are considered to be homogeneous, isotropic, and extending infinitely in the horizontal direction.
- The interface between layers is continuous, such that the resistance from friction between layers is greater than that developed by shear forces.
- The characteristics of all loads are that they are static, circular in shape, and uniform over the contact area.

Input values used in the back-calculation procedure include the measured deflections, the material structure layer type and thickness, the material Poisson's ratio, the layer interface condition, the initial seed modulus value, and the minimum and maximum ranges of modulus values.

The back-calculation procedure for the six test sections focused on the deflection measurements at the 16 kip load (drops 13–16). Deflections under this loading condition represent traffic highway speeds. For all six test sections, the structure was represented as a three-layer system: asphalt concrete overlying a base layer, overlying a subgrade layer. This approach simplified the representation of the structure to produce comparable results between sections of similar asphalt thickness. The field investigation provided the values for the asphalt thickness and the materials and thicknesses of the underlying supporting layers. The total thickness of the structure modeled was 240 in. with any bedrock assumed very deep. Table 15 shows the material layering inputs for each test section. Table 16 gives the material input parameters, including the seed modulus values and ranges. There are no strict criteria in the selection of the material modulus values for either the initial modulus or the minimum and maximum limits. For the asphalt layer, the upper limit of 1×10^6 psi was the average within the range of recommended values of 5×10^5 (ASTM 2008) and 2×10^6 (DOD 2001). The initial seed modulus and ranges can be adjusted should the calculated error be unreasonably high. ASTM (2008) suggests an acceptable error range of 7% to 14% when using seven deflection sensors.

Table 15. Material layer thicknesses for each test section used as input in the back-calculation procedure.

Layer Number	Material	Layer Thicknesses					
		EB MM 123.2 (in.)	EB MM 124.2 (in.)	EB MM 128.4 (in.)	WB MM 123.4 (in.)	WB MM 128.0 (in.)	WB MM 131.5 (in.)
1	Asphalt	10	10	6	9	6	6
2	Base	37	37	38.5	46	43	44.4
3	Natural Subgrade	193	193	195.5	185	191	189.6
	Total Depth	**240**	**240**	**240**	**240**	**240**	**240**

Table 16. Material input parameters used in the WESDEF back-calculation procedure.

Layer Number	Material	Modulus Initial	Modulus Min.	Modulus Max.	Poisson's Ratio	Slip
1	Asphalt	350,000	100,000	1,000,000	0.35	1
2	Base	61,000	5,000	150,000	0.35	1
3	Natural Subgrade	24,567	19,567	29,567	0.4	1

Tables 17 to 18 provide the back-calculated values for each test section. For this initial run, the back-calculated material values for the 6 in. asphalt

sections were somewhat high, yet the error values were within ASTM's recommended range. In this first attempt, the modulus values were back-calculated for all three material layers. Table 17 and Figure 42 show the results of the initial back-calculation for the thin asphalt test sections, and Table 18 and Figure 43 show the results for the thick asphalt test sections.

Figure 42. Thin asphalt sections back-calculated asphalt modulus using initial material layer input values and measured deflection data.

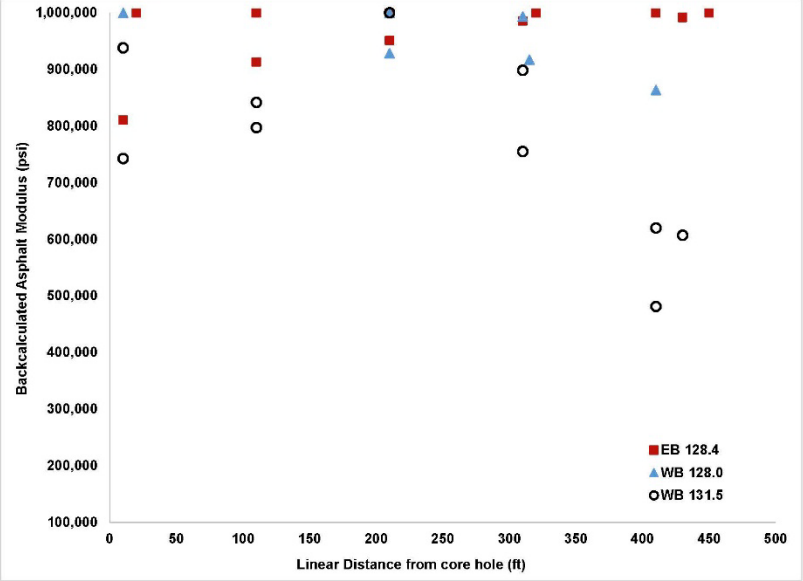

Figure 43. Thick asphalt sections back-calculated asphalt modulus using initial material layer input values and measured deflection data

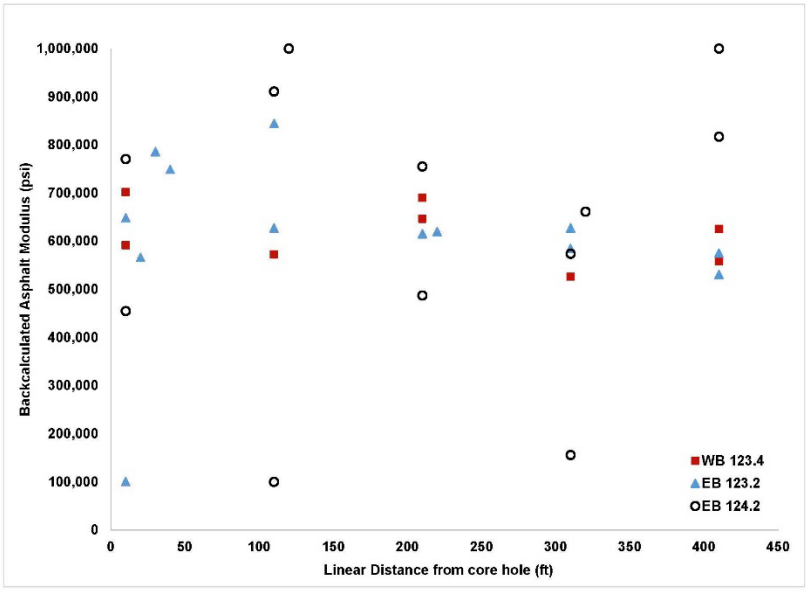

Table 17. Average back-calculated layer values for thin asphalt test sections.

WB MM 131.5							EB MM 128.4							WB MM 128.0						
			Average							Average							Average			
Lane Location	Test Point	(ft)	% Error	Asphalt (psi)	Base (psi)	Subgrade (psi)	Lane Location	Test Point	(ft)	% Error	Asphalt (psi)	Base (psi)	Subgrade (psi)	Lane Location	Test Point	(ft)	% Error	Asphalt (psi)	Base (psi)	Subgrade (psi)
WP	31	10	1.8	742,701	25,785	30,868	WP	21	10	2.0	810,701	27,369	19,639	WP	41	10	3.7	1,000,000	26,586	20,939
WP	32	110	2.1	841,774	28,229	27,662	WP	22	110	2.2	913,115	30,710	19,645	WP	43	210	1.3	928,392	24,916	20,283
WP	33	210	5.2	1,000,000	28,573	27,121	WP	23	210	2.2	951,299	30,238	21,636	WP	44	310	1.4	993,394	23,700	21,802
WP	34	310	2.3	754,782	19,896	30,132	WP	24	310	1.8	985,691	31,380	20,341	CL	46	10	4.5	1,000,000	31,273	22,181
WP	35	410	2.4	481,206	26,805	27,121	WP	25.2	430	2.2	991,913	32,965	18,862	CL	48	210	2.7	1,000,000	29,142	21,054
WP	35.2	430	2.8	606,873	27,697	27,121	WP	25.4	450	4.8	1,000,000	34,560	17,799	CL	49.1	315	1.5	916,824	26,008	22,537
CL	36	10	1.3	938,274	26,745	35,394	CL	26.1	20	2.7	1,000,000	30,357	21,938	CL	50	410	2.3	863,551	23,655	23,604
CL	37	110	2.0	797,191	28,471	29,403	CL	27	110	2.7	1,000,000	31,631	20,305							
CL	38	210	4.7	1,000,000	32,035	27,320	CL	28	210	2.9	1,000,000	31,834	21,396							
CL	39	310	2.7	898,456	20,922	34,823	CL	29.1	320	2.3	1,000,000	33,236	21,420							
CL	40	410	1.3	619,914	28,615	28,589	CL	30	410	3.2	1,000,000	39,394	17,799							
Asphalt modulus values back-calculated; Base and subgrade modulus values set																				
WP	31	10	16.9	319,318	44,000	22,654	WP	21	10	10.7	339,585	44,000	19,567	WP	41	10	16.1	1,000,000	44,000	19,567
WP	32	110	13.4	413,315	44,000	21,558	WP	22	110	7.9	466,889	44,000	19,567	WP	43	210	12.9	327,524	44,000	19,567
WP	33	210	14.3	1,000,000	44,000	19,567	WP	23	210	8.4	516,676	44,000	19,567	WP	44	310	15.4	668,726	44,000	19,567
WP	34	310	25.6	210,503	44,000	19,717	WP	24	310	7.4	537,673	44,000	19,567	CL	46	10	13.1	799,234	44,000	19,567
WP	35	410	14.4	212,246	44,000	20,217	WP	25.2	430	7.6	546,936	44,000	19,567	CL	48	210	9.9	473,678	44,000	19,567
WP	35.2	430	12.4	287,009	44,000	20,261	WP	25.4	450	15.2	1,000,000	44,000	19,567	CL	49.1	315	11.9	371,071	44,000	19,567
CL	36	10	16.2	385,309	44,000	26,495	CL	26.1	20	8.9	551,979	44,000	19,567	CL	50	410	14.0	299,896	44,000	19,567
CL	37	110	13.6	394,676	44,000	22,937	CL	27	110	8.0	553,929	44,000	19,567							
CL	38	210	14.5	1,000,000	44,000	21,665	CL	28	210	9.1	779,066	44,000	19,567							
CL	39	310	33.0	1,000,000	44,000	19,567	CL	29.1	320	8.2	907,321	44,000	19,567							
CL	40	410	13.5	306,462	44,000	22,428	CL	30	410	9.3	1,000,000	44,000	19,567							
Asphalt modulus values back-calculated; Base and subgrade modulus values set, normalized deflection values used																				
WP	31	10	11.0	245,696	44,500	24,500	WP	21	10	22.0	253,812	44,500	24,500	WP	41	10	7.5	1,000,000	44,500	19,392
WP	32	110					WP	22	110					WP	43	210	13.5	306,013	44,500	19,392
WP	33	210	15.9	812,905	44,500	24,500	WP	23	210	16.2	253,812	44,500	24,500	WP	44	310	14.8	494,038	44,500	19,392
WP	34	310	20.5	173,468	44,500	24,500	WP	24	310	17.6	409,543	44,500	24,500	CL	46	10	13.8	1,000,000	44,500	19,392
WP	35	410					WP	25.2	430					CL	48	210	10.4	438,569	44,500	19,392
WP	35.2	430					WP	25.4	450					CL	49.1	315	12.2	357,762	44,500	19,392
CL	36	10	17.6	330,334	44,500	24,921	CL	26.1	20	12.1	469,550	44,500	24,500	CL	50	410	14.4	287,664	44,500	19,392
CL	37	110					CL	27	110											
CL	38	210	14.3	1,000,000	44,500	24,500	CL	28	210	16.3	854,945	44,500	24,500							
CL	39	310	21.6	260,028	44,500	24,500	CL	29.1	320	12.0	529,163	44,500	24,500							
CL	40	410	11.4	280,466	44,500	24,500	CL	30	410	20.4	1,000,000	44,500	24,500							

WP = wheel path

CL = center of lane

Table 18. Average back-calculated layer values for thick asphalt test sections.

EB MM 123.2							EB MM 124.2							WB MM 123.4						
			Average							Average							Average			
Lane Location	Test Point	(ft)	% Error	Asphalt (psi)	Base (psi)	Subgrade (psi)	Lane Location	Test Point	(ft)	% Error	Asphalt (psi)	Base (psi)	Subgrade (psi)	Lane Location	Test Point	(ft)	% Error	Asphalt (psi)	Base (psi)	Subgrade (psi)
WP	1	10	1.4	648,634	25,370	27,002	WP	11	10	45.2	454,904	9,931	24,821	WP	51	10	0.9	591,514	22,114	25,162
WP	2	110	1.1	627,476	19,335	20,541	WP	12	110	15.5	910,937	6,699	24,821	WP	52	110	0.8	572,203	22,141	20,764
WP	3	210	1.0	615,326	21,514	19,567	WP	13	210	38.1	487,301	5,000	24,821	WP	53	210	1.5	690,575	22,973	21,591
WP	4	310	2.6	627,398	25,399	20,931	WP	14	310	60.9	155,836	10,644	24,821	WP	54	310	2.6	526,169	27,835	29,389
WP	5	410	6.0	530,691	29,521	29,567	WP	14.1	320	40.3	661,295	5,000	24,821	WP	55	410	0.8	625,054	23,384	21,398
CL	6	10	7.2	100,585	45,944	20,213	WP	15	410	13.5	817,079	5,586	24,821	CL	56	10	1.6	701,906	25,459	25,430
CL	6.1	20	2.4	566,215	24,223	24,884	CL	16	10	33.3	770,693	16,113	24,821	CL	58	210	2.6	646,154	32,070	30,220
CL	6.2	30	0.5	785,980	24,022	21,978	CL	17	110	62.6	100,000	48,798	24,821	CL	60	410	3.1	558,407	28,915	20,220
CL	6.3	40	0.8	749,187	24,795	25,358	CL	17.1	120	17.1	1,000,000	7,920	24,821							
CL	7	110	0.7	844,423	18,607	20,373	CL	18	210	34.0	755,161	5,000	24,821							
CL	8.1	220	2.4	619,779	17,878	19,567	CL	19	310	38.1	573,773	6,751	24,821							
CL	9	310	0.8	584,742	23,515	20,784	CL	20	410	13.1	1,000,000	6,195	24,821							
CL	10	410	6.4	575,067	27,206	29,567														
Asphalt modulus values back-calculated; Base and subgrade modulus values set																				
WP	1	10	9.3	424,080	44,000	21,002	WP	11	10	8.7	414,070	44,000	24,906	WP	51	10	9.9	270,134	44,000	19,567
WP	2	110	13.7	297,419	44,000	19,910	WP	12	110	9.9	368,196	44,000	23,496	WP	52	110	16.2	237,292	44,000	19,567
WP	3	210	15.4	260,928	44,000	19,567	WP	13	210	14.3	227,628	44,000	19,567	WP	53	210	14.3	299,268	44,000	19,567
WP	4	310	9.8	352,796	44,000	19,567	WP	14	310	22.7	111,103	44,000	20,053	WP	54	310	12.5	262,959	44,000	21,963
WP	5	410	11.9	376,350	44,000	25,865	WP	14.1	320	17.1	290,506	44,000	21,311	WP	55	410	13.5	279,732	44,000	19,567
CL	6	10	15.8	100,172	44,443	19,737	WP	15	410	16.4	185,544	44,000	19,567	CL	56	10	10.3	378,112	44,000	19,567
CL	6.1	20	11.6	375,132	44,000	20,918	CL	16	10	4.6	622,706	44,000	29,567	CL	58	210	12.0	341,606	44,000	19,567
CL	6.2	30	8.8	439,801	44,000	19,567	CL	17	110	15.2	155,460	44,000	19,567	CL	60	410	10.8	306,733	44,000	19,567
CL	6.3	40	8.8	479,906	44,000	19,600	CL	17.1	120	11.3	416,256	44,000	19,567							
CL	7	110	16.7	344,115	44,000	19,567	CL	18	210	16.6	348,241	44,000	19,945							
CL	8.1	220	8.8	479,906	44,000	19,600	CL	19	310	14.1	333,174	44,000	23,140							
CL	9	310	10.8	302,823	44,000	19,567	CL	20	410	14.5	294,397	44,000	19,567							
CL	10	410	14.0	383,672	44,000	25,027														
Asphalt modulus values back-calculated; Base and subgrade modulus values set, normalized deflection values used																				
WP	1	10	9.4	359,865	44,500	21,130	WP	11	10	8.6	423,662	44,500	25,804	WP	51	10	10.1	260,581	44,500	20,211
WP	2	110	12.2	325,641	44,500	21,130	WP	12	110	12.4	317,964	44,500	25,565	WP	52	110	15.8	246,708	44,500	20,211
WP	3	210	21.1	219,261	44,500	21,130	WP	13	210	17.5	183,536	44,500	25,488	WP	53	210	14.3	309,256	44,500	20,211
WP	4	310	13.5	313,801	44,500	21,130	WP	14	310					WP	54	310	11.3	314,705	44,500	22,620
WP	5	410	12.4	360,806	44,500	25,260	WP	14.1	320	15.5	286,113	44,500	25,488	WP	55	410	13.3	294,041	44,500	20,211
CL	6	10					WP	15	410	23.8	186,869	44,500	25,488	CL	56	10	9.8	408,434	44,500	20,211
CL	6.1	20	11.7	356,134	44,500	22,269	CL	16	10	3.3	624,846	44,500	32,358	CL	58	210	10.6	384,901	44,500	20,211
CL	6.2	30					CL	17	110					CL	60	410	9.8	336,595	44,500	20,211
CL	6.3	40					CL	17.1	120											
CL	7	110					CL	18	210	15.0	346,102	44,500	25,488							
CL	8.1	220	23.0	200,210	44,500	21,130	CL	19	310											
CL	9	310					CL	20	410	18.4	316,176	44,500	25,488							
CL	10	410	13.8	394,184	44,500	25,638														

WP = wheel path
CL = center of lane

In Table 17 for the thin asphalt sections, particularly both sections with grid reinforcement, the asphalt modulus frequently hit the upper limit of 1,000,000 psi. This was especially the case for EB MM 128.4 and WB MM 128.0. The back-calculation results for the asphalt layer for the thick asphalt test sections, both with and without grid reinforcement, ranged between 500,000 to 800,000 psi. However, no clear trend is apparent for either asphalt thickness.

A second back-calculation attempt using the measured deflection data reduced and narrowed the range of the base-course modulus to 44,000 to 46,000 psi and the subgrade modulus to 19,000 to 21,000 psi. Only the modulus for the asphalt layer was back-calculated. Figures 44 and 45 show the results for the thick and thin asphalt test sections, respectively. This approach reduced the range of the asphalt modulus values although, similar to the initial back-calculation run, the data is scattered. However, the scatter appears to be somewhat reduced for the thicker asphalt sections than the thin asphalt sections.

Figure 44. Back-calculated asphalt modulus for the thick asphalt layer test sections setting the base and subgrade modulus values.

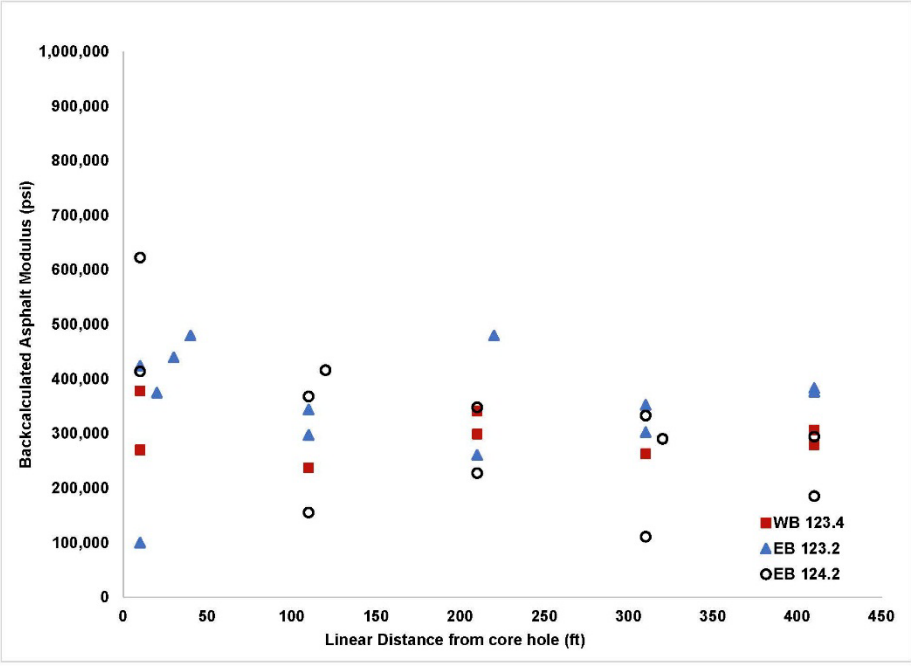

Figure 45. Back-calculated asphalt modulus for the thin asphalt layer test sections setting the base and subgrade modulus values.

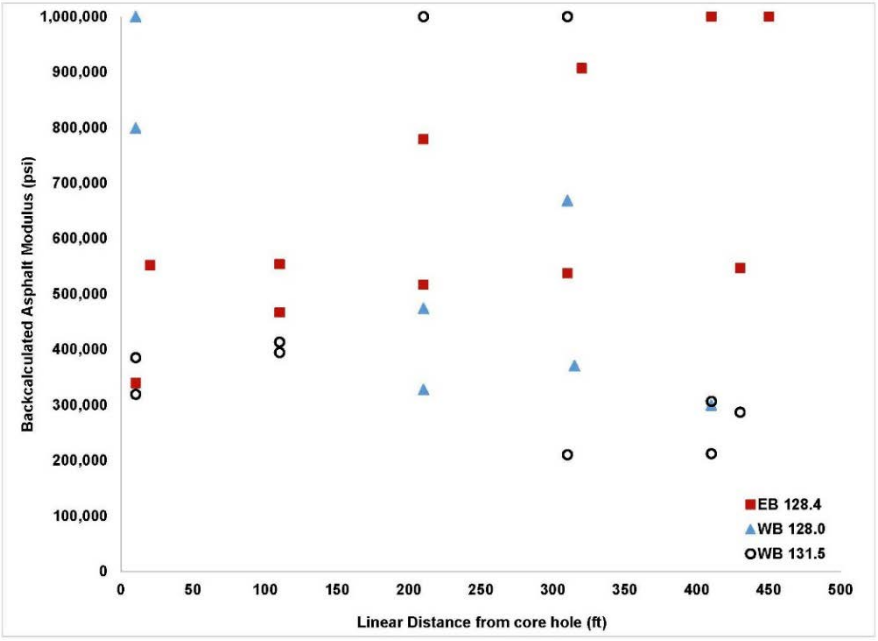

The normalized deflection data was used in the next back-calculation run. The asphalt modulus was back-calculated, and the base and subgrade modulus values were fixed using the same values as in the previous attempt (Figures 46 and 47).

Figure 46. Back-calculated asphalt modulus for the thick asphalt layer test sections using normalized deflection data and setting the base and subgrade modulus values.

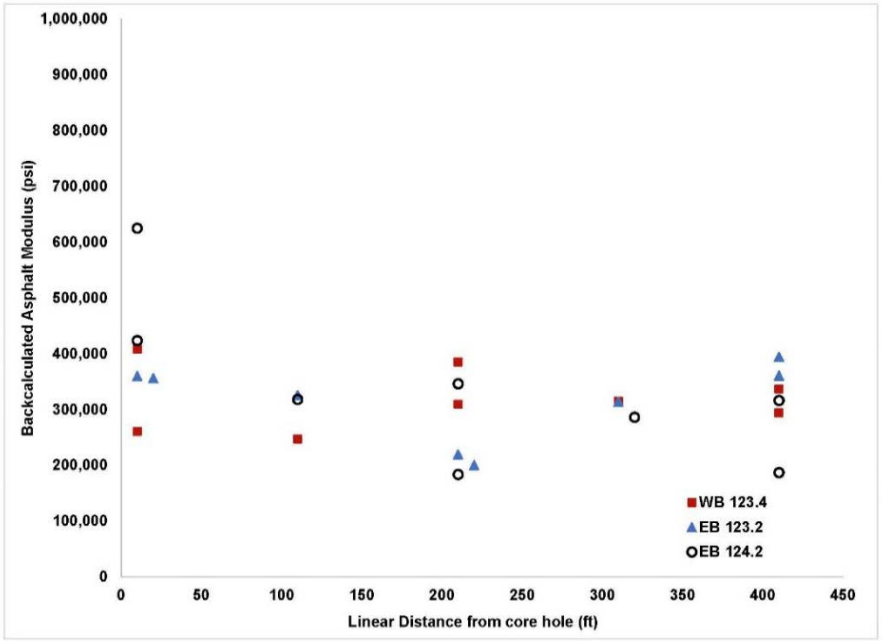

Figure 47. Back-calculated asphalt modulus for the thin asphalt layer test sections using normalized deflection data and setting the base and subgrade modulus values.

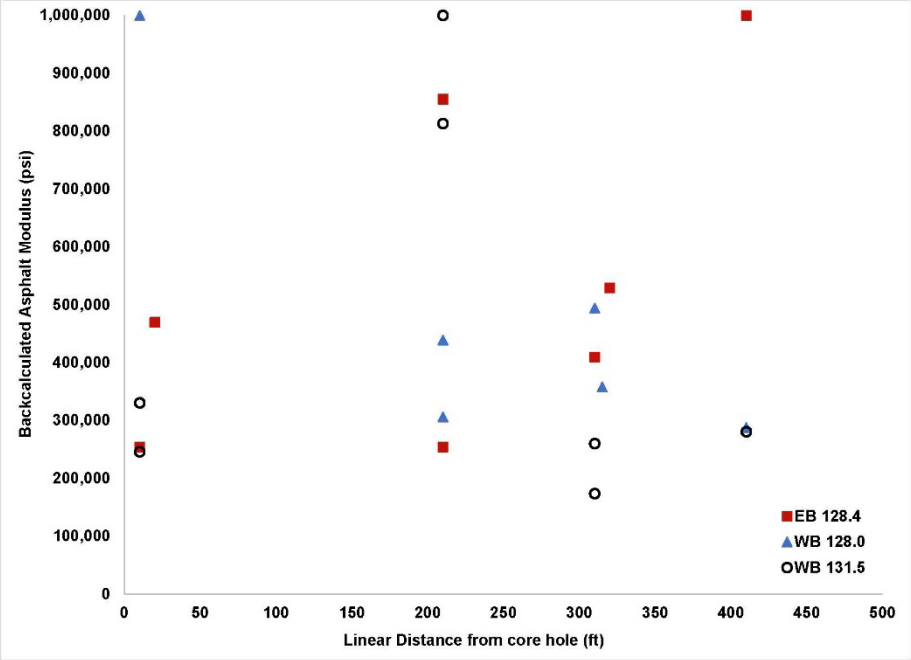

We attempted a final back-calculation run splitting the asphalt layer on the thick asphalt test section. We used the normalized deflection data from WB MM 123.4 and EB MM 124.2, with asphalt thicknesses of 9 and 10 in., respectively. A thickness of 5 in. was used for the top asphalt layer, and 4 in. for the bottom asphalt layer for WB MM 123.4, and 5 in. for the bottom asphalt layer for EB MM 124.2. Based on input from NHDOT, the original asphalt layer prior to reconstruction was greatly deteriorated and would likely have a lower modulus strength. In this back-calculation attempt, the bottom asphalt layer was assigned a lower initial modulus value of 250,000 psi as estimated using the FWD data collected in 2008. To run a split pavement layer in PCASE, the bottom asphalt layer was set as a high-quality stabilized base (Harrison 2015). The remainder of the input values were unchanged. Similar to all of the previous results, the back-calculated asphalt modulus values were inconclusive with scattered values.

7 Conclusions

To reduce the damage from fatigue cracking in sections of NH 101, NHDOT installed a reinforcing grid at mid-depth of the asphalt layer during a rehabilitation project of the roadway. The reinforcing grid has been in place now for several years, and thus far the roadway sections continue to perform well. CRREL completed a structural evaluation using FWD and analyzed the deflection data obtained during testing to determine if any benefit gained by the inclusion of the grid reinforcement could be quantified. Six sections were tested at two different asphalt thicknesses. As a comparison, control sections (without grid reinforcement) were tested in close proximity to the grid-reinforced sections.

Using the deflection measurements, CRREL calculated the basin area, ISM, and radius of curvature by using accepted methods. Comparisons between test sections with and without grid were inconclusive. In case the measured deflection data was too variable, the deflection data was normalized to a common load of 16,000 lb. A recalculated ISM for the thin asphalt sections showed a somewhat linear trend compared to the scatter of the test section without grid reinforcement. However, it is unclear the source of this trend. No trend was observed in the recalculated ISM of the thick asphalt test sections.

For consistency, we used the ISM value to compare the test sections. The calculated ISM values for all of the test sections appeared to be reasonable to categorize them as similar for analysis purposes. For these test sections, this may be a realistic assumption.

Likewise, for the thin asphalt test sections, the control section was located some distance away from the grid-reinforced test sections. The control section may not have been as comparable to the two grid sections given the locations and traffic conditions.

Similarly, the moisture content in the subsurface layers may have had a larger impact than initially thought. The rainfall that occurred a short time before the field testing may not have completely drained out of the pavement structure, causing a greater impact on the deflection data.

Additionally, the deflection measurements between the grid and non-grid test sections did not show conclusively that the grid reinforcement provided structural benefit.

The first back-calculation attempt used the measured deflection data in a three-layer system to back-calculate the modulus for all three layers. There was considerable scatter in the back-calculated modulus values. This was the case for both the thin and thick asphalt layers. The normalized deflection data was used in a second back-calculation attempt producing similar results.

The conventional approach for rehabilitating existing flexible pavements is an asphalt overlay. The literature reports that increasing the thickness of the asphalt layer, while adding both cost and design adjustments to the project, is an effective and accepted method to reduce reflective cracking in the asphalt layer. It is possible, given the total thickness of an asphalt layer of 6 and 10 in. in the rehabilitated portions of NH 101, that the additional asphalt has significantly reduced cracking due to traffic loading. It is also possible that this hampers the ability to parse out of the data structural benefit of grid reinforcement. However, we would have then expected to see a benefit in the thinner asphalt sections, which there was not. Additionally, the FWD may be too coarse of a test apparatus to capture this in the measurements. While laboratory testing of specimens have been conducted, a method is still needed to accurately assess reinforcing grid in the asphalt layer.

It is possible that the grid reinforcement may help arrest cracking by holding cracked portions of the asphalt material close together, but the effect of grid reinforcement on the overall stiffness of the pavement structure was not apparent based on the FWD data.

8 Recommendations

This investigation provided an initial understanding of the performance of grid-reinforced asphalt pavement. Follow-up investigations would further build on this knowledge. We therefore make the following recommendations:

- For more representative data, locate test and control selections in closer proximity to each other. The selection of the control test section for the thin asphalt sections may not have been ideal. Differences in traffic count and direction, slope, and aspect may contribute to the performance of grid reinforced pavements. The test section orientation should be in the same lane and direction.

- Consider conducting laboratory testing on either the field asphalt cores or laboratory fabricated test specimens to understand the performance of grid reinforcement with the NHDOT asphalt mixture.

- Conduct laboratory testing under varying environmental conditions to quantify the effects of grid reinforcement within the asphalt material.

- Consider the impacts of environmental conditions. Conduct FWD testing during a time period when the pavement structure is naturally weaker, such as during the spring or following several rain events, when subsurface moisture contents are high, to examine if the grid is providing additional structural benefit.

- Conduct a series of follow-up FWD tests in the same test locations in 2 to 5 years to assess any changes to the pavement structure.

References

Air Force. 2002. *Airfield Pavement Evaluation Standards and Procedures.* Engineering Technical Letter 02-19. Tyndall Air Force Base, FL: Department of the Air Force, Headquarters Air Force Civil Engineer Support Agency.

AASHTO (American Association of State Highway and Transportation Officials). 1993. *Guide for the Design of Pavement Structures.* Washington, DC: American Association of State Highway and Transportation Officials.

———. 2005. *Standard Method of Test for Pavement Deflection Measurements.* AASHTO Designation: T 256-01. Washington, DC: American Association of State Highway and Transportation Officials.

———. 2009. *Standard Method of Test for Materials Finer than 75 µm (No. 200) Sieve in Mineral Aggregates by Washing.* AASHTO Designation T 11-09. Washington, DC: American Association of State Highway and Transportation Officials.

———. 2011. *Standard Practice for Calibrating the Load Cell and Deflection Sensors for a Falling Weight Deflectometer.* AASHTO Designation R 32-11. Washington, DC: American Association of State Highway and Transportation Officials.

———. 2014. *Standard Method of Test for Sieve Analysis of Fine and Coarse Aggregates.* AASHTO Designation T 27-14. Washington, DC: American Association of State Highway and Transportation Officials.

ASTM (American Society for Testing and Materials). 2008. *Standard Guide for Calculating In Situ Equivalent Elastic Moduli of Pavement Materials Using Layered Elastic Theory*. ASTM D5858. West Conshohocken, PA: ASTM International.

———. 2009. *Standard Test Method for Deflections with a Falling-Weight-Type Impulse Load Device*. ASTM D4694. West Conshohocken, PA: ASTM International.

Caltabiano, M. A., and J. M. Brunton. 1991. Reflection Cracking in Asphalt Overlays. *Journal of the Association of Asphalt Paving Technologists* 60:310–329.

Darling, J. R., and J. H. Woolstencroft. 2004. Fibreglass Pavement Reinforcements Used in Dissimilar Climatic Zones for Retarding Reflective Cracking in Asphalt Overlays. In Proceedings of the 5th International RILEM Conference on Cracking in Pavements, 5–7 May, Limoges, France, 435–442.

DOD (Department of Defense). 2001. *Airfield Pavement Evaluation*. Unified Facilities Criteria UFC 3-260-03. Washington, DC: U.S. Army Corps of Engineers.

Doré, G., and H. K. Zubeck. 2009. *Cold Regions Pavement Engineering*. McGraw Hill. Reston, VA: American Society of Civil Engineers.

Francken, L. 2005. Prevention of Cracks in Pavements. *Road Materials and Pavement Design* 6 (3): 407–425. doi:10.1080/14680629.2005.9690014.

Harrison, J. A. 2015. Personal communication. 2 November. Vicksburg, MS: U.S. Army Engineer Research and Development Center.

Hassan, H. F., R. M. Mousa, and A. A. Gadallah. 2003. Comparative Analysis of Using AASHTO and WESDEF Approaches in Back-Calculation of Pavement Layer Moduli. *Journal of Transportation Engineering* 129 (3): 322–329.

Horak, E. 1987. The Use of Surface Deflection Basin Measurements in the Mechanistic Analysis of Flexible Pavements. In *Proceedings of the Sixth International Conference on Structural Design of Asphalt Pavements, 13–17 July, University of Michigan, Ann Arbor, MI*, 1:990–1001.

Lee, S. J. 2008. Mechanical Performance and Crack Retardation Study of a Fiberglass-Grid-Reinforced Asphalt Concrete System. *Canadian Journal of Civil Engineering* 35 (10): 1042–1049.

Lukanen, E. O., R. Stubstad, and R. Briggs. 2000. *Temperature Predictions and Adjustment Factors for Asphalt Pavement*. FHWA-RD-98-085. McLean, VA: Federal Highway Administration.

Pasquini, E., M. Bocci, G. Ferrotti, and F. Canestrari. 2013. Laboratory characterization and field validation of geogrid-reinforced asphalt pavements. *Road Materials and Pavement Design* 14 (1): 17–35. http://dx.doi.org/10.1080/14680629.2012.735797.

Roberts, F. L., P. S. Kandhal, E. R. Brown, D-Y. Lee, T. W. Kennedy. 1996. *Hot Mix Asphalt Materials, Mixture, Design and Construction*. 2nd ed. Lanham, MD: National Asphalt Pavement Association Research and Education Foundation.

Romeo, E., F. Freddi, and A. Montepara. 2014. Mechanical Behavior of Surface Layer Fiberglass-Reinforced Flexible Pavements. *International Journal of Pavement Engineering* 15 (2): 95–109. doi:10.1080/10298436.2013.828838.

Saint-Gobain ADFORS. 2011. *GlasGrid 8501 (International Spec)*. Grand Island, NY: Saint-Gobain ADFORS America.

Smart, A. L. 2011. *Pilot Study – Rolling Wheel Deflectometer, Falling Weight Deflectometer, and Ground Penetrating Radar on New Hampshire Roadways*. FHWA-NH-RD-14282N. Concord, NH: New Hampshire Department of Transportation, Bureau of Materials and Research.

Tensar. 2011. *Pavement Reinforcement Systems Overview*. Alpharetta, GA: Tensar International Corporation.

Van Cauwelaert, F. J., D. R. Alexander, T. D. White, and W. R. Barker. 1989. Multilayer Elastic Program for Backcalculating Layer Moduli in Pavement Evaluation. In *Nondestructive Testing of Pavements and Backcalculation of Moduli*. ASTM STP 1026, ed. A. J. Bush III and G. Y. Baladi, 171-188. West Conshohocken, PA: American Society for Testing and Materials.

Webster, S. L., R. H. Grau, and T. P. Williams. 1992. *Description and Application of Dual Mass Dynamic Cone Penetrometer*. Instruction Report GL-92-3. Vicksburg, MS: U.S. Army Corps of Engineers, Waterways Experiment Station.

Appendix A: Test Boring and Soil Grain Size Distribution Reports

TEST BORING REPORT

STATE OF NEW HAMPSHIRE DEPARTMENT OF TRANSPORTATION
MATERIALS & RESEARCH BUREAU - GEOTECHNICAL SECTION

PROJECT NAME **EPPING-EXETER 15680S** BRIDGE NO. N/A
DESCRIPTION NH101 Reinforced Pavement

BORING NO. PC1
SHEET NO. 1 OF 1
STA. _____ OFF. _____
BASELINE NH101 EB
ELEVATION (ft) _____
START/END 9/4/14 / 9/4/14
DRILLER C. Cleveland (NHDOT)
INSPECTOR Aaron Smart
CLASSIFIER ALS
EAST/NORTH (ft) -- / --

GROUNDWATER						EQUIPMENT	SAMPLER	CASING	CORE
DATE	TIME	DEPTH (ft)	ELEV. (ft)	BOTTOM OF CASING	BOTTOM OF HOLE	TYPE:	SL	NW	
						SIZE I.D. (in):	3	3	
						HAMMER WT. (lb):	140	DRILL RIG	
						HAMMER FALL (in):	30	CME 45-C Trlr	
						HAMMER TYPE:	Automatic		

DEPTH (ft)	STRATUM CHANGE (ft) DEPTH	STRATUM CHANGE (ft) ELEVATION	BLOWS PER 0.5 ft	SAMPLE NUMBER	SAMPLER RECOVERY (ft) [%]	DEPTH RANGE (ft)	FIELD CLASSIFICATION AND REMARKS	STRATUM SYMBOL
0							-ASPHALT PAVEMENT-	
	0.7			SL1	2.0 [100]	0.7	Mostly gray to light brown, fine to coarse subangular GRAVEL, some sand.	
							-FILL-	
						2.7	Mostly brown fine to medium SAND.	
	3.9			SL2	2.0 [100]	2.7		
5						4.7	Mostly grayish brown dessicated silty CLAY.	
							-GLACIAL MARINE DEPOSIT-	
							Bottom of Exploration @ 4.7 ft	
							NOTE: NH101 EB MP 123.2	
10								
15								
20								
25								

Sampler	Identification
S	Standard Split Spoon
SL	Large Spoon (O.D.= 3 in)
T	Thin Wall Tube
U	Undisturbed Piston
O	Open End Rod
A	Auger Flight
C	Core Barrel
NR	Not Recorded

COHESIVE SOILS	
Blows/foot (N)	Consistency
0 - 1	Very Soft
2 - 4	Soft
5 - 8	Medium Stiff
9 - 15	Stiff
16 - 30	Very Stiff
> 30	Hard

NON-COHESIVE SOILS	
Blows/foot (N)	Apparent Density
0 - 4	Very Loose
5 - 10	Loose
11 - 30	Medium Dense
31 - 50	Dense
> 50	Very Dense

WOR - Weight of Rod
WOH - Weight of Hammer

Soil Descriptions	Proportion
Capitalized Soil Name	Major Component
Lower Case Adjective	35% - 50%
Some	20% - 35%
Little	10% - 20%
Trace	1% - 10%

ENGLISH

TB-12 S:\MATERIALS-RESEARCH\RESEARCH\RESEARCH PROJECTS\SPR PROJECTS\15680S - STRUCTURAL CONDITION ASSESSMENT OF BASE COURSE\NH101\LOGS\15680S EPPING EXETER NH101.PCS.GPJ 3/23/2015 2:19:02 PM TB-12

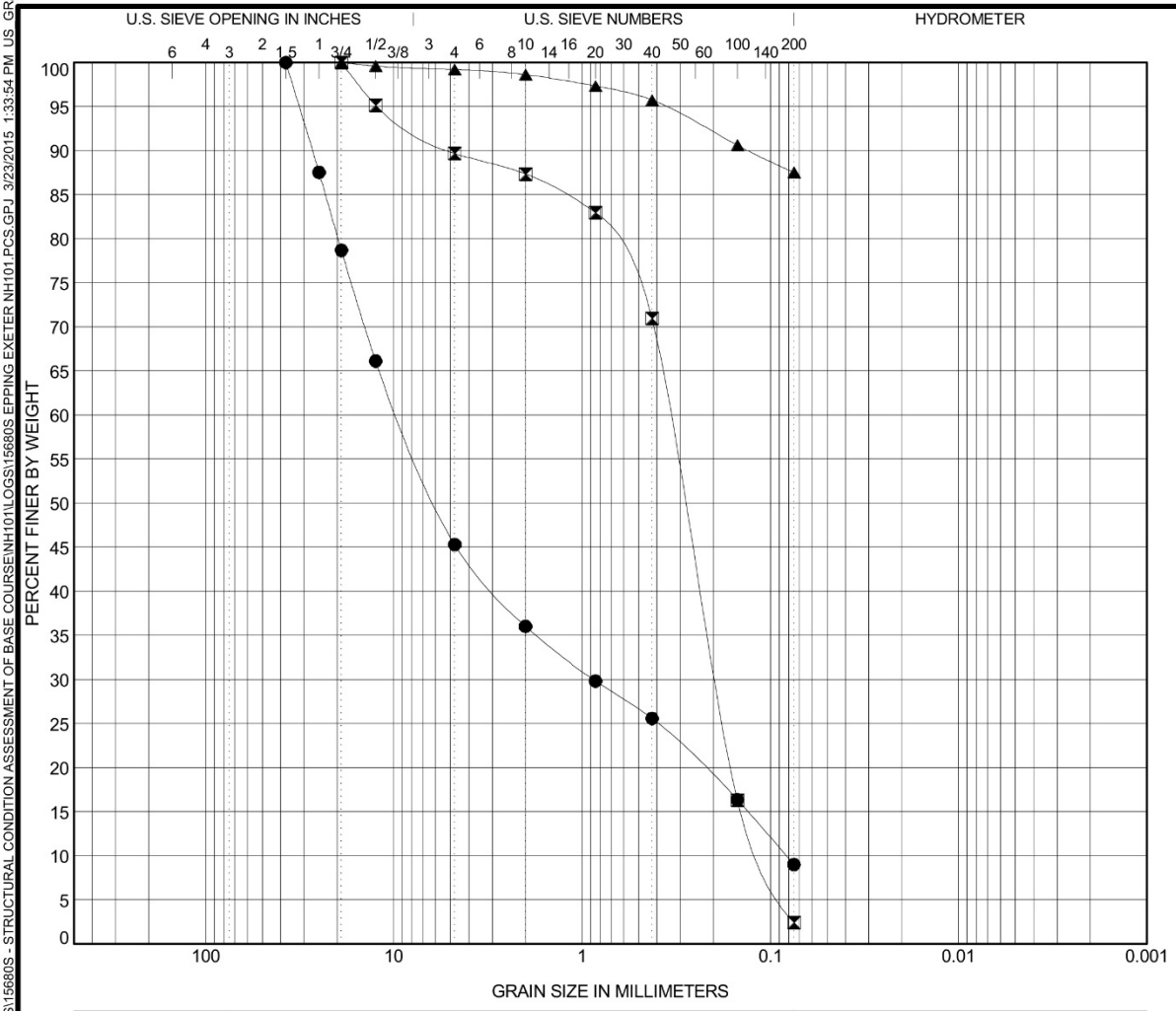

COBBLES	GRAVEL		SAND			SILT OR CLAY
	coarse	fine	coarse	medium	fine	

Specimen Identification			USCS Classification	LL	PL	PI	Cc	Cu
●	PC1, SL1	0.7	poorly graded GRAVEL w/silt & sand (GP-GM)				0.98	114.10
⧓	PC1, SL2	1.5	poorly graded SAND (SP)				1.00	3.15
▲	PC1, SL3	3.9	silty CLAY (CL)					

Specimen Identification			D100	D60	D30	D10	%Gravel	%Sand	%Silt	%Clay
●	PC1, SL1	0.7	37.5	9.4	0.871	0.082	54.7	36.3	9.0	
⧓	PC1, SL2	1.5	19	0.345	0.195	0.109	10.3	87.3	2.4	
▲	PC1, SL3	3.9	19				0.8	11.7	87.5	

State of New Hampshire
Department of Transportation
Bureau of Materials & Research

Project: Epping-Exeter
Location: NH101 Reinforced Pavement
Number: 15680S

GRAIN SIZE DISTRIBUTION

AASHTO T27/T11 - Sieve Analysis of Fine and Coarse Aggregates/Materials Finer Than No. 200 Sieve in Mineral Aggregates by Washing

TEST BORING REPORT

STATE OF NEW HAMPSHIRE DEPARTMENT OF TRANSPORTATION
MATERIALS & RESEARCH BUREAU - GEOTECHNICAL SECTION

PROJECT NAME **EPPING-EXETER 15680S** BRIDGE NO. N/A
DESCRIPTION NH101 Reinforced Pavement

BORING NO. PC2
SHEET NO. 1 OF 1
STA. _____ OFF. _____
BASELINE NH101 EB
ELEVATION (ft) _____
START/END 9/4/14 / 9/4/14
DRILLER C. Cleveland (NHDOT)
INSPECTOR Aaron Smart
CLASSIFIER ALS
EAST/NORTH (ft) -- / --

GROUNDWATER						EQUIPMENT	SAMPLER	CASING	CORE
DATE	TIME	DEPTH (ft)	ELEV. (ft)	BOTTOM OF CASING	BOTTOM OF HOLE	TYPE:	SL	NW	
						SIZE I.D. (in):	3	3	
						HAMMER WT. (lb):	140	DRILL RIG	
						HAMMER FALL (in):	30	CME 45-C Trlr	
						HAMMER TYPE:	Automatic		

DEPTH (ft)	STRATUM CHANGE (ft) DEPTH	STRATUM CHANGE (ft) ELEVATION	BLOWS PER 0.5 ft	SAMPLE NUMBER	SAMPLER RECOVERY (ft) [%]	DEPTH RANGE (ft)	FIELD CLASSIFICATION AND REMARKS	STRATUM SYMBOL
0							-ASPHALT PAVEMENT-	
	0.7			SL1	2.0 [100]	0.7	Mostly dark gray, medium to coarse subangular GRAVEL, some sand.	
						2.7	-FILL- Mostly brown, fine to medium SAND.	
	3.9			SL2	2.0 [100]	2.7	Mostly brownish gray, silty fine SAND & GRAVEL.	
5						4.7	-GLACIAL TILL DEPOSIT-	
							Bottom of Exploration @ 4.7 ft	
							NOTE: NH101 EB MP 124.2	
10								
15								
20								
25								

Sampler	Identification
S	Standard Split Spoon
SL	Large Spoon (O.D.= 3 in)
T	Thin Wall Tube
U	Undisturbed Piston
O	Open End Rod
A	Auger Flight
C	Core Barrel
NR	Not Recorded

COHESIVE SOILS Blows/foot (N)	Consistency
0 - 1	Very Soft
2 - 4	Soft
5 - 8	Medium Stiff
9 - 15	Stiff
16 - 30	Very Stiff
> 30	Hard

NON-COHESIVE SOILS Blows/foot (N)	Apparent Density
0 - 4	Very Loose
5 - 10	Loose
11 - 30	Medium Dense
31 - 50	Dense
> 50	Very Dense

WOR - Weight of Rod
WOH - Weight of Hammer

Soil Descriptions	Proportion
Capitalized Soil Name	Major Component
Lower Case Adjective	35% - 50%
Some	20% - 35%
Little	10% - 20%
Trace	1% - 10%

ENGLISH

TB-12 S:\MATERIALS-RESEARCH\RESEARCH\RESEARCH PROJECTS\SPR PROJECTS\15680S - STRUCTURAL CONDITION ASSESSMENT OF BASE COURSE\NH101\LOGS\15680S EPPING EXETER NH101.PCS.GPJ 3/23/2015 2:19:04 PM TB-12

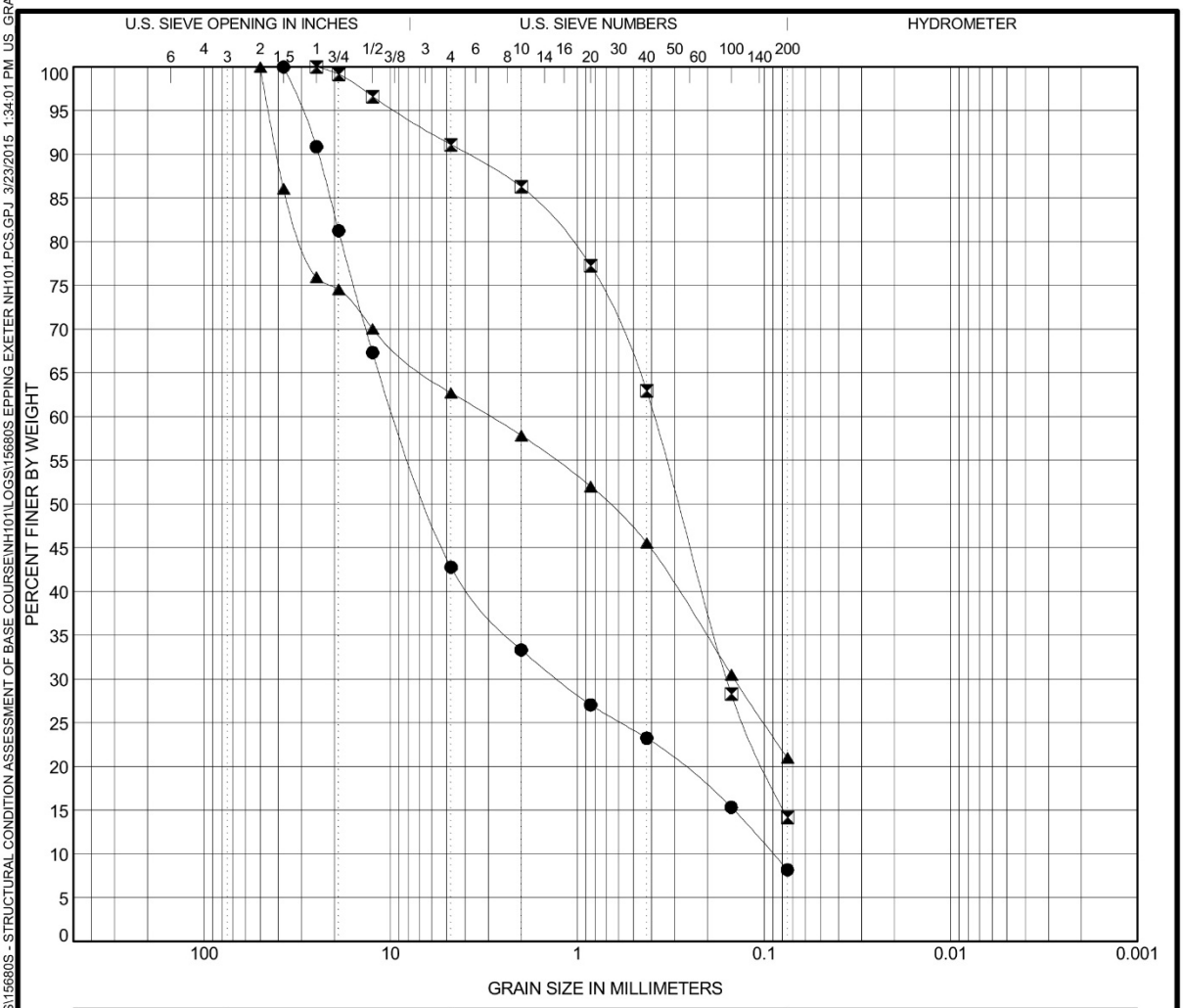

COBBLES	GRAVEL		SAND			SILT OR CLAY
	coarse	fine	coarse	medium	fine	

Specimen Identification		USCS Classification	LL	PL	PI	Cc	Cu
● PC2, SL1	0.7	well graded GRAVEL w/silt & sand (GW-GM)				1.93	104.75
⧓ PC2, SL2	1.5	poorly graded SAND w/silt (SP-SM)					
▲ PC2, SL3	3.9	silty SAND w/gravel (SM)					

Specimen Identification		D100	D60	D30	D10	%Gravel	%Sand	%Silt	%Clay
● PC2, SL1	0.7	37.5	9.358	1.269	0.089	57.2	34.6	8.2	
⧓ PC2, SL2	1.5	25	0.389	0.158		8.9	76.9	14.2	
▲ PC2, SL3	3.9	50	2.925	0.144		37.3	41.7	21.0	

State of New Hampshire
Department of Transportation
Bureau of Materials & Research

Project: Epping-Exeter
Location: NH101 Reinforced Pavement
Number: 15680S

GRAIN SIZE DISTRIBUTION

AASHTO T27/T11 - Sieve Analysis of Fine and Coarse Aggregates/Materials Finer Than No. 200 Sieve in Mineral Aggregates by Washing

US_GRAIN_SIZE S:\MATERIALS-RESEARCH\RESEARCH\RESEARCH PROJECTS\SPR PROJECTS\15680S - STRUCTURAL CONDITION ASSESSMENT OF BASE COURSE\NH101\LOGS\15680S EPPING EXETER NH101.PCS.GPJ 3/23/2015 1:34:01 PM US_GRAIN_S

TEST BORING REPORT

STATE OF NEW HAMPSHIRE DEPARTMENT OF TRANSPORTATION
MATERIALS & RESEARCH BUREAU - GEOTECHNICAL SECTION

PROJECT NAME **EPPING-EXETER 15680S** BRIDGE NO. N/A
DESCRIPTION NH101 Reinforced Pavement

BORING NO. PC3
SHEET NO. 1 OF 1
STA. _____ OFF. _____
BASELINE NH101 EB
ELEVATION (ft) _____
START/END 9/4/14 / 9/4/14
DRILLER C. Cleveland (NHDOT)
INSPECTOR Aaron Smart
CLASSIFIER ALS
EAST/NORTH (ft) -- / --

GROUNDWATER						EQUIPMENT	SAMPLER	CASING	CORE
DATE	TIME	DEPTH (ft)	ELEV. (ft)	BOTTOM OF CASING	BOTTOM OF HOLE	TYPE:	SL	NW	
						SIZE I.D. (in):	3	3	
						HAMMER WT. (lb):	140	DRILL RIG	
						HAMMER FALL (in):	30	CME 45-C Trlr	
						HAMMER TYPE:	Automatic		

DEPTH (ft)	STRATUM CHANGE (ft) DEPTH	STRATUM CHANGE (ft) ELEVATION	BLOWS PER 0.5 ft	SAMPLE NUMBER	SAMPLER RECOVERY (ft) [%]	DEPTH RANGE (ft)	FIELD CLASSIFICATION AND REMARKS	STRATUM SYMBOL
0	0.5					0.5	-ASPHALT PAVEMENT-	
				SL1	2.0 [100]		Mostly dark gray to black, fine to medium SAND, some coarse gravel-sized asphalt pavement fragments.	
						2.5	-FILL-	
				SL2	2.0 [100]	2.5	Mostly brown to reddish brown, fire to coarse SAND & GRAVEL, gravel portion is medium to coarse and subrounded to subangular.	
	3.7						Mostly fine to medium SAND, little fine subrounded gravel.	
5						4.5	Mostly brown, silty fine SAND, some medium subangular gravel.	
							-GLACIAL TILL DEPOSIT-	
							Bottom of Exploration @ 4.5 ft	
							NOTE: NH101 EB MP 128.4	
10								
15								
20								
25								

Sampler	Identification
S	Standard Split Spoon
SL	Large Spoon (O.D.= 3 in)
T	Thin Wall Tube
U	Undisturbed Piston
O	Open End Rod
A	Auger Flight
C	Core Barrel
NR	Not Recorded

COHESIVE SOILS	
Blows/foot (N)	Consistency
0 - 1	Very Soft
2 - 4	Soft
5 - 8	Medium Stiff
9 - 15	Stiff
16 - 30	Very Stiff
> 30	Hard

NON-COHESIVE SOILS	
Blows/foot (N)	Apparent Density
0 - 4	Very Loose
5 - 10	Loose
11 - 30	Medium Dense
31 - 50	Dense
> 50	Very Dense

WOR - Weight of Rod
WOH - Weight of Hammer

Soil Descriptions	Proportion
Capitalized Soil Name	Major Component
Lower Case Adjective	35% - 50%
Some	20% - 35%
Little	10% - 20%
Trace	1% - 10%

ENGLISH

TB-12 S:\MATERIALS-RESEARCH\RESEARCH\RESEARCH PROJECTS\SPR PROJECTS\15680S - STRUCTURAL CONDITION ASSESSMENT OF BASE COURSE\NH101\LOGS\15680S EPPING EXETER NH101.PCS.GPJ 3/23/2015 2:19:05 PM TB-12

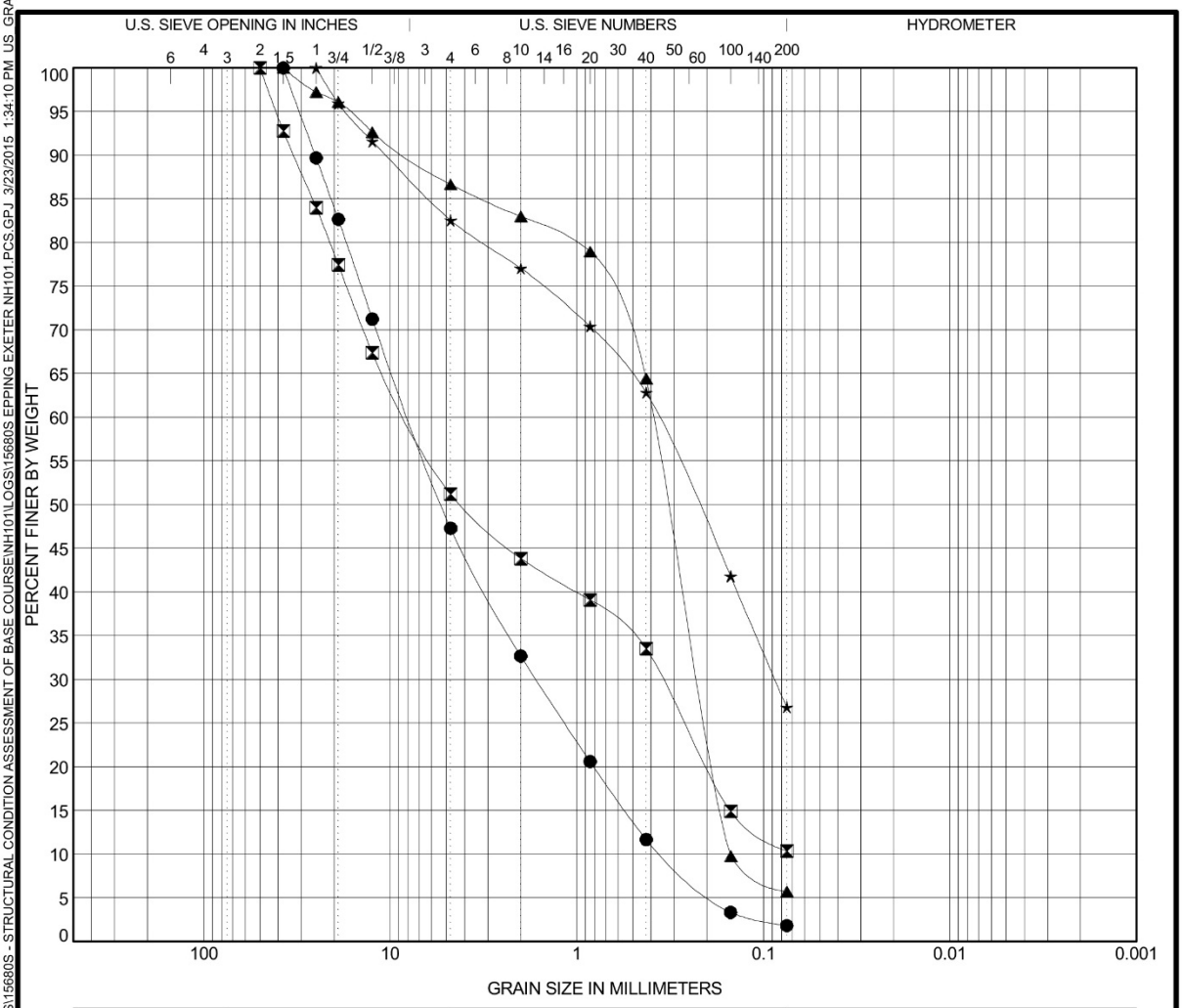

COBBLES	GRAVEL		SAND			SILT OR CLAY
	coarse	fine	coarse	medium	fine	

Specimen Identification			USCS Classification	LL	PL	PI	Cc	Cu
●	PC3, SL1	0.5	well graded GRAVEL w/sand (GW)				1.00	23.00
⧓	PC3, SL1	1.0	poorly graded GRAVEL w/silt & sand (GP-GM)				0.21	112.83
▲	PC3, SL2	2.5	poorly graded SAND w/silt & gravel (SP-SM)				0.83	2.59
★	PC3, SL2	3.7	silty SAND w/gravel (SM)					

Specimen Identification			D100	D60	D30	D10	%Gravel	%Sand	%Silt	%Clay
●	PC3, SL1	0.5	37.5	7.935	1.654	0.345	52.7	45.5	1.8	
⧓	PC3, SL1	1.0	50	8.036	0.349		48.8	40.9	10.3	
▲	PC3, SL2	2.5	37.5	0.39	0.22	0.151	13.3	80.9	5.7	
★	PC3, SL2	3.7	25	0.369	0.087		17.5	55.7	26.8	

State of New Hampshire
Department of Transportation
Bureau of Materials & Research

Project: Epping-Exeter
Location: NH101 Reinforced Pavement
Number: 15680S

GRAIN SIZE DISTRIBUTION

AASHTO T27/T11 - Sieve Analysis of Fine and Coarse Aggregates/Materials Finer Than No. 200 Sieve in Mineral Aggregates by Washing

US_GRAIN_SIZE S:\MATERIALS-RESEARCH\RESEARCH\RESEARCH PROJECTS\SPR PROJECTS\15680S - STRUCTURAL CONDITION ASSESSMENT OF BASE COURSE\NH101\LOGS\15680S EPPING EXETER NH101.PCS.GPJ 3/23/2015 1:34:10 PM US_GRAIN_S

TEST BORING REPORT

STATE OF NEW HAMPSHIRE DEPARTMENT OF TRANSPORTATION
MATERIALS & RESEARCH BUREAU - GEOTECHNICAL SECTION

PROJECT NAME **EPPING-EXETER 15680S** BRIDGE NO. N/A
DESCRIPTION NH101 Reinforced Pavement

BORING NO. PC4
SHEET NO. 1 OF 1
STA. _____ OFF. _____
BASELINE NH101 WB
ELEVATION (ft) _____
START/END 9/4/14 / 9/4/14
DRILLER C. Cleveland (NHDOT)
INSPECTOR Aaron Smart
CLASSIFIER ALS
EAST/NORTH (ft) -- / --

GROUNDWATER						EQUIPMENT	SAMPLER	CASING	CORE
DATE	TIME	DEPTH (ft)	ELEV. (ft)	BOTTOM OF CASING	BOTTOM OF HOLE	TYPE:	SL	NW	
						SIZE I.D. (in):	3	3	
						HAMMER WT. (lb):	140	DRILL RIG	
						HAMMER FALL (in):	30	CME 45-C Trlr	
						HAMMER TYPE:	Automatic		

DEPTH (ft)	STRATUM CHANGE (ft) DEPTH	STRATUM CHANGE (ft) ELEVATION	BLOWS PER 0.5 ft	SAMPLE NUMBER	SAMPLER RECOVERY (ft) [%]	DEPTH RANGE (ft)	FIELD CLASSIFICATION AND REMARKS	STRATUM SYMBOL
0							-ASPHALT PAVEMENT-	
	0.5			SL1	2.0 [100]	0.5 – 2.5	Mostly dark gray to white, fine to coarse subangular GRAVEL, some sand. -FILL- Mostly brown, fine to medium SAND.	
				SL2	2.0 [100]	2.5 – 4.5		
	4.2						Mostly gray, silty fine SAND, some medium to coarse subangular gravel. -GLACIAL TILL DEPOSIT-	
5							Bottom of Exploration @ 4.5 ft	
10							NOTE: NH101 WB MP 131.5	
15								
20								
25								

Sampler	Identification
S	Standard Split Spoon
SL	Large Spoon (O.D.= 3 in)
T	Thin Wall Tube
U	Undisturbed Piston
O	Open End Rod
A	Auger Flight
C	Core Barrel
NR	Not Recorded

COHESIVE SOILS	
Blows/foot (N)	Consistency
0 - 1	Very Soft
2 - 4	Soft
5 - 8	Medium Stiff
9 - 15	Stiff
16 - 30	Very Stiff
> 30	Hard

NON-COHESIVE SOILS	
Blows/foot (N)	Apparent Density
0 - 4	Very Loose
5 - 10	Loose
11 - 30	Medium Dense
31 - 50	Dense
> 50	Very Dense

WOR - Weight of Rod
WOH - Weight of Hammer

Soil Descriptions	Proportion
Capitalized Soil Name	Major Component
Lower Case Adjective	35% - 50%
Some	20% - 35%
Little	10% - 20%
Trace	1% - 10%

ENGLISH

TB-12 S:\MATERIALS-RESEARCH\RESEARCH\RESEARCH PROJECTS\SPR PROJECTS\15680S - STRUCTURAL CONDITION ASSESSMENT OF BASE COURSE\NH101\LOGS\15680S EPPING EXETER NH101.PCS.GPJ 3/23/2015 2:19:06 PM TB-12

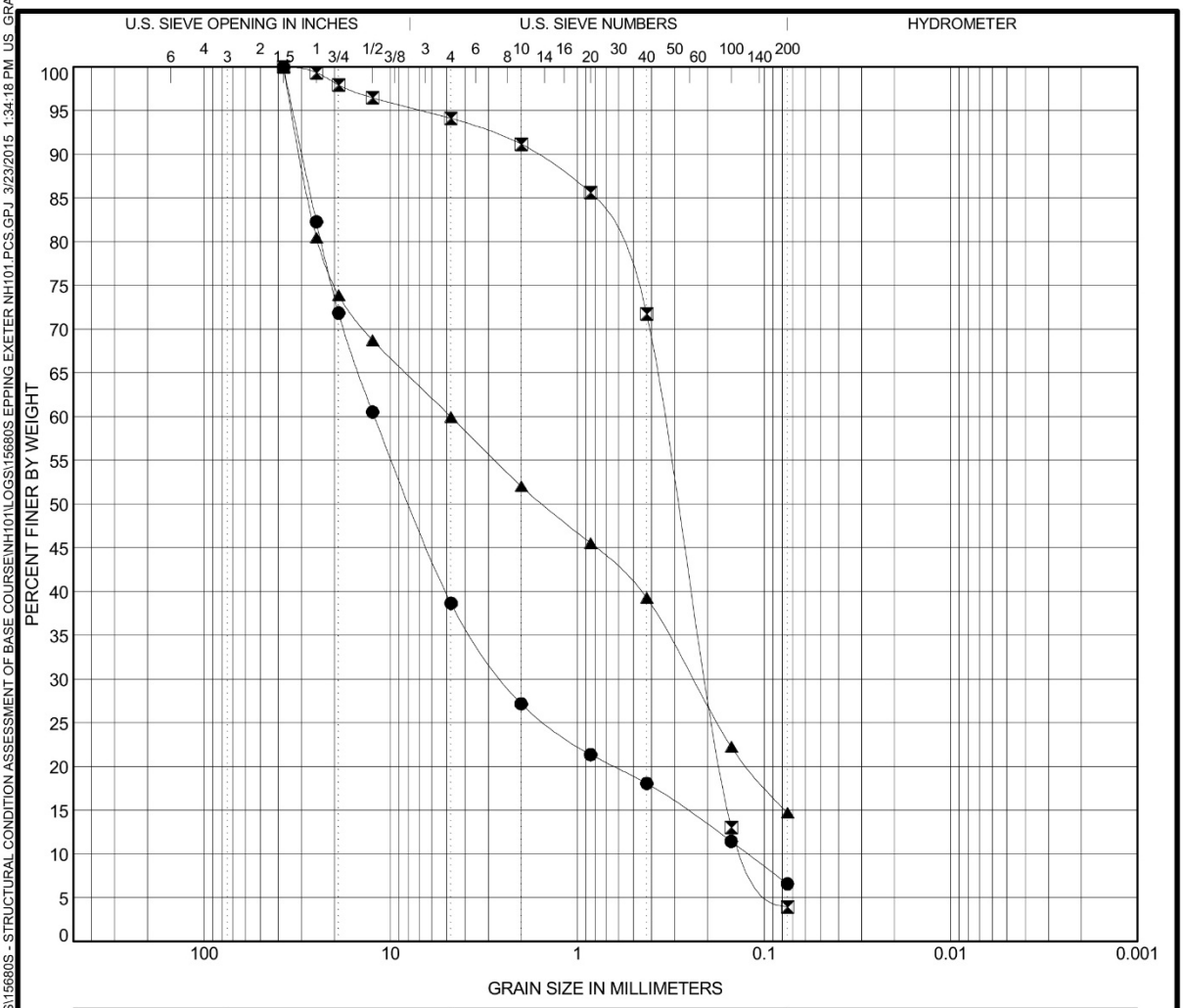

COBBLES	GRAVEL		SAND			SILT OR CLAY
	coarse	fine	coarse	medium	fine	

Specimen Identification		USCS Classification	LL	PL	PI	Cc	Cu
● PC4, SL1	0.5	poorly graded GRAVEL w/silt & sand (GP-GM)				4.11	100.07
⧓ PC4, SL1	1.2	poorly graded SAND (SP)				1.00	2.90
▲ PC4, SL2	4.2	poorly graded SAND w/silt & gravel (SP-SM)					

Specimen Identification		D100	D60	D30	D10	%Gravel	%Sand	%Silt	%Clay
● PC4, SL1	0.5	37.5	12.209	2.473	0.122	61.3	32.1	6.6	
⧓ PC4, SL1	1.2	37.5	0.345	0.203	0.119	5.9	90.2	3.9	
▲ PC4, SL2	4.2	37.5	4.756	0.241		40.0	45.3	14.7	

State of New Hampshire
Department of Transportation
Bureau of Materials & Research

Project: Epping-Exeter
Location: NH101 Reinforced Pavement
Number: 15680S

GRAIN SIZE DISTRIBUTION

AASHTO T27/T11 - Sieve Analysis of Fine and Coarse Aggregates/Materials Finer Than No. 200 Sieve in Mineral Aggregates by Washing

US_GRAIN_SIZE S:\MATERIALS-RESEARCH\RESEARCH\RESEARCH PROJECTS\SPR PROJECTS\15680S - STRUCTURAL CONDITION ASSESSMENT OF BASE COURSE\NH101\LOGS\15680S EPPING EXETER NH101.PCS.GPJ 3/23/2015 1:34:18 PM US_GRAIN_S

TEST BORING REPORT

STATE OF NEW HAMPSHIRE DEPARTMENT OF TRANSPORTATION
MATERIALS & RESEARCH BUREAU - GEOTECHNICAL SECTION

PROJECT NAME **EPPING-EXETER 15680S** BRIDGE NO. N/A
DESCRIPTION NH101 Reinforced Pavement

BORING NO. PC5
SHEET NO. 1 OF 1
STA. _____ OFF. _____
BASELINE NH101 WB
ELEVATION (ft) _____
START/END 10/28/14 / 10/28/14
DRILLER C. Cleveland (NHDOT)
INSPECTOR Aaron Smart
CLASSIFIER ALS
EAST/NORTH (ft) -- / --

GROUNDWATER						EQUIPMENT	SAMPLER	CASING	CORE
DATE	TIME	DEPTH (ft)	ELEV. (ft)	BOTTOM OF CASING	BOTTOM OF HOLE	TYPE:	SL	NW	
						SIZE I.D. (in):	3	3	
						HAMMER WT. (lb):	140	DRILL RIG	
						HAMMER FALL (in):	30		
						HAMMER TYPE:			

DEPTH (ft)	STRATUM CHANGE (ft) DEPTH	STRATUM CHANGE (ft) ELEVATION	BLOWS PER 0.5 ft	SAMPLE NUMBER	SAMPLER RECOVERY (ft) [%]	DEPTH RANGE (ft)	FIELD CLASSIFICATION AND REMARKS	STRATUM SYMBOL
0	0.5					0.5	-ASPHALT PAVEMENT-	
				SL1	2.0 [100]		Mostly dark gray to white, fine to coarse subangular GRAVEL, some sand.	
						2.5	-FILL- Mostly brown, fine to medium SAND.	
				SL2	2.0 [100]	2.5		
	4.1					4.5	Mostly gray, silty fine SAND, some medium to coarse subangular gravel.	
5							-GLACIAL TILL DEPOSIT-	
							Bottom of Exploration @ 4.5 ft	
							NOTE: NH101 WB MP 131.5	
10								
15								
20								
25								

Sampler	Identification
S	Standard Split Spoon
SL	Large Spoon (O.D.= 3 in)
T	Thin Wall Tube
U	Undisturbed Piston
O	Open End Rod
A	Auger Flight
C	Core Barrel
NR	Not Recorded

COHESIVE SOILS	
Blows/foot (N)	Consistency
0 - 1	Very Soft
2 - 4	Soft
5 - 8	Medium Stiff
9 - 15	Stiff
16 - 30	Very Stiff
> 30	Hard

NON-COHESIVE SOILS	
Blows/foot (N)	Apparent Density
0 - 4	Very Loose
5 - 10	Loose
11 - 30	Medium Dense
31 - 50	Dense
> 50	Very Dense

WOR - Weight of Rod
WOH - Weight of Hammer

Soil Descriptions	Proportion
Capitalized Soil Name	Major Component
Lower Case Adjective	35% - 50%
Some	20% - 35%
Little	10% - 20%
Trace	1% - 10%

ENGLISH

TB-12 S:\MATERIALS-RESEARCH\RESEARCH\RESEARCH PROJECTS\SPR PROJECTS\15680S - STRUCTURAL CONDITION ASSESSMENT OF BASE COURSE\NH101\LOGS\15680S EPPING EXETER NH101.PCS.GPJ 3/23/2015 2:19:07 PM TB-12

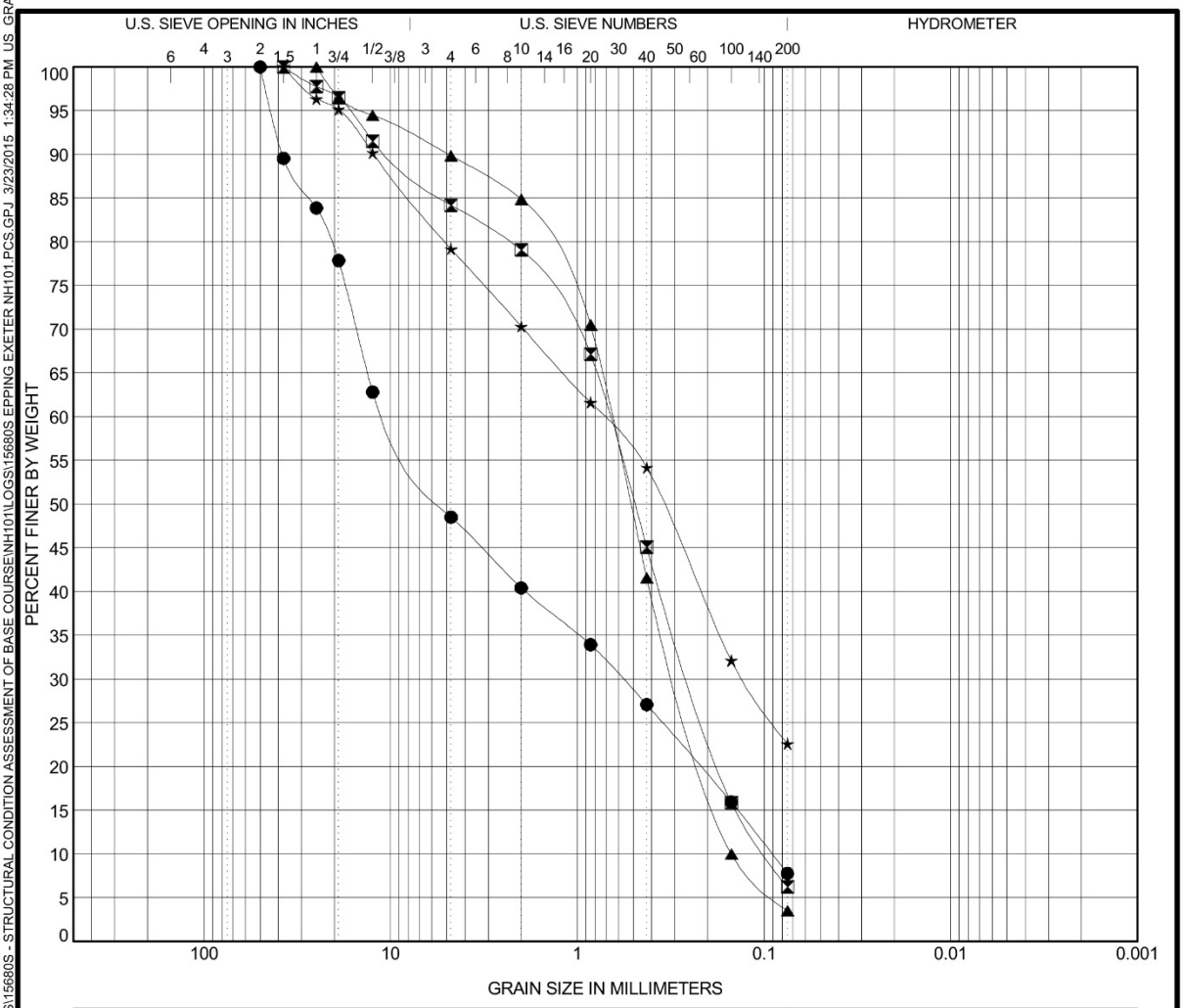

COBBLES	GRAVEL		SAND			SILT OR CLAY
	coarse	fine	coarse	medium	fine	

Specimen Identification			USCS Classification	LL	PL	PI	Cc	Cu
●	PC5, SL1	0.6	poorly graded GRAVEL w/silt & sand (GP-GM)				0.35	114.01
⧓	PC5, SL1	2.1	poorly graded SAND w/silt (SP-SM)				0.92	6.90
▲	PC5, SL2	2.6	poorly graded SAND (SP)				0.85	4.41
★	PC5, SL2	4.1	silty SAND w/gravel (SM)					

Specimen Identification			D100	D60	D30	D10	%Gravel	%Sand	%Silt	%Clay
●	PC5, SL1	0.6	50	10.329	0.571	0.091	51.5	40.7	7.8	
⧓	PC5, SL1	2.1	37.5	0.679	0.248	0.098	15.8	78.0	6.2	
▲	PC5, SL2	2.6	25	0.661	0.29	0.15	10.2	86.3	3.5	
★	PC5, SL2	4.1	37.5	0.73	0.129		20.8	56.6	22.6	

State of New Hampshire
Department of Transportation
Bureau of Materials & Research

Project: Epping-Exeter
Location: NH101 Reinforced Pavement
Number: 15680S

GRAIN SIZE DISTRIBUTION

AASHTO T27/T11 - Sieve Analysis of Fine and Coarse Aggregates/Materials Finer Than No. 200 Sieve in Mineral Aggregates by Washing

US_GRAIN_SIZE S:\MATERIALS-RESEARCH\RESEARCH\RESEARCH PROJECTS\SPR PROJECTS\15680S - STRUCTURAL CONDITION ASSESSMENT OF BASE COURSE\NH101\LOGS\15680S EPPING EXETER NH101.PCS.GPJ 3/23/2015 1:34:28 PM US_GRAIN_S

TEST BORING REPORT

STATE OF NEW HAMPSHIRE DEPARTMENT OF TRANSPORTATION
MATERIALS & RESEARCH BUREAU - GEOTECHNICAL SECTION

PROJECT NAME **EPPING-EXETER 15680S** BRIDGE NO. N/A
DESCRIPTION NH101 Reinforced Pavement

BORING NO. PC6
SHEET NO. 1 OF 1
STA. _____ OFF. _____
BASELINE NH101 WB
ELEVATION (ft) _____
START/END 10/28/14 / 10/28/14
DRILLER C. Cleveland (NHDOT)
INSPECTOR Aaron Smart
CLASSIFIER ALS
EAST/NORTH (ft) -- / --

GROUNDWATER						EQUIPMENT	SAMPLER	CASING	CORE
DATE	TIME	DEPTH (ft)	ELEV. (ft)	BOTTOM OF CASING	BOTTOM OF HOLE	TYPE:	SL	NW	
						SIZE I.D. (in):	3	3	
						HAMMER WT. (lb):	140	DRILL RIG	
						HAMMER FALL (in):	30		
						HAMMER TYPE:			

DEPTH (ft)	STRATUM CHANGE (ft) DEPTH	STRATUM CHANGE (ft) ELEVATION	BLOWS PER 0.5 ft	SAMPLE NUMBER	SAMPLER RECOVERY (ft) [%]	DEPTH RANGE (ft)	FIELD CLASSIFICATION AND REMARKS	STRATUM SYMBOL
0							-ASPHALT PAVEMENT-	
	0.8			SL1	2.0 [100]	0.8 – 2.8	Mostly dark gray to white, fine to coarse subangular GRAVEL, some sand. -FILL- Mostly brown, fine to medium SAND.	
				SL2	2.0 [100]	2.8 – 4.8		
5	4.6						Mostly gray, silty fine SAND, some medium to coarse subangular gravel. -GLACIAL TILL DEPOSIT-	
10							Bottom of Exploration @ 4.8 ft NOTE: NH101 WB MP 131.5	
15								
20								
25								

Sampler	Identification
S	Standard Split Spoon
SL	Large Spoon (O.D.= 3 in)
T	Thin Wall Tube
U	Undisturbed Piston
O	Open End Rod
A	Auger Flight
C	Core Barrel
NR	Not Recorded

COHESIVE SOILS	
Blows/foot (N)	Consistency
0 - 1	Very Soft
2 - 4	Soft
5 - 8	Medium Stiff
9 - 15	Stiff
16 - 30	Very Stiff
> 30	Hard

NON-COHESIVE SOILS	
Blows/foot (N)	Apparent Density
0 - 4	Very Loose
5 - 10	Loose
11 - 30	Medium Dense
31 - 50	Dense
> 50	Very Dense

WOR - Weight of Rod
WOH - Weight of Hammer

Soil Descriptions	Proportion
Capitalized Soil Name	Major Component
Lower Case Adjective	35% - 50%
Some	20% - 35%
Little	10% - 20%
Trace	1% - 10%

ENGLISH

TB-12 S:\MATERIALS-RESEARCH\RESEARCH\RESEARCH PROJECTS\SPR PROJECTS\15680S - STRUCTURAL CONDITION ASSESSMENT OF BASE COURSE\NH101\LOGS\15680S EPPING EXETER NH101.PCS.GPJ 3/23/2015 2:19:08 PM TB-12

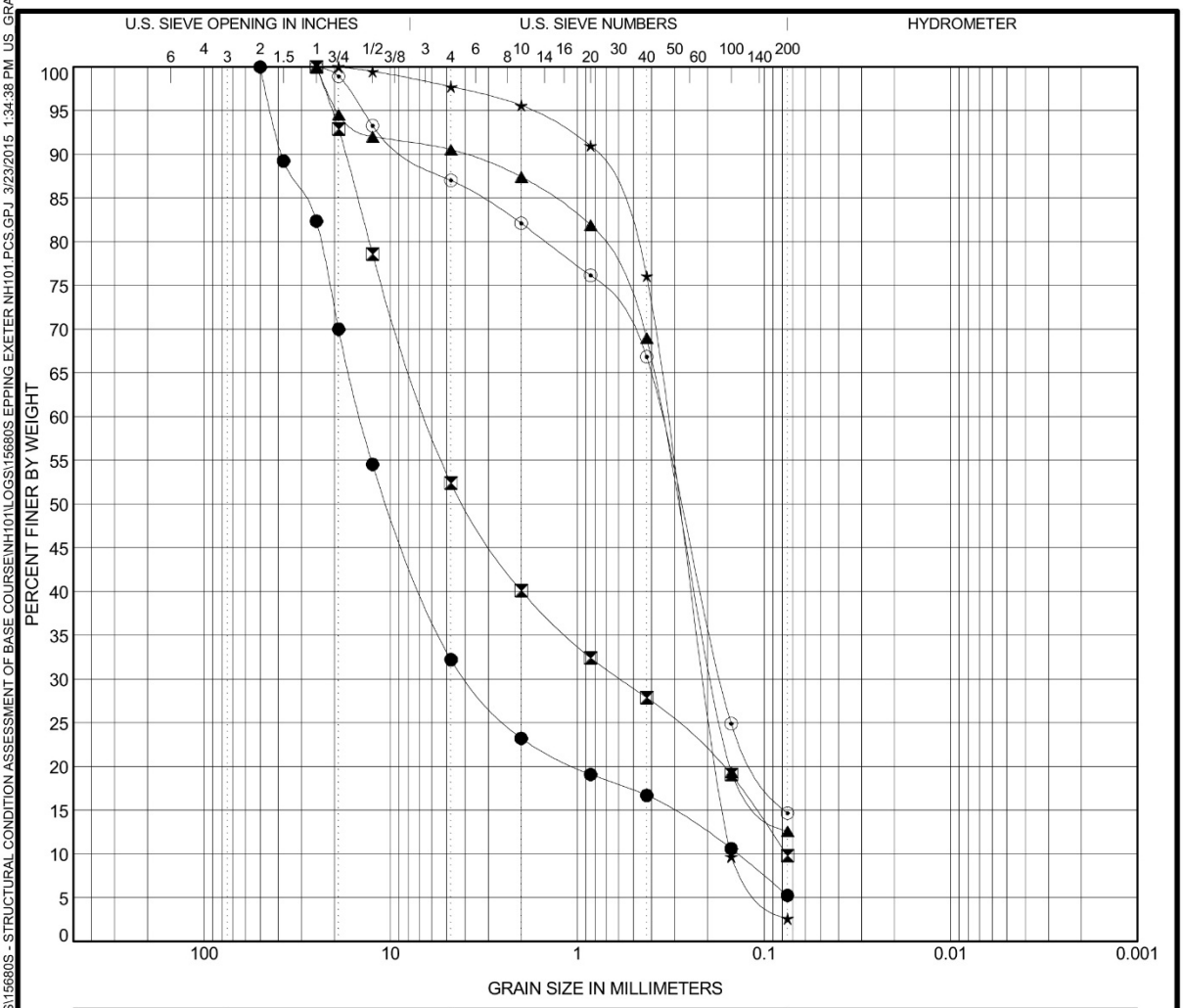

COBBLES	GRAVEL		SAND			SILT OR CLAY
	coarse	fine	coarse	medium	fine	

Specimen Identification		USCS Classification	LL	PL	PI	Cc	Cu
● PC6, SL1	0.8	poorly graded GRAVEL w/silt & sand (GP-GM)				7.33	104.59
⧓ PC6, SL1	1.1	poorly graded SAND w/silt & gravel (SP-SM)				0.72	82.54
▲ PC6, SL1	2.1	poorly graded SAND w/silt (SP-SM)					
★ PC6, SL2	2.8	poorly graded SAND (SP)				0.85	2.19
⊙ PC6, SL2	4.5	poorly graded SAND w/silt (SP-SM)					

Specimen Identification		D100	D60	D30	D10	%Gravel	%Sand	%Silt	%Clay
● PC6, SL1	0.8	50	14.486	3.836	0.138	67.8	27.0	5.3	
⧓ PC6, SL1	1.1	25	6.289	0.588	0.076	47.6	42.6	9.8	
▲ PC6, SL1	2.1	25	0.352	0.188		9.5	77.9	12.6	
★ PC6, SL2	2.8	19	0.33	0.206	0.151	2.3	95.1	2.6	
⊙ PC6, SL2	4.5	25	0.359	0.17		13.0	72.3	14.7	

State of New Hampshire
Department of Transportation
Bureau of Materials & Research

Project: Epping-Exeter
Location: NH101 Reinforced Pavement
Number: 15680S

GRAIN SIZE DISTRIBUTION

AASHTO T27/T11 - Sieve Analysis of Fine and Coarse Aggregates/Materials Finer Than No. 200 Sieve in Mineral Aggregates by Washing

US_GRAIN_SIZE S:\MATERIALS-RESEARCH\RESEARCH\RESEARCH PROJECTS\SPR PROJECTS\15680S - STRUCTURAL CONDITION ASSESSMENT OF BASE COURSE\NH101\LOGS\15680S EPPING EXETER NH101.PCS.GPJ 3/23/2015 1:34:38 PM US_GRAIN_S

REPORT DOCUMENTATION PAGE

Form Approved
OMB No. 0704-0188

1. REPORT DATE *(DD-MM-YYYY)*
May 2016

2. REPORT TYPE
Technical Report/Final

3. DATES COVERED *(From - To)*

4. TITLE AND SUBTITLE
Assessment of Asphalt Concrete Reinforcement Grid in Flexible Pavements

5a. CONTRACT NUMBER
CRADA 13-CRL-01

5b. GRANT NUMBER

5c. PROGRAM ELEMENT NUMBER

6. AUTHOR(S)
Lynette A. Barna, Charles E. Smith Jr., Andrew Bernier, Aaron Smart, and Ann M. Scholz

5d. PROJECT NUMBER
26962A

5e. TASK NUMBER

5f. WORK UNIT NUMBER

7. PERFORMING ORGANIZATION NAME(S) AND ADDRESS(ES)
U.S. Army Engineer Research and Development Center (ERDC)
Cold Regions Research and Engineering Laboratory (CRREL)
72 Lyme Road
Hanover, NH 03755-1290

8. PERFORMING ORGANIZATION REPORT NUMBER
ERDC/CRREL TR-16-7

9. SPONSORING / MONITORING AGENCY NAME(S) AND ADDRESS(ES)
New Hampshire Department of Transportation (NHDOT) in cooperation with the U.S. Department of Transportation, Federal Highway Administration
PO Box 483, 5 Hazen Drive
Concord, NH 03302

10. SPONSOR/MONITOR'S ACRONYM(S)
NHDOT

11. SPONSOR/MONITOR'S REPORT NUMBER(S)

12. DISTRIBUTION / AVAILABILITY STATEMENT
Approved for public release; distribution is unlimited.

13. SUPPLEMENTARY NOTES
New Hampshire DOT SPR2 Program

14. ABSTRACT

This report investigated the application of accepted methods of pavement structural evaluation to independently assess the potential structural benefit of asphalt geogrid reinforcement of an operational flexible highway pavement. The asphalt interlayer consisted of an elastomeric polymer coated fiberglass grid with an open configuration. The reinforcing grid was installed in the asphalt layer during construction of a maintenance overlay and has been subjected to trafficking for several years.

Our structural evaluation included a geotechnical investigation and non-destructive testing using a falling weight deflectometer. Field testing was conducted when both air temperatures were above 50°F and no recent precipitation events had occurred. Standard testing methods were applied during the field data collection and back-calculation procedure.

The back-calculation results showed no clear quantifiable benefit from including the reinforcing grid in the asphalt layer, but this study developed a methodology to test and evaluate in situ flexible pavements with asphalt grid reinforcement. We recommend that a future structural evaluation be completed to monitor any changes in the pavement's performance.

15. SUBJECT TERMS
Asphalt concrete--Evaluation
Fiberglass geogrid
Flexible pavement
Geogrids—Testing
Modulus backcalculation
Pavements, Asphalt concrete--Cracking
Pavements, Asphalt concrete--Design and construction--Data processing
Pavements, Flexible--Design and construction

16. SECURITY CLASSIFICATION OF:			17. LIMITATION OF ABSTRACT	18. NUMBER OF PAGES	19a. NAME OF RESPONSIBLE PERSON
a. REPORT	b. ABSTRACT	c. THIS PAGE			19b. TELEPHONE NUMBER *(include area code)*
Unclassified	Unclassified	Unclassified	SAR	91	